GEOSTATISTICAL DYNAMIC SIMULATION ON UNSTRUCTURED GRID

NIVEDHITHA AJITHKUMAR

March, 2019

SUPERVISORS:
MR.HARI SHANKAR (IIRS)
DR.FRANK.B.OSEI (ITC)
ADVISOR: MR.PRABHAKAR ALOK VERMA (IIRS)

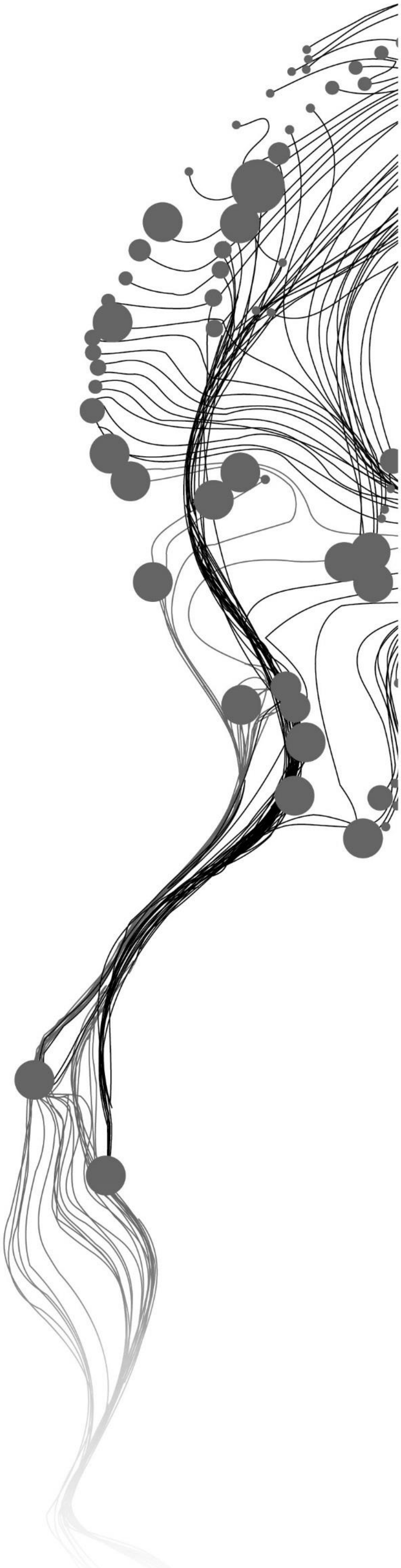

GEOSTATISTICAL DYNAMIC SIMULATION ON UNSTRUCTURED GRID

NIVEDHITHA AJITHKUMAR
Enschede, The Netherlands,

March, 2019

Thesis submitted to the Faculty of Geo-Information Science and Earth Observation of the University of Twente in partial fulfilment of the requirements for the degree of Master of Science in Geo-information Science and Earth Observation.
Specialization: Geoinformatics

SUPERVISORS:
MR.HARI SHANKAR
DR.FRANK.B.OSEI
ADVISOR: MR.PRABHAKAR ALOK VERMA

THESIS ASSESSMENT BOARD:
Prof. Dr.Ir.A.Stein (Chair, ITC Professor)
Prof. S.K.Ghosh (External Examiner ,IIT Roorkee)

Dedicated to my parents

ABSTRACT

Geostatistical simulations are generally performed on the structured grid or regular grid. Due to uniform size and pattern of the structured grid, it has drawbacks like the support size effect or change of support is not considered, cell distortion and artefacts are caused during simulation. This might lead to many consequences like the symmetry of the grid is disturbed which in turn reduces the numerical accuracy of the grid. To overcome these, unstructured grids were introduced. But for performing geostatistical simulation on the unstructured grid, the support size effect is needed to be taken into consideration as the volume difference between each block in the unstructured grid is different. Moreover accounting for support size effect is important in ore and petroleum reservoir for estimation and planning. In the area of hydrology change of support is not taken into account unless it is sub-surface flow estimation. In this research two methods have been used for accounting the change of support and studying its effect on surface flow estimation in hydrology. One is the classical fine-scale simulation approach and the other approach is using Discrete Gaussian Model (DGM). In accordance with the application in hydrology, elevation value is taken as the point support data to perform the simulation. Furthermore, to understand the effect of support size the resultant output is applied for steady flow simulation.

The unstructured grid is generated depending upon the requirements of the study area. In the fine-scale simulation, the change of support model is addressed after performing simulation while in Discrete Gaussian model, simulation is performed after changing the support. It was observed that due to regularisation of the data the spatial variability decreases as the area of the support increases. The outputs of the geostatistical simulation, which is basically a Digital Elevation Model (DEM) is given as an input along with other parameters for steady flow simulation. Cartosat 10m DEM is taken as reference DEM in order to validate the simulated output. The flow velocity of unstructured DEM generated using DGM approach shows similar behaviour to that of reference DEM. While for the water surface elevation difference, DEM generated using fine-scale simulation is the same as the reference DEM. The resultant flow output for all the generated DEM is validated with the reference DEM. The minimum RMSE for water surface elevation is 0.83m for DGM generated unstructured DEM while the minimum RMSE for flow discharge is 0.38m^3/s. The maximum coefficient of determination of flow channel velocity and water surface elevation is 0.709m/s and 0.86m respectively.

The results suggest that the unstructured DEM generated using DGM approach shows a high correlation to reference DEM than the simulated structured DEM. The flow output shows variation in both structured and unstructured DEM, affecting not only the vertical resolution of DEM but the horizontal resolution as well. Thus resulting in that the variation or the change in support affects the surface flow estimation.

Keywords: Unstructured grid, Support size effect, Geostatistical simulation, Digital Elevation Models, Steady flow analysis

ACKNOWLEDGEMENTS

To my first teachers, my parents who have been with me in all the situations inspired me and provided me with moral, emotional and financial support, without them I would be nowhere. I take this opportunity to thank them. I would like to thank my brother who was always there for me whenever I needed.

I would like to thank my supervisors, Mr Hari Shankar, Dr Frank.B.Osei, who gave me direction on how to do the research. I would especially like to thank my advisor Mr Prabhakar Alok Varma, who took his time in explaining and clearing all my queries whenever I ran into trouble with patience and guided and supported me throughout the research. I would also like to thank Dr Sameer Saran, who helped us throughout by solving all the problems that we had faced during the research.

Brainstorming is the most difficult part of the research and without discussing and sharing thoughts with friends, it wouldn't have been possible for me to go on with the research. I would like to thank all my friends for helping me to go through those tough times. They have supported and guided me along the way.

I want to extend my gratitude to Dr Prakash Chauhan (Director, IIRS), Dr S.K.Srivastav Dean (Academics), Dr. Valentyn Tolpekin (M.Sc. Course co-ordinator, ITC) for their constant support throughout this period and I would also like to thank all the organizers and teachers both IIRS and ITC involved in this M.Sc. Course programme.

Finally, I would like to acknowledge all the software and programming language developer community especially Rstudio, HEC-RAS and Arc GIS without which this research wouldn't be possible.

TABLE OF CONTENTS

LIST OF FIGURES

LIST OF TABLES

1. INTRODUCTION

1.1. Motivation

Most geostatistical simulations are performed over structured grids or regular grids, which are uniform in size and pattern. They are grids with identical blocks, made up of rectangular box subdivided equally into regions (blocks), that are modelled into a set of small control volume elements ("Grid Systems," 2015; Zaytsev, Biver, Wackernagel, & Allard, 2016b). In structured grids, these small control volume elements are well ordered and simulate the centroid of the cell. They are fast and memory efficient i.e. these grids find neighbours faster and they use less memory than another kind of grids. They are highly spaced efficient, with better convergence and have higher resolution (Biver, Zaytsev, Allard, & Wackernagel, 2017; Manchuk & Deutsch, 2009). For example, in hydrology, the flow of fluid has stronger gradients (multi-variables) in one direction and milder gradients in opposite direction (Chawner, 2013). These regular grids have been used for a long time in the industries as they follow stratigraphy in corner point grids geometry. They were also convenient in optimizing algorithms of various kinds such as sequential simulation, Fast Fourier transform etc. (Dusserre, Garbolino, Jaber, Guarnieri, & Karim, 2016b; Zaytsev, Biver, Wackernagel, & Allard, 2016a).

Although structured grids have been used for a long time in the industries, they have certain drawbacks. It is very difficult to deform the shape of regular grids, which is generally known as the support size effect. Typically the shape of this grid has fixed area or volume (Bergamaschi, 2005; Hengl, 2006; Manchuk, 2010). So if we had to add or remove any points from the grid it will affect the whole grid structure. Another disadvantage of the structured grids is that due to some artefacts, cell distortions are caused. These distortions might lead to many consequences like disturbing the symmetry of the grid which makes the numerical approximation no longer in centre of the volume element, thereby reducing the numerical accuracy of the grid (Braun, Molnar, & Kleeberg, 1997; Fields et al., 1996; Loseille, 2017; Mavriplis, 1997). For example in hydrology, if we take a Digital Elevation Model (DEM), the error produced in DEM will severely affect the ability to represent terrain which indirectly affects the hydrological modelling. DEM is affected by many factors in which artefacts of grid cell size (resolution) is one among them. So if grid cell size (resolution) is decreased, DEM decreases progressively (Usul & Pasaogullari, 2004; Yakar, Yilmaz, & Yurt, 2010; Zhou, Pilesjö, & Chen, 2011). In order to address these drawbacks of structured grids, unstructured grids were introduced (Mavriplis, 1997).

In the last few decades, many new unstructured grid geometries have emerged such as tetrahedral meshes, Voronoi grids etc. They are mainly used in areas like hydrogeology for reservoir modelling and mining in petroleum industries. These newly emanated grids are more convenient to solve physical equations of flow and transport in permeable media (Biver et al., 2017; Dusserre, Garbolino, Jaber, Guarnieri, & Karim, 2016a; Manchuk & Deutsch, 2009; Manchuk, Leuangthong, & Deutsch, 2005). Adaptive resolutions are enabled in building the models of unstructured grids, i.e., less important regions are coarser and for important and interested regions, it is finer. For instance, a petroleum reservoir can be modelled with fine blocks in the vicinity of the wells in order to solve the flow equations with better accuracy, whereas the aquifer can be modelled with lower resolution in order to reduce the computation time(Zhou et al., 2011).

The advantages of unstructured grids are that it solves complex structures in a short period of time. They are automated compared to regular grids and require less effort and will generate full mesh under most situations. Basically, the unstructured grids were introduced as a practical alternative to regular grids for discretizing complex geometries. This increases the flexibility in the mesh and enabling the technique to add, delete, move mesh points and to enhance solution accuracy (Balan & Schlumberger, 1997). Most grids are used to discretize a reservoir as it is easy to do numerical flow computation over grids. But designing a grid structure to depict a reservoir structure is a demanding task as it is computationally complex to show the heterogeneous behaviour of the reservoir. The unstructured grid helps to solve this complexity as the generation of this grid can be constrained depending upon the flow simulator requirements(Manchuk, 2010).

There are various algorithm and simulation techniques on unstructured grid generation. Manchuk et al. (2005) have implemented Direct Statistical Simulation technique to generate unstructured grids. Zaytsev et al (2016b) use a discrete Gaussian model algorithm for the un-conditioning simulation to eliminate the artefacts imposed by the mesh, providing a full-size model of unstructured grids. Dusserre, Garbolino, Jaber, Guarnieri, & Karim (2016b) have proposed truncated Gaussian modelling as a solution to the problem of geostatistical simulation on unstructured grids with support change effect. Even though unstructured grids existed earlier in grid generation, they are new generation grids in the domain of hydrology and petroleum industries. Thus, there are many theoretically proved simulation technique on unstructured grids and less practically applied research on these domains.
This research will aim to address the issue of support size effect by using direct simulation technique on unstructured grids and also show the surface flow simulation on these grids and compare it with the normal structured grids.

1.2. Research identification

Generally, most of the change of support is addressed in the area of ore and petroleum reservoirs as volume support data is an important parameter in geomodelling. In the application of hydrology, unless the estimation of flow is in sub-surface, there is no research which accounts of the change of support in surface flow. Moreover, the unstructured grid has been used for complex geometry to show geological features. As per literature in hydrology, the unstructured grid is generated as different stratigraphic layers for sub-surface estimation. In this research considering the application on surface flow estimation, the unstructured grid and change of support will be studied. As Digital Elevation Model play as an important parameter in hydrological modelling, the sample point support data will be taken as elevation value, which will be further used in the study for simulation.
Thus the main objective of this research will be to explore and implement the simulation on unstructured grids and to find the effects of support size in hydrology by addressing the change of support on the unstructured grid.
The foremost issues addressed in the current research project can be defined through the following research objectives and research questions.

1.2.1. Main Objective

1. Literature review for identification of suitable simulation technique and grid structures
2. To implement the geostatistical dynamic simulation on the unstructured grid in hydrology

1.2.2. Sub Objective

1. To identify the best suited unstructured grid for hydrological modelling from existing structures and to generate a grid for the study area.
2. To simulate the unstructured grid dynamically to show the variation of grid structure by addressing the issue of support size effect.

3. To undertake surface flow simulation on unstructured grids and compare it with structured grid flow simulation.
4. To access the performance of the model

1.3. Research question

In order to achieve the research objectives, many research question aroused during the study like-

1. What are the different types of unstructured grid structures available in the previous study and which can be used for hydrological modelling?
2. How is the issue of support size effect relevant in relation to unstructured grids and hydrological modelling?
3. How does the structure of grid vary over a typical terrain?
4. How to address this support size effect?
5. How to validate the results?

1.4. Innovation

Till now the unstructured grid simulation and the support size effect issue is being addressed in the areas of mining and petroleum industries, due to their complexity in estimation because of multivariable inputs and in hydrology, the support size is addressed over sub-surface estimations. It is being studied previously that due to the complexity of the data, and to represent different stratigraphy layers, it was easier in representing the data in the unstructured grid as it reduces the complexity. This research focuses on the application of hydrology and will address the support size effect in the unstructured grid using the proposed methodology. Furthermore, as an application, this study aims to understanding the effect of surface flow simulation on the unstructured grid due to support size effect. Additionally, the base input parameter for calculating any hydrological model is the Digital Elevation Model (DEM) data. Like for example, it helps in finding the flow accumulation, flow direction, catchment area of the reservoir and all these models were simulated in structured grids. In this study, elevation data is used as a proposed variable to do surface flow simulation directly on the unstructured grids.

1.5. Research flow

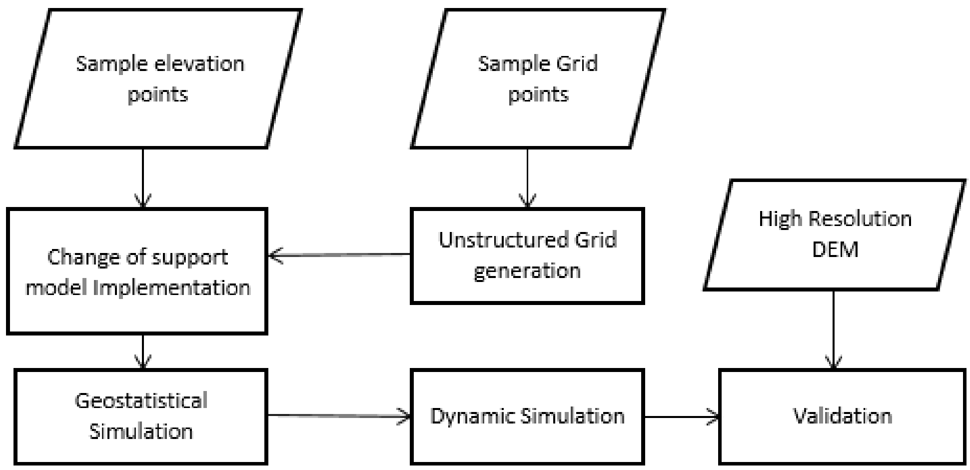

Figure 1-1 Generic workflow of the research

The generic workflow is generated (Figure 1-1) based on the objectives. In the objective, one part is about geostatistical simulation on the unstructured grid by addressing the issue of support size effect. In order to address this in research two methods are used, which is explained further in chapter 2 and 5. The second part of the objective is based on dynamic simulation in Hydrological domain. For this flow simulation is been executed on the output of the geostatistical simulation, which in detail is mentioned in chapter 5. Overall in order to attain the objective 1 and 2 the above generic workflow is designed.

1.6. Thesis outline

This thesis consists of 8 chapters. Chapter 1 introduces the motivation and problem statement. It also explains the main objective of the research. Chapter 2 provides the theoretical background and the literature studies behind this research objective mentioned in chapter 1. Chapter 3 is about the theoretical algorithm which is used for implementation in this research. Chapter 4 is a description of the study area and dataset used for this research. Chapter 5 states the methodology which is used to attain the research objective. Chapter 6 will explain the results and analysis of the work which includes answers to the research questions as well. Chapter 7 is a discussion about the analysis obtained in the study Chapter 8 concludes the research by stating further recommendation to improve the research.

2. LITERATURE REVIEW

This chapter summarises the theoretical background on the use of geostatistical simulation and its application on grids. It starts with a discussion on Geostatistical simulation, different types of geostatistical simulation and the impact of these simulations on grids. The next section is about structured and unstructured grid structure and how they are different from each other. Further section focuses on the support size effect issues and methods to address them. The final section is about the dynamic simulation on the unstructured grids.

2.1. Overview of geostatistics

Geostatistics aims at providing quantitative descriptions of natural variables distributed in space or in time and space. Examples of such variables are rainfall over a catchment area, porosity and permeability in a porous medium, soil properties in a region (Delfiner, 2012). These variables exhibit a huge complex of details that exclude description from simpler models. They provide methods to quantify spatial randomness. In order to quantify the spatial randomness, a model specifying spatial uncertainty is required and this is where statistics comes into the role. Its probability distribution is one of the best ways to define a range of possible values of interest and geo highlights the spatial aspect of the problem (Gómez, Rodrigo, Rodrigo, & Vargas, 2017). In hydrology some hydrological properties like rainfall, porosity, permeability, hydraulic conductivity etc. are all function of space (and time) and exhibit high spatial variability, which is also known as heterogeneity. Generally, these properties show a so-called "support size effect", i.e. it is the difference between the measured value and inferred value during modelling (also known as a change of support problem) (Emery, 2007).

Simulation is a process of replicating reality using a model. In Geostatistics, simulation is the realization of a random function (surface) having the same statistical features as the sample data, which is used to generate it. The random functions rely on statistical models to model uncertainty associated with spatial simulation or estimation. Normally geostatistical techniques include estimation and simulation. Estimation includes different interpolation techniques but the output of these shows smoothing effect and those techniques provide only one value for every location in the study area which may not provide all information for decision making. Simulation gives continuous results, they generate many interpolated surfaces which is a replication of spatial characteristics found in the given data (Chilès & Delfiner, 2014). Thus Geostatistical simulation is a well-accepted simulation in fields like petroleum industries as a method of characterizing heterogeneous reservoirs in a continuous surface (Bertoncello, Caers, Biver, Caumon, & France, 2009).

2.2. Geostatistical simulation

Geostatistical simulation addresses a wide range of problems related to natural and environmental aspects. The common application consists of generating realistic observation of a spatial or spatial-temporal phenomenon. Apart from capturing the heterogeneity in the data, geostatistical simulation also performs other important functions like honouring and integrating multiple data types, quantifying and assessing the uncertainty in the data (Webster & Oliver, 2002). Geostatistical simulation specifically follows for continuous data and it is assumed that the data or the transform of the data follow a certain distribution, an example in case of Gaussian geostatistical simulation, it is assumed that the data follows Gaussian distribution. As mentioned previously, this geostatistical simulation is the realization of a random function. Random function is defined by a set of random variables and is represented by the equation given below.

$$\{Z(x), x\epsilon\Omega\} \qquad 2.2.1$$

Where, $Z(x)$ is a random function having a random variable at a location x and Ω is fixed spatial region whose spatial index x varies at different location in that region Ω. If values of $n\ th$ number of locations (x) has to be estimated then the realization of these *n* number of variables in random function $Z(x)$ are referred to as the regionalized variable $z(x)$. n Number of realization gives simulated output (figure.2.1). Mathematically, they are represented by as a function $F(x)$, which locates the value of each variable at n location (equation 2.2.2).

$$\{z(x_i): i\ = 1\ to\ n\ ,\ x_i\ \epsilon\ \Omega\} \qquad 2.2.2$$

Where $z(x)$ is regionalised variable

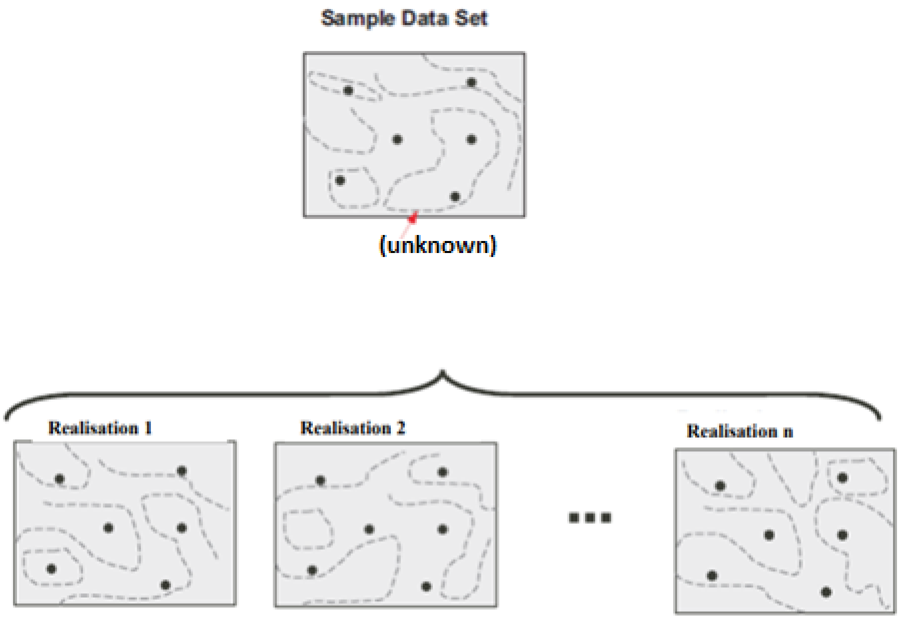

Figure 2-1 General Geostatistical workflow (Desbarats, 1996)

2.2.1. Non-conditional simulation

A non-conditional simulation of the random function $\{Z(x): x\ \epsilon\ R_n\}$ is the realization of a random function (RF) $S(x)$, which is randomly selected from the set of all possible observations $\{x_a\ :\ \alpha = 1\ ...\ N\}$, chosen in a class of RF with same second order moments as $Z(x)$ like covariance, variogram. The methods for generating non-conditional simulation generally produce realization of strictly stationary RFs with zero mean.

2.2.2. Conditional simulation

Sometimes the random function $S(x)$ mentioned in the sub-section 2.1.1 will have infinite number of realization. In such cases it is assumed that the samples collected at points have same values as in regions where it is observed and thus it can be considered to represent the regionalized variable $z(x)$ from the subset of realization. They are quantitatively useful to obtain realistic depiction of spatial variability.

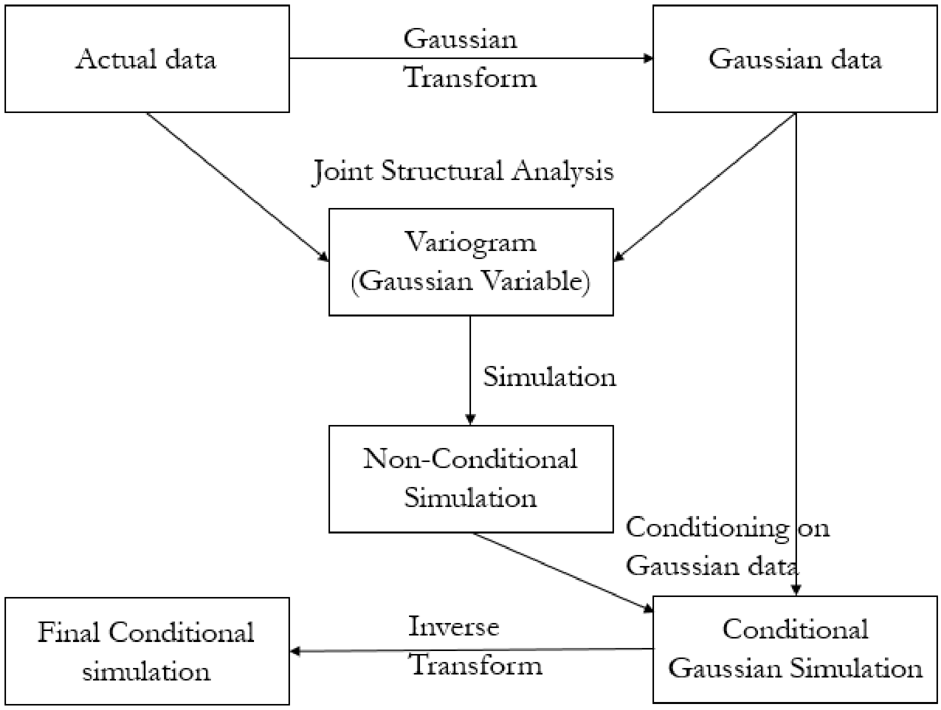

Figure 2-2 Flowchart of various stages of conditional simulation (Delfiner, 2012)

Below are the steps, adapted from Delfiner (2012), for generation of a conditional simulation (Figure 2.2):
1. Transformation of the $Z\ (x_a)$ data into $Y\ (x_a)$ by the inverse transformation $Y\ (x_a)\ = \phi^{-1}\ (Z\ (x_a))$.
2. Structural analysis of the $Y\ (x_a)$ data, or, better, joint structural analysis of the $Y\ (x_a)$ and $Z\ (x_a)$ data, to obtain the variogram of $Y(x)$.
3. Non-conditional simulation of $Y(x)$, leading to $S_y(x)$, using a Gaussian simulation method.
4. Conditioning of $S_y(x)$, on the Gaussian data $Y\ (x_a)$, leading to $T_y(x)$.
5. Application of the transformation (back Transformation) $T_z(x)\ = \phi\ (T_y(x))$.

Mostly in these simulation techniques $z(x)$ is to be estimated at places where it has not been measured. Generally, these places are the nodes of the grids laid out on the studied domain and usually these grids are regular in structure. Once these grids are set they are used as the representation to reality irrespective to the original data. They are obtained by algebraic or Boolean operations, contour maps, volumetric calculation etc. The estimated quantity is not necessarily the value at a point but it is in many cases the grid node is also to represent the grid cell and surrounding it.

2.3. Basics of variography

Variogram or semi-variogram, statistical inference or structural analysis of random function $Z(x)$, is a graph showing the relationship between the variance of regionalised variables to the separation distance between those variables. Depending on isotropic and anisotropic of data, graph can also be calculated for direction.
The stationarity of random function (equation 2.2.1) is defined from the equation given below

$$E\big(Z(x+h) - Z(x)\big) = 0 \qquad \forall x, x+h \in \Omega \qquad 2.5.1$$

and variance is defined below

$$Var(E(Z(x+h)-Z(x)) = 2\gamma(\mathrm{h}) \qquad \forall x, x+h \in \Omega \qquad 2.5.2$$

2.3.1. Estimation of semi-variogram

The most common method for estimating a semi-variogram (Morgan, 2005) is defined below:
For n measurements of spatial attributes, semi-variogram is calculated as

$$\hat{\gamma}(h) = \frac{1}{2|N(h)|} \sum_{N(h)} (z(x_i) - z(x_j))^2 \qquad 2.5.3$$

where, $N(h) = \{(x_i, x_j): x_i - x_j = h; i, j = 1,2, \dots, n\}$ is set of pair samples located at a vector distance *h*.

2.4. Support size effect

As mentioned in section 2.2, geostatistics is realization of random function. But it is not necessary that this random function of a variable x should be defined from a point location. It can also be defined over a large area or volumes which are usually square or rectangular in shape and the cell centres are at the location x inside Ω. This 'spatial region' which is represented by $Z(x)$ is referred as the support of the random variable. If that spatial region is referred by a point then they are referred as point support and if they are represented over a large area or volume then they are referred as block support (Usul & Pasaogullari, 2004) . The support of random variable has some properties like shapes and orientation of area with the measurement. The spatial support in terms of spatial prediction has two spatial discretization levels: size of the block for the sampled location, and grid resolution (Hengl, 2009).

Mostly during these geostatistical calculations the available data mentioned in equation 2.2.2 are defined for a particular support size, while the calculation (variography or estimation) is carried out over different support size. This support size effect was earlier found in the areas of mining and petroleum industries. For example, in gold mining industry, initial data is generally a point support size, while the estimated support size was on actual panel sizes, which are smallest blocks which can be extracted from ground (Morgan, 2012) .

2.4.1. Regularization

Theoretically, the spatial attribute value of a block *v* is the mean value of all the points that are contained in v. Let a block having area or volume be v and spatial attribute of a point support be (equation 2.6.1)

$$z_v(x) = \frac{1}{v} \int_{v(x)} z(y)dy \qquad 2.6.1$$

Where $z_v(x)$the spatial attribute value is defined for a block $v(x)$ and $z(y)$ is all the points inside $v(x)$. Here $z_v(x)$ is the mean value which is said to be the regularization of $z(y)$ over $v(x)$. Generally, geostatistical calculation like for example calculating a semi-variogram of a different support size to that of given data is calculated using two ways (Morgan, 2012) :

- Data regularization
- Semi-variogram regularization

2.4.1.1. Data regularization

As mentioned previously, regularization basically is an averaging method where all the available data required for the new support size are averaged. Once the averaging is done, a new spatial dataset is generated and the semi-variogram is calculated as usual for the new support size with the generated spatial data.

For example a point support random function $Z(y)$ is considered with expectation m and semi-variogram $\gamma(h)$ then, according to Journel and Huijbregts (1978) the data regularization of $Z(y)$ over block volume $v(x)$ (equation 2.6.2)

$$Z_v(x) = \frac{1}{v} \int\limits_{v(x)} Z(y)dy \qquad 2.6.2$$

is then also a second-order random function with expectation (equation 2.6.3)

$$\begin{aligned} E\{Z_v(x)\} &= \frac{1}{v}\int_{v(x)} E\{Z(y)\}dy \\ &= \frac{1}{v}\int_{v(x)} m.dy \\ &= m \end{aligned} \qquad 2.6.3$$

and variogram

$$2\gamma_v(h) = E\{[Z_v(x+h) - Z_v(x)]^2\} \qquad 2.6.4$$

2.4.1.2. Semi-variogram regularization

In semi-variogram regularization, the semi-variogram of desired support size is directly calculated from the available data of different support size (i.e. without regularizing the original data). Thus, in this method the semi-variogram for support v is directly calculated from point support data. Morgan (2005) shows that the semi-variogram from equation 2.6.4 can then be written as

$$\gamma_v(h) = \bar{\gamma}(v, v_h) - \bar{\gamma}(v, v) \qquad 2.6.5$$

Where, as adapted from Journel and Huijbregts (1978), v_h denotes support v separated by vector distance h, $\bar{\gamma}(v, v_h)$ represents the mean value of point support semi-variogram $\gamma(h)$ for vector distance h and $\bar{\gamma}(v, v)$ represents the mean value of point support semi-variogram of domain v. Mathematically,

$$\bar{\gamma}(v, v_h) = \frac{1}{v^2}\int\limits_{v} du \int\limits_{v_h} \gamma(u-u')du' \qquad 2.6.6$$

And

$$\bar{\gamma}(v, v) = \frac{1}{v^2}\int\limits_{v} du \int\limits_{v} \gamma(u-u')du' \qquad 2.6.7$$

In most Geostatistics, the mean point semi-variogram is generally denoted as:

$$\bar{\gamma}(V, v) = \frac{1}{vV}\int\limits_{V(x)} du \int\limits_{v(y)} \gamma(u-u')du' \qquad 2.6.8$$

However, mean point semi variogram ($\bar{\gamma}(v, v_h)$ and $\bar{\gamma}(v, v)$) mentioned in equation 2.6.6 and 2.6.7 can be considered by simply replacing V and v in Equation 2.6.8 with the actual two desired support sizes.

Basically the support size and the semi-variogram are related to each other. That is, when the support of a spatial data increases the sill value of the semi-variogram decreases which means spatial variability decreases. As mentioned earlier, regularization involves averaging of data over a particular support size. When data is averaged over larger and larger support size some of the data's inherent variability will be reduced which technically reduces the sill value.

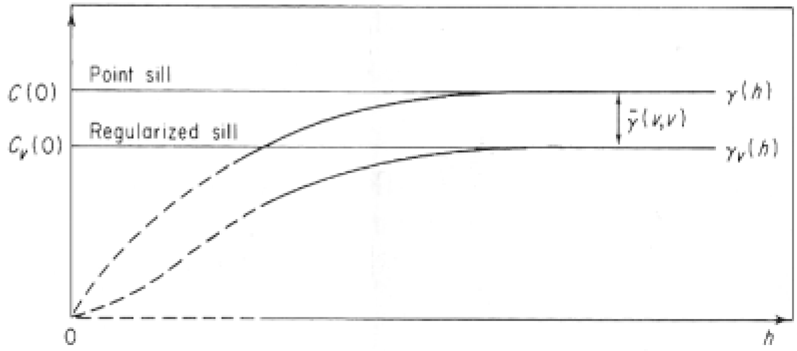

Figure 2-3 Variogram plotted for point and regularized support size. Taken from Journel and Huijbregts, (1978)

2.4.2. Effects of support size effect on semi-variogram

Theoretically analysing from figure 2.3, It can be said that as the support size of the data increases

- The sill of the semi-variogram decreases
- The nugget effect decreases
- The range of the semi-variogram increases

The decrease in sill of the semi-variogram is being already mentioned in the section 2.6.1.1.
In regularized semi-variogram, the range parameter for block support v is equal to the range parameter of the point support plus the scalar diameter of the blocks of support v (show in figure 2.4). This can be explained by the fact that the range of the semi-variogram is defined as the location (distance) at which any two points become spatially uncorrelated (Delfiner, 1999). As previously mentioned and given in equation 2.6.2, the block support size is the average of all the points which lie inside the block, so if the distance between any points within one block to the any points in different block is larger than the range of the point support semi-variogram then that is the block support semi variogram range. Rendu (1981) also mentions in his book that the smallest distance at which two blocks are uncorrelated is equal to the point semi-variogram range plus the distance between the block centres v.

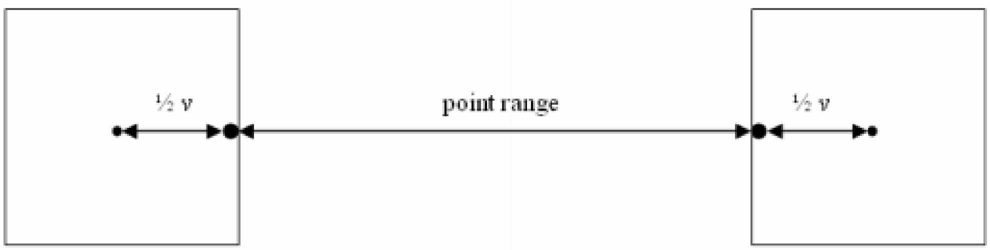

Figure 2-4 Two blocks separated at distance of point range (taken from (Morgan, 2012))

Generally nugget effect is the variability of the regionalised variables $z(x)$ at a small distance. As mentioned in previous section that regularization due to averaging of data reduces the inherent small scale variability which in turn reduces the nugget effect in semi-variogram. This also makes sense that the when semi-variogram for block support is calculated the nugget effect is decreased. Figure 2.5 shows the graphical explanation to the effect of support size on semi-variogram.

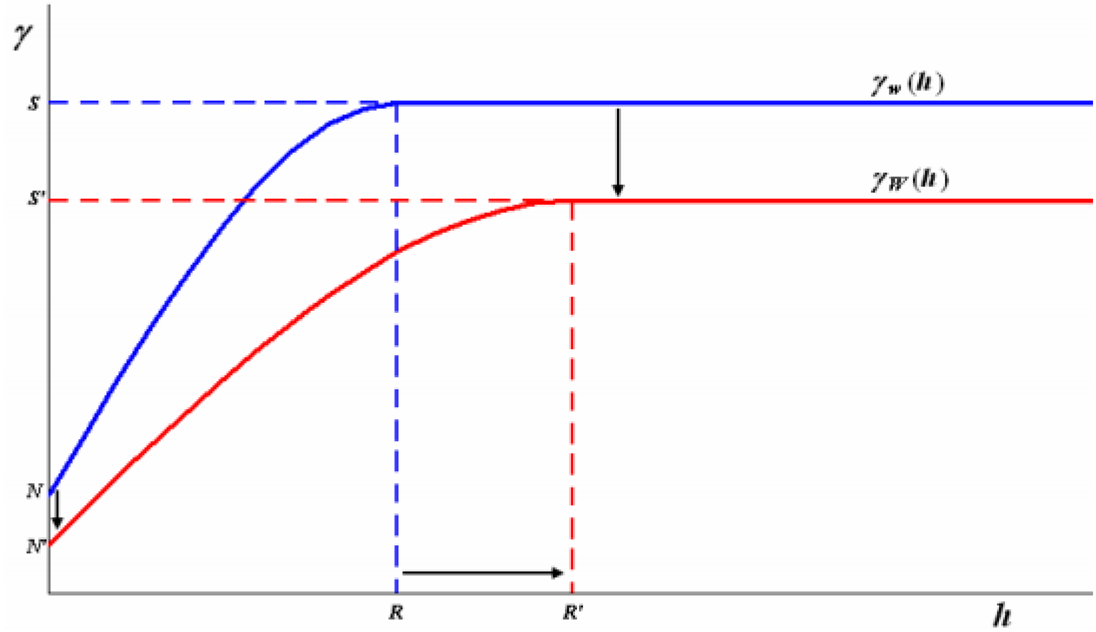

Figure 2-5 Semi-variogram for different support sizes, w and W, where w<W (Craig John Morgan, 2012)

The figure 2.5 is taken from the PhD thesis by Morgan (2012), where the illustration explains the relationship between the regionalised variable and the regularised variable. Here, $\gamma_w(h)$ is the semi-variogram of support w, having Nugget N, sill S and range R while $\gamma_W(h)$ is the semi-variogram of support W having range R, sill S and Nugget N. We can see in the above figure that greater the support size effect lesser the sill and nugget and larger the range.

2.4.3. Calculating the values of $\bar{\gamma}(v, v_h)$ and $\bar{\gamma}(v, v)$

There are many methods to calculate the value of $\bar{\gamma}(v, v_h)$ and $\bar{\gamma}(v, v)$. One straight forward method is to solve the integral in the equation 2.6.6 and 2.6.7, but it is a tedious approach. An alternative method mentioned in the thesis by Morgan (2005) is the use of auxiliary functions. These functions are pre-calculated values of $\bar{\gamma}(V, v)$, in form of tables, corresponding to different geometries of V and v. Another method explained by Morgan (2012) is discretization. In discretization $\bar{\gamma}(V, v)$ is being approximated by taking equal number of finite points in the domain of V and v.The finite number of points can be a regular grid of points. For example, considering a regular grid of points,

$$x_i, i = 1,2, \dots n$$

And

$$x_j, j = 1,2, \dots m$$

placed in the domain of V and v respectively, then $\bar{\gamma}(V, v)$ is approximated as the double sum as shown in equation 2.6.9

$$\bar{\gamma}(V, v) \approx \frac{1}{n.m} \sum_{i=1}^{n} \sum_{j=1}^{n} \gamma(x_i - x_j) \qquad 2.6.9$$

Additionally, Clark & Harper (2000) have mentioned that in above case, it should be made sure that each grid has equal number of points which occur within the given domain.

2.5. Grids

From the previous sections it is known that the main goal of geostatistics is to sample and analyse the random function $Z(x)$, conditionally or unconditionally to the available data. It was also seen that in addition to the available data another parameter that influence the characteristics of the random variable is the support size of the random variable. That is, consider in petroleum, usually the data collected on the ground will be in point support while in analysis, the work unit is taken as block with specific size and shape. And this change of support is usually not considered due to CPU limitation (Bertoncello et al., 2009; J. Manchuk et al., 2005). In Previous researches some methods had been introduced to address this change of support issue but mostly they are computationally intensive and give approximate results.

Mostly in reservoir modelling in order to represent the reservoir geometry accurately grid blocks are used. These grid blocks are discretized by the volume of the reservoir, which in turn used as support to integrate data and to perform modelling. Technically, grid/gridding is process of converting a given region or domain into a set of control volumes or blocks ("Grid Systems," 2015). This support, which are represented in terms of grids and can be classified into two types: Structured and unstructured grids.
The general process for grid generation includes the following steps:

1. Decompose the problem domain or spatial domain into a set of sub domain (boundary definition).
2. In each block, generate the requisite grid (definition of element size distribution function). A typical sequence of operation would be
    a. Generate edge grid in 1-dimension
    b. Using the edge grids, generate the grid on block-surface.
    c. Use surface grids to generate volume mesh (Mesh generation).
3. Check the quality of mesh and modify the mesh (optimization).

2.5.1. Structured grids

A structured grid are grids having equal size and shape, that is they are means whose volume elements or blocks are well ordered and i,j,k coordinate format can be used to identify the neighbour blocks easily. The simplest grid is generated from rectangular box by subdividing the box to n- blocks (rectangular elements). The elements are ordered by x, y and z direction, i.e. they are commonly defined over Cartesian coordinates, and they lack the ability to represent complex reservoir geometries such as boundaries and faults.

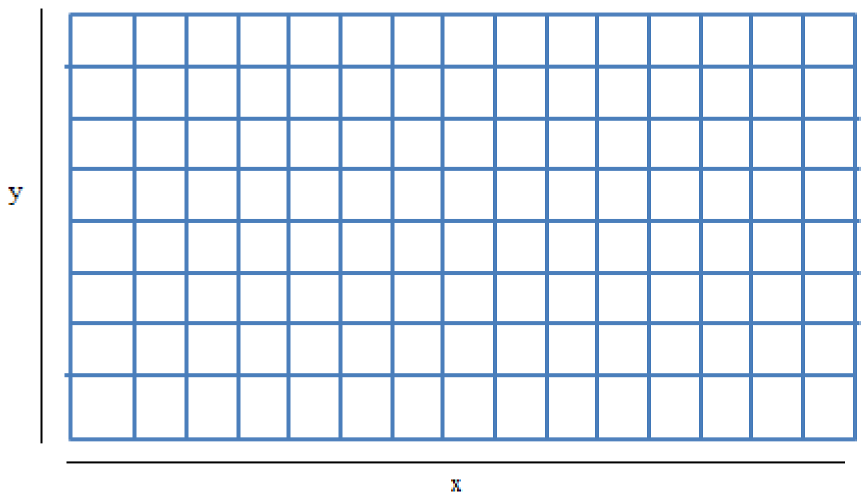

Figure 2-6 illustration of structured grid

These structured grids are highly space efficient as the relationship of the neighbourhood blocks are defined by storage arrangement. They have higher resolution and better convergence. However they do have disadvantages like they cannot easily handle abrupt changes in the data, the size of grid mesh affects the computational efficiency (Dusserre et al., 2016b). In terms of hydrological application, the computed flow path in structured grid tend to move in zig-zag direction which is somewhat unrealistic (Hodges, 2014). For this reason structured grids must be adjusted to roughest terrain creating redundancy but they are not adaptive to spatial phenomenon whereas introducing of unstructured grids gave more flexible and efficient results in such circumstances(Dehotin & Braud, 2008) . The basic steps for generating mesh is as same technique as explained in previous section i.e.

1. Boundary definition
2. Nodalization (grid discretization)
3. Mesh generation
4. optimization

2.5.2. Unstructured grids

Unstructured grids are also known as irregular grids. It is a tessellation by simple shapes which are mostly used for finite element analysis for computational fluid. As structured grids lack the ability to model complex geometries unstructured grids were introduced which has ability to model complex geometries as well as provide improved accuracy. They are adaptive grids defining high cell density in important areas and low cell density in less important areas of reservoir geometry (Yakar et al., 2010). This means that the grid volume may be of many different sizes. So it is difficult to find the neighbourhood blocks easily like the structured grids. There is no relation to co-ordinate direction. There are many types of unstructured grid like triangular grids and Voronoi grids. Most of the unstructured grids are usually triangular grids in 2-dimension or tetrahedral grids in 3-dimension. Figure 2.7 shows an illustration of an unstructured grid generated using Voronoi polygons. The basic concept is that, the unstructured grid is mainly focused to fill the complex geometry that are created by random elements. Therefore, the problem of unstructured mesh generation is designing algorithm that are automatic, robust and yield element and shapes that are convenient to the flow solver (Conroy, Kubatko, & West, 2012; Mavriplis, 1997). Thus, due to its adaptive nature, accuracy of modelling geographical features is increased, which made unstructured grid as the building block for reservoir modelling.

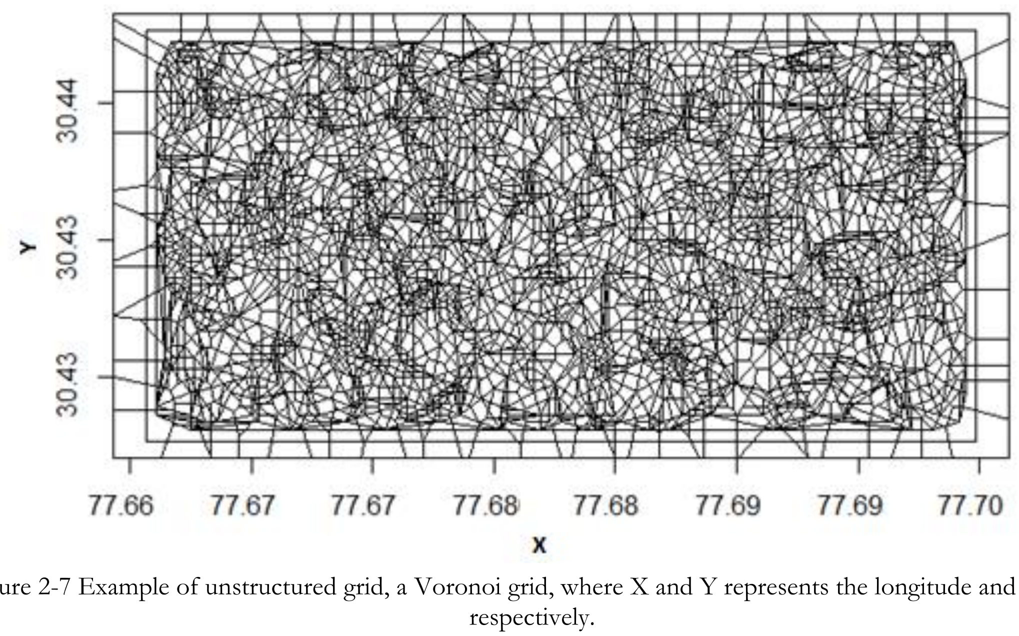

Figure 2-7 Example of unstructured grid, a Voronoi grid, where X and Y represents the longitude and latitude respectively.

2.5.2.1. Unstructured grid generation techniques

There are many methods to generate unstructured grids. It involves systematic sub-division of the problem domain into cells of desired size and shape (example: triangle in 2-D and tetrahedron in 3-D). Some most common methods are advancing front method, Delaunay –Voronoi generation, and Quad-tree (2-D)/Octree (3-D) methods. As mentioned earlier Delaunay generation is purely based on the computational geometrical principle that is these methods systematically decompose the problem geometry in a set of packed convex polygons based on Delaunay tessellation or Voronoi polygons. While in Advancing front method boundary grid generation technique is used for grid generation, in Quad tree method Cartesian decomposition technique is used to generate grid.

- **Advancing front method**

In this technique grid generation begins with boundary discretization of geometry boundary into set of edges and then using the generated individual elements the mesh is created by adding those elements at a time with front generated elements. The elements are added in such a way that the edges from initial front are advanced out into the field, and the process continues till it completes all the edges.

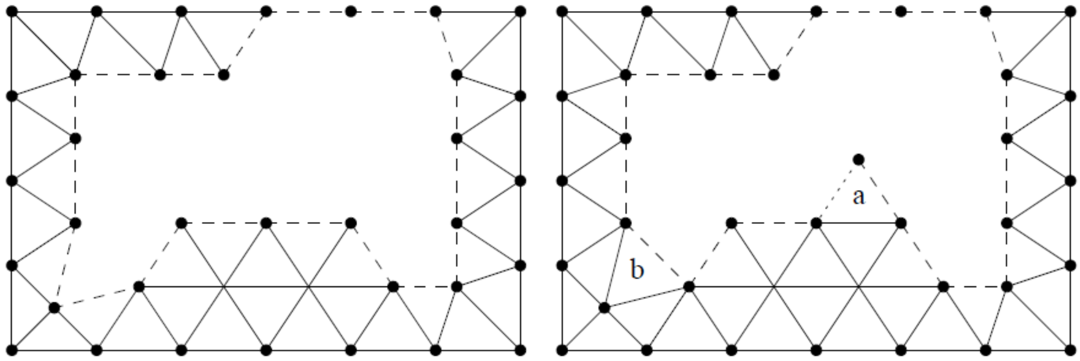

Figure 2-8 grid generated using advancing front method where the triangle is generated using either point a or using existing front point b (Mavriplis, 1997).

- **Delaunay-Triangulation method**

In this method the grid is generated using the circumcircle property of the Bowyer-Watson algorithm. Consider a set of points given in a plane then there exist many possible ways to do triangulation using the given set of points. To minimise all the possibilities the Delaunay-triangulation follows the algorithm of Bowyer-Watson. The property states that "no triangle in a Delaunay-triangulation can contain a point other than its three forming vertices within its circumcircle" (Bowyer, 1981; Watson, 1981).

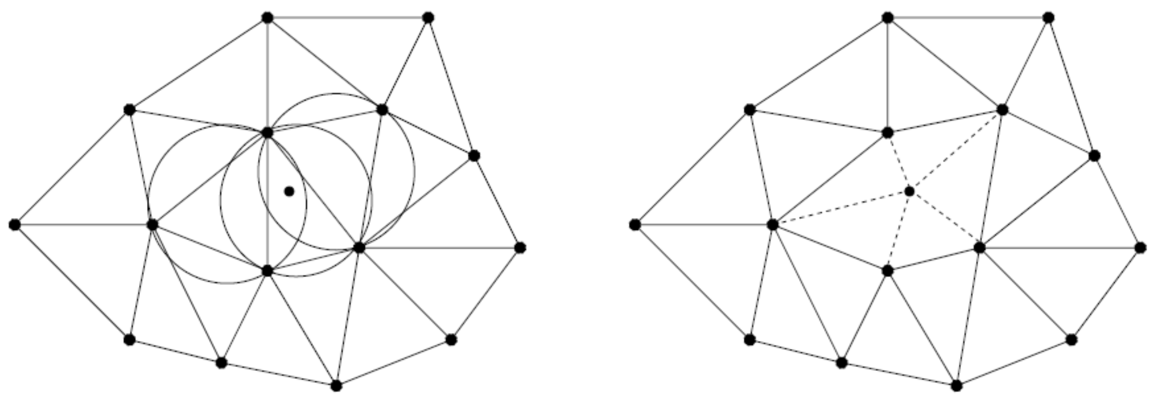

Figure 2-9 illustration of Delaunay triangle generation (Mavriplis, 1997)

2.6. Summary of related works on unstructured grids

From section 2.4, it is taken into account that the support of the data should be properly considered so as to avoid over estimation of ore grades and effectively optimize mining. Thus it can be stated that support of the data is an important factor in reservoir or geological modelling. Recently geostatistical simulations Algorithm, which are done on unstructured grids, often have to address this change of support problem due to geological properties. Studies have generalized the above mentioned problem by integrating point support data to simulation on irregular supports. Zaytsev et al. (2016a) gives critical review on the existing methods on unstructured grid simulation algorithm, including fine scale simulation with upscaling, direct sequential simulation algorithm and simulation using Discrete Gaussian Model, which address the above mentioned problem.

Many studies have been carried out and several methods exist for simulation of unstructured grids. It is to be noted that classical geostatistical simulation methods cannot be applied on unstructured grids due to uneven support sizes. Manchuk, Leuangthong, & Deutsch (2005) have implemented Direct Statistical Simulation twice. First, without correcting the kriging variance and second, by correcting the kriging variance. Zaytsev, Biver, Wackernagel, & Allard (2016b) uses discrete Gaussian model which eliminates the artefacts imposed by the mesh, providing a full size model. Dusserre, Garbolino, Jaber, Guarnieri, & Karim (2016b) has proposed truncated Gaussian modelling as a solution to the problem of geostatistical simulation on unstructured grids with support change effect. Zhou, Pilesjö, & Chen (2011) have estimated the surface flow paths on digital elevation model using triangular facet network (TFN). Manchuk (2010) has done his PhD work on geostatistical simulation on unstructured grid for flow simulation where he had used dual approach method on different stratigraphic layers. One main disadvantage was that in his workflow geological modelling was done twice. Hurtado (2004) has worked on numerical modelling for simulating petroleum reservoir using element based finite volume method. Chiles (2014) has investigated a special case of lognormal random functions for finding the accuracy of change of support model. He has also explained the principle of the validation method used for discrete Gaussian model.

In this research we will implement geostatistical simulation by addressing the support size effect using one of the mentioned methods in the literature. The main focus of implementing the algorithm is to find the effect of support size in areas other than mining and petroleum industries. Thus this research focuses on doing geostatistical simulation on unstructured grid which further is applied on hydrological domain to compute flow simulation on the given data and find its effect due to different supports.

2.7. Flow simulation

Numerical modelling of surface or sub-surface flow and transport in geological formation such as in areas like mining, petroleum reservoirs is called flow simulation. Most numerical simulation is done on sub-surface flow for mining and petroleum reservoir modelling. In those reservoirs, accumulation of hydrocarbon is analysed based on the geological properties which are highly heterogeneous in nature (Moog, 2013). In hydrology also there are some problem caused due to heterogeneity like runoff and material transport on surface and sub-surface due to complex surface and heterogeneous material. Unlike other models, in hydrology modelling requires very different parameters, like water network structures, cell size for precipitation, topographic relief, land-use, soil and other characteristics (Dehotin & Braud, 2008; Marsh, Spiteri, Pomeroy, & Wheater, 2018; Vieux, 2016). One of the main primary parameter for hydrological modelling is the altitude value, which can be derived from Digital Elevation Model (DEM) (Braun et al., 1997). Thus secondary parameters like slope, flow directions, flow routes can be related as they are derived from DEM.

DEM is a numerical representation of topographical structure which is usually represented in terms of equal sized grid made up with elevation values. The widespread availability of DEM sources has enhanced their utilization in many natural and environmental applications. Applications like visibility analysis, erosion modelling, surface hydrology, watershed modelling, are some examples. Thus, error caused while constructing DEM, will adversely affect the topographical/terrain representation, which in turn will affect the usefulness for certain application (Bergamaschi, 2005; Jamal, 2018; Usul & Pasaogullari, 2004; Yakar et al., 2010).For example simulation of geophysical data for mass flow use certain set of elevation values for mapping areas which are said as low or high risk regions. However, due to slight change in elevation difference may lead to prediction as high risk regions.

Surface hydrology includes dynamics of surface flow of water networks like rivers, canals, streams, lakes, ponds etc. It also includes the relationship between rainfall and surface run-off (Wikipedia contributors, 2018).A typical hydrological model requires an understanding of interrelationship between stream flow data and the catchment area which generates such streamflow (Gold, 2012). It can be stated that, the key parameter for catchment topography is flow distribution as it shows how much water flow is distribution in that area. Slope of the terrain controls the surface flow path which in turn influences the sub-surface flow pattern and DEM has made it easy to estimate this surface flow distribution over a location. Zhou et al. (2011) mentions that there are numerous algorithm, such as single flow direction (SFD) and Multi-flow direction (MFD) that approximates surface flow and catchment area. SFD allows flow restricting to one single down-hill direction at a time while MFD considers more than one flow direction. Basically when it comes to simulate the flow in grid level depending upon the grid size and pattern the flow changes. Durlofsky, (2005) governs an upscaling techniques that is depending upon the flow, the grids are up scaled from finer to coarser resolution. The upscaling technique is classified into two, single or two phase flow parameter upscaling.

1. **Single phase flow equation**

Darcy's law

$$u = -\frac{1}{\mu} k . \nabla p \tag{2.7.1}$$

Mass of conservation 2.7.2

$$\frac{\delta}{\delta t}(\emptyset \rho) + \nabla . (\rho u) + \bar{m} = 0$$

Pressure 2.7.3

$$\frac{\delta}{\delta t}(\emptyset \rho) - \nabla . \left(\frac{\rho}{\mu} k . \nabla p\right) + \bar{m} = 0$$

Where, u is the Darcy velocity, μ is the viscosity, k is the permeability, p is the pressure, $\emptyset$ is the porosity, ρ is the density and $\bar{m}$ is the sink.

2. **Multi-phase flow equation**

Darcy's law

$$u_j = -\frac{k_{rj}}{\mu_j} k . \nabla p_j \tag{2.7.4}$$

Mass of conservation 2.7.5

$$\frac{\delta}{\delta t}(\emptyset \rho_j S_j) + \nabla . (\rho_j u_j) + \overline{m_j} = 0$$

Where, subscript j refers to water and k_{rj} refers to relative permeability and S_j is the volume fraction.

Hagen, Huthoff, & Warmink (2014) use D-flow flexible mesh method for hydrodynamic model on unstructured grid. In this research, one of the numerical flow simulation techniques is used to simulate the surface flow on unstructured grid. This simulation will be performed to the output of the previous model, so as to understand the effect of the support size on flow simulation. Additionally the flow simulation is done on structured grid as well and is comparative analysis will be done with unstructured grid.

The above mentioned flows can be differed in two ways depending upon their aspect of flow (velocity, depth, pressure, etc.) with time. One way is steady flow analysis and other type is unsteady flow analysis. Steady flow and unsteady flow of a system helps in defining the flow of interest of that system. Steady flow can be uniform or non-uniform in nature. Uniform steady flow has a constant variable with respect to time and distance, while gradually varied steady flow has a varying value with respect to distance and constant with time.

2.7.1. Steady Flow analysis

In steady flow analysis the flow is known at all the points in the channel and the trivial case of solving the computational element here is to find the water surface elevation at each end points. In order to find the surface elevation, the surface flow channel is computed sequentially with given initial values. Generally, in steady flow analysis the direction of flow is upstream if it is subcritical case and the flow is supercritical if the direction is downstream (Franz, 2015). HEC-RAS is software designed to simulate such kind of flow hydraulic model analysis.

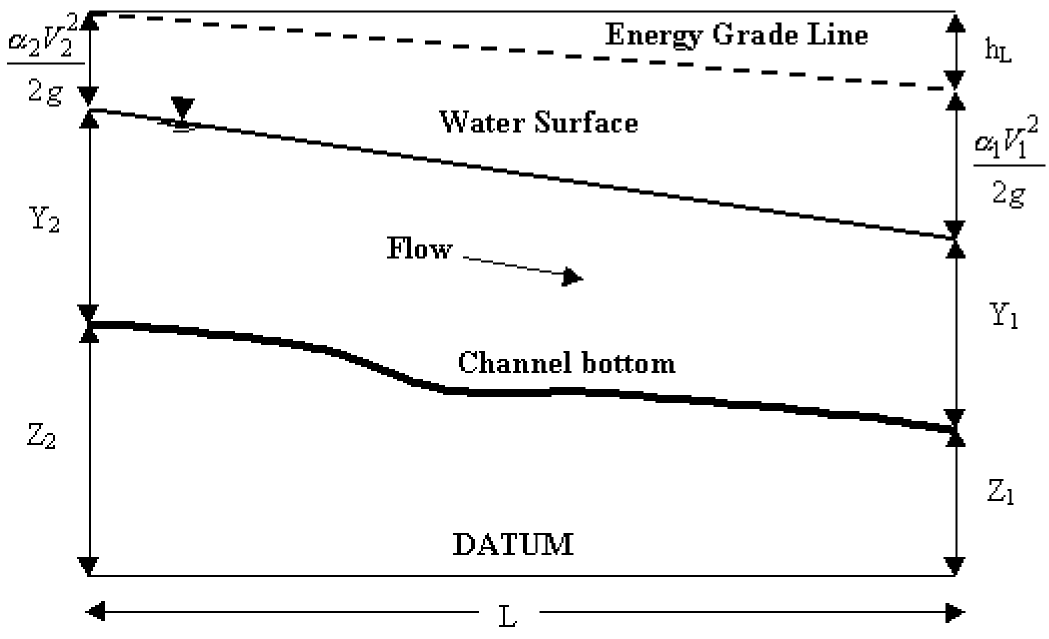

Figure 2-10 Steady flow profile, where the x axis represent the length of the river, while y axis represents the energy parameters as described in manning's equation (adapted from Tate, (1999))

2.7.1.1. HEC-RAS

HEC-RAS is a hydraulic flow model tool designed for determining the steady and unsteady channel flow analysis, and flood determination. As mentioned in earlier section, in steady flow analysis depth and velocity can change over distance but doesn't change over time, in HEC-RAS gradual variation of the channel flow is characterized by changes from cross-section to cross-section (U.S. Army Corps of

Engineers, 2019). This modelling system is planned in calculating the water surface profiles for steady flow (figure 2-10). The steady flow component in HEC-RAS has the capability to model subcritical, critical and mixed flow water surface profiles. Initially, HEC-RAS uses direct step method to calculate the water surface profile by assuming the flow to be steady. The computation for this is based on one-dimensional energy equation (equation 2.7.6) where the energy loss are calculated by manning's equation (for friction).

$$H = Z + Y + \frac{\alpha V^2}{2g} \qquad 2.7.6$$

Where, H is the energy at given location, $Z + Y$ is the potential energy and $\frac{\alpha V^2}{2g}$ is the kinetic energy and the change in energy between two cross-section is head loss (h_L). Flow depends on the flow regime as to know whether the calculation is upstream to downstream or vice versa (Tate, 1999). This flow regime is described using the dimensionless Froude number, where:

- F_r<1, subcritical flow
- F_r>1,supercritical flow
- F_r=1,critical flow

Many researches has been done using HEC_RAS tool. Yang, Townsend, & Daneshfar (2006) have used HEC-RAS to develop a model for floodplain delineation. In their research the first objective was to construct and validate a HEC-RAS river network using a generated model. Ahmad, Bhat, & Ahmad (2016) have done research on one dimensional steady flow analysis using HEC-RAS. Zainalfikry & Ghani, (2018) did their research on HEC-RAS for one dimension flood modelling in certain area. They did water level, stream discharge and river cross-section analysis. In this research different DEM obtained from the geostatistical simulation is used as elevation feature, and steady flow analysis is applied to each DEM with fixed geometric data. The resultant data is compared to find the DEM gives relative results with less uncertainty.

3. CHANGE OF SUPPORT MODELS

Geostatistical simulation, effect of support size in geostatistical simulation, different types of grid structures was explained in previous chapter. It was found that unstructured grids constitute an important role in reservoir modelling and geostatistical simulation on reservoir properties needs to take support of the data into consideration. Thus in order to do simulation on unstructured grid the change of support has to be addressed. Many methods exists which address this support size effect issue. Some method includes fine-scale simulation followed by upscaling (Manchuk, 2010), direct block simulation (Manchuk et al., 2005) and simulation using discrete Gaussian model (Delfiner, 1999, 2012). This chapter explains the theoretical concept behind the models used in this thesis.

3.1. Fine-scale simulation approach

This method is one of the classical approach followed for simulating on an unstructured grids. In this technique point support simulation is performed on auxiliary regular fine-scale grid and later the results are up-scaled to targeted unstructured grids. This classical approach in simulation use the most classical assumption about the spatial structure of the random function which is to be simulated is the multigaussian assumption (equation 3.1.1)

$$Z(x) = \phi(Y(x)) \tag{3.1.1}$$

The assumption states that a non-linear function $Z(x)$ is a transform of a multivariate Gaussian random function $Y(x)$. In this technique using certain assumption, geostatistical simulation like Sequential Gaussian simulation, Spectral decomposition, turning band, direct sequential simulation is performed over the random function $Z(x)$. After performing the simulation on fine-scale grids, whose grid cells are considered as point support, the results are up-scaled on the target unstructured grid. One main advantage of this approach is assumption of change of support law for $Z(x)$ and $Z(v)$ is not taken into consideration.
Another point to be noted in this approach is that, the size of the fine scale grid should be equal to the smallest area of the unstructured grid generated.

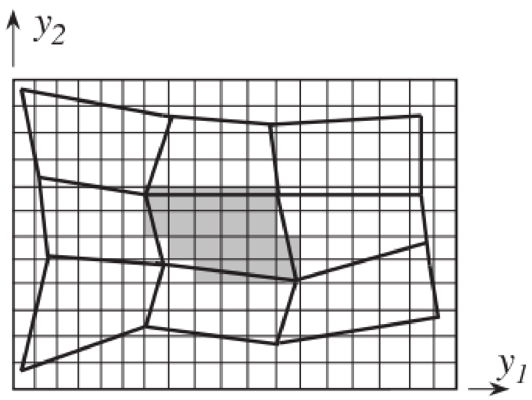

Figure 3-1 upscaling illustration, y1 and y2 representing the longitude and latitude respectively (adapted from Durlofsky, (2005))

3.2. Discrete Gaussian Model (DGM)

Matheron (1985) first attempts to integrate diffusion-type of random function by evaluating the change of support for showing the variation in probability distributive function (pdf). He compared usual models and came to conclusion that isofactorial model is true for first order and multigaussian case is correct for second-order approximation. Initial model of DGM was proposed by Matheron where he provides second order approximation for density of average values $Z(v)$, when support v is constant throughout the domain. Then Delfiner (1999) in his book on geostatistical simulation on uncertainty gave a generalised description of the discrete Gaussian model. Later Emery (2007) studies about the properties of DGM model and offers a streamlined method for deriving the change of support coefficient. The application of DGM to geostatistical simulation to address the issue of support size effect was introduced due to Emery & Ortiz (2011). In their paper the author applies this DGM to address the problem on geostatistical simulation on structured grids. As mentioned by Matheron the model developed rely on multi Gaussian random fields thus simulating using this model requires simulating realization of multivariate Gaussian random vectors.

Consider a stationary random function (SRF) $Z(x)$, which can be expressed as transform of an SRF $Y(x)$ (equation 3.1), with standard normal marginal distribution.

$$Z(x) = \phi(Y(x)) \tag{3.1}$$

With transformation function

$$\phi = F^{-1}.G \tag{3.2}$$

Where, F is the marginal cumulative distributive function (c.d.f.) of $Z(.)$ and G is the standard normal c.d.f. Similarly, as explained in section 2.4 of chapter 2, if we consider a spatial region having mean grade $Z(v)$ of the block v then the equation 3.1 can be rewritten as

$$Z(v) = \phi_v(Y(v)) \tag{3.3}$$

Where, $Y(v)$ is standard normal random variable and ϕ_v is block transformation function. The distribution of the block can be written as

$$Z_v = \frac{1}{|v|}\int_v Z(x)dx \tag{3.4}$$

From the above equation it can be said that the distribution of the block depends on the support size v of the block in such a way that the dispersion is inversely proportional to the support of the block. Now considering a uniform random point $\underline{x}$ within v then SRF from equation 3.1 for $Z(\underline{x})$ will be written as

$$Z(\underline{x}) = \phi(Y(\underline{x})) \tag{3.5}$$

The main assumption in DGM is that the bivariate distribution of $(Y(\underline{x}), Y_v)$ pair is Gaussian which is characterised a by correlation coefficient r.

As per the theorem mentioned in (Delfiner, 2012) stating that, "The c.d.f. F_1 is more selective than F_2 if and only if there exists a bivariate distribution $F_{12}(dz_1, dz_2)$ with marginal F_1 and F_2" and such that

$$E(Z_1|Z_2) = Z_2 \tag{3.6}$$

if and only if

$$\int \phi(z)F_1(dz) \geq \int \phi(z)F_2(dz) \tag{3.7}$$

Equation 3.6 is called Cartier's relation.
Now according to DGM assumption the transformation function and its distribution are derived using Cartier's relation. That is,

$$E\big(\phi Y(\underline{x})\big|Y_v\big) = \phi_v(Y_v) \tag{3.8}$$

$$(\phi_v(Y_v)) = \int \phi(ry_v + \sqrt{1+r^2}\,u)g(u)du \tag{3.9}$$

The above equation can be written in the form of a convolution product (equation 3.10)

$$\phi_v(Y_v) = \phi * g_{1-r^2}(\mathrm{r}(Y_v) \tag{3.10}$$

Where, g_{1-r^2} = Zero mean normal with variance $1-r^2$
Hermite polynomial as represented in equation 3.11, is used to calculate ϕ_v (equation 3.12)

$$\phi(y) = \sum_{n=0}^{\infty} \phi_n \ \chi_n(y) \tag{3.11}$$

$$\phi_v(y) = \sum_{n=0}^{\infty} \phi_{vn}(\chi_n\,(y)) \tag{3.12}$$

By applying Cartier's Relation from equation 3.8 and equation 3.13,

$$E(\chi_n(y')|Y) = \rho^n \chi_n(y) \tag{3.13}$$

We get,

$$\sum_{n=0}^{\infty} r^n \phi_n \ (\chi_n(y_v)) = \sum_{n=0}^{\infty} \phi_{vn}(\chi_n\,(y_n)) \tag{3.14}$$

$$\phi_{vn} = r^n \phi_n \tag{3.15}$$

Thus using equation 3.14 and 3.15, equation 3.12 can be written as,

$$\phi_v(y) = \sum_{n=0}^{\infty} r^n \phi_n(\chi_n\,(y)) \tag{3.16}$$

Where r is known as co-relation coefficient, or support size coefficient or point-block covariance and to solve the above equation r is to be determined.
There are two options available to determine support coefficient. One is using DGM1, which was proposed by Matheron in his paper (Matheron, 1985) where he uses equation 3.17 to find r.

$$\sum_{n=1}^{\infty} r^{2n} {\phi_n}^2 = \frac{1}{|v^2|} \iint_v c(x',x)dx\,dx' = Var(Z(\underline{x})) \tag{3.17}$$

Where v is the block area, Matheron had introduced DGM1 by applying it in structured grid, whose block area was same throughout the domain, in that case r was a single value but in case of unstructured grid, block area is different throughout the domain in such cases $r = r_p$ and $v = v_p$, p is different blocks in the domain.
And the covariance matrix for $Y(\underline{x_1}), Y(\underline{x_2}), Y(\underline{x_3}) \dots Y(\underline{x_n})$ is defined by the equation 3.18

$$\frac{1}{|v_p||v_q|} \iint_{v} c(x', x) dx\, dx' = \sum_{n=1}^{\infty} {\phi_n}^2 r_p^n r_q^n\, cov(Y_{v_p} Y_{v_q})^n \tag{3.18}$$

The other option to determine r is using DGM 2 which was proposed by Emery (2007), where author introduces an additional assumption. That is the bivariate distribution of $Y(x)$ and $Y(\underline{x'})$ for 2 independent random points within same block v is Gaussian. Introducing this assumption enables simpler way of determining the support coefficient and correlation between the block $Y(\underline{x_1}), Y(\underline{x_2}), Y(\underline{x_3}) \dots Y(\underline{x_n})$ is defined by equation 3.19 and 3.20 respectively.

$$r_p^2 = \frac{1}{|v_p||v_p|} \iint_{v} \rho(x', x) dx\, dx' \tag{3.19}$$

$$Cov\left(Y_{v_p} Y_{v_q}\right) = \frac{1}{r_p r_q} \frac{1}{|v_p||v_q|} \iint_{v_p v_q} \rho(x', x) dx\, dx' \tag{3.20}$$

The output of both DGM1 and DGM2 is the correlation coefficient and covariance matrix for the multivariate Gaussian random vector $Y(\underline{x_1}), Y(\underline{x_2}), Y(\underline{x_3}) \dots Y(\underline{x_n})$. This can then be simulated using classical techniques, for instance Sequential Gaussian Simulation (SGS)).

4. STUDY AREA AND DATASET USED

This chapter gives the information about the resources and dataset used. Section 4.1 shows the study area chosen for this research. Section 4.2 gives the details about the dataset used for the study area for analysis. Section 4.3 gives the detail information about the software and the packages used for the work.

4.1. Study area

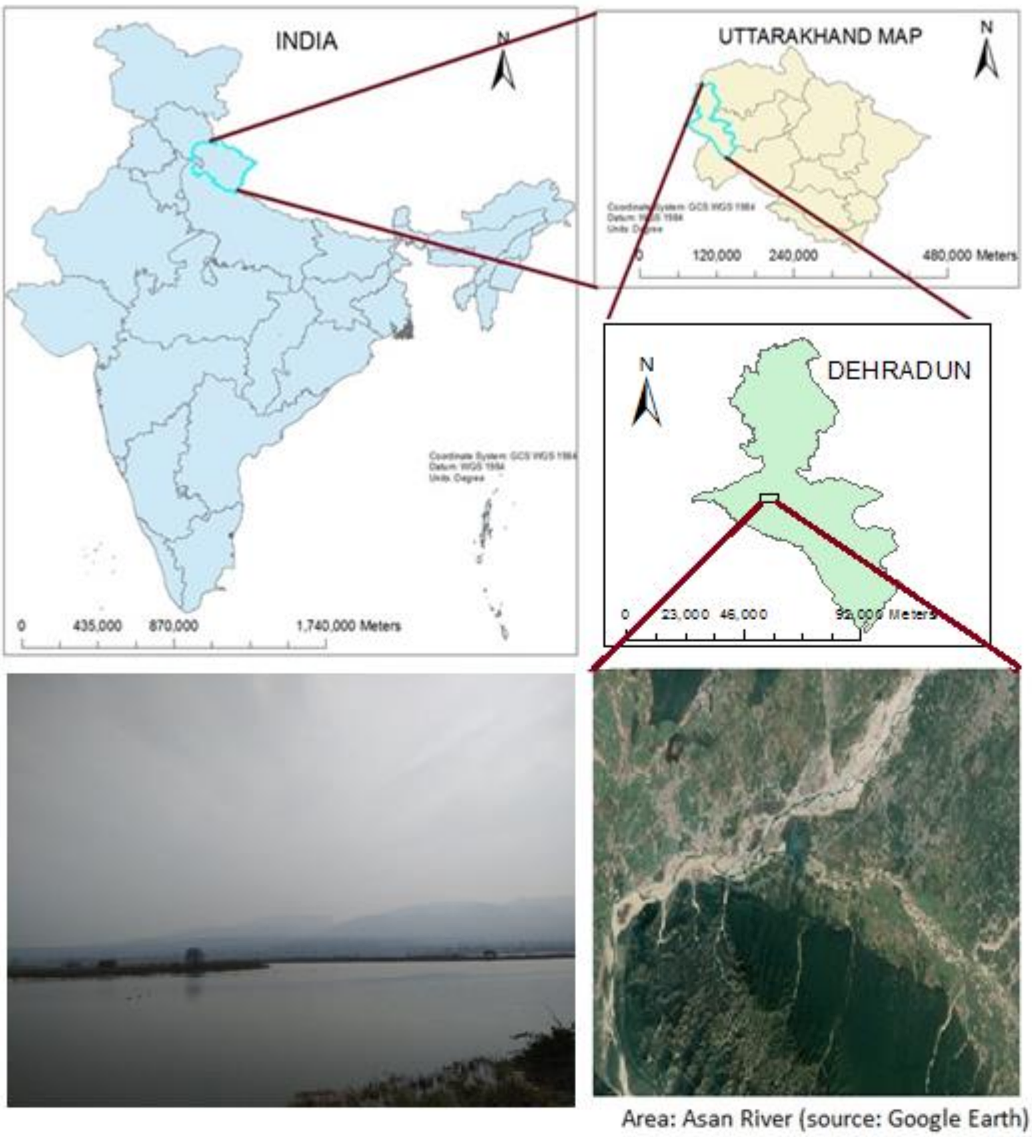

Figure 4-1 Study area - Google earth imagery of Asan River which is located in Dehradun.

Since the application is on hydrology, the study area chosen to test the proposed methodology is Asan River, Dehradun, Uttarakhand state, India (figure 4.1). The river is fed by the streams of western part of Doon valley and flows into the Yamuna River. The Test area is chosen in such a way that it constitute a Barrage in the middle of the river which is known as Asan Barrage (figure 4.2). This Asan Barrage is situated in the confluence of eastern Yamuna canal and Asan River and having a surface area of 4km^2 and its coordinates are 30°26'09"N latitude and 77°39'56"E longitude at the location Dakpathar in Dehradun. This Dam creates Asan Reservoir which is also called as Dhalipur Lake. The spatial extent taken for the study lies between longitudes 77.55 to 77.77 decimal degrees, and latitudes from 30.34 to 30.49 decimal degrees.The overall Elevation of that region varies from 335m to 935m from mean sea level with mean elevation of 630m from mean sea level.

4.2. Dataset used

Two CartoDEM of different location are taken for the study area as shown in Table 1. The 30m resolution DEM is taken for generating random sample elevation points which is used as the ground truth points for further estimation. In addition to that, from 30m DEM, slope map is generated which is later converted to vector points and taken for grid generation purpose. The CartoDEM 10m resolution is used as the reference data to compare the flow simulated results with the other generated DEMs.

Table 1 Dataset used for the study

NAME	SPATIAL RESOLUTION	SATELLITE
CartoDEM	30m	Cartosat-1
CartoDEM	10m	Cartosat-1

4.3. Software used

The workflow is divided into two parts, geostatistical simulation and flow simulation. All the process done in Geostatistical simulation are applied using R and RStudio (Team, 2018). The R-libraries that are used for specific process are spatstat (Baddeley, Turner, & Rubak, 2019) for tessellation, gstat (Pebesma & Graeler, 2018) for variogram analysis and simulation, CTT (Willse, 2018) for transformation and other packages like raster, rgdal, sp, maptools were also used. All the methods that are applied in flow simulation are done in HEC-RAS (U.S. Army Corps of Engineers, 2019)and ArcGIS software(Environmental Systems Research Institute, 2018).

5. METHODOLOGY

This research work mainly focuses on addressing the issue of support size effect and also to apply geostatistical simulation on unstructured grids. As an application in hydrological domain, the output of this geostatistical simulation is applied to undertake flow simulation on both structured and unstructured grids, and comparative study is done to find the effect of support size on flow simulation. As a reason the flow diagram is divided into 2 main parts, one Figure 5-1 representing the workflow which helps in achieving the objective 1, that is geostatistical simulation and the other one (Figure 5-2) representing the workflow on flow simulation. Furthermore the workflow 1 is divided into 2 parts depending on the method used for addressing the change of support model.

This chapter gives the detailed information about the workflow of this research. Section 5.1 shows the flow diagram of this research. In section 5.2 basic description of flow diagram for geostatistical simulation is mentioned. Section 5.3 explains about the sequential flow of method-1 mentioned in the flow diagram 1 and Section 5.4 explains about the mathematical flow of method-2 mentioned in the flow diagram 2. Section 5.5 mentions the second part of the research, Flow simulation analysis.

5.1. Flow diagram

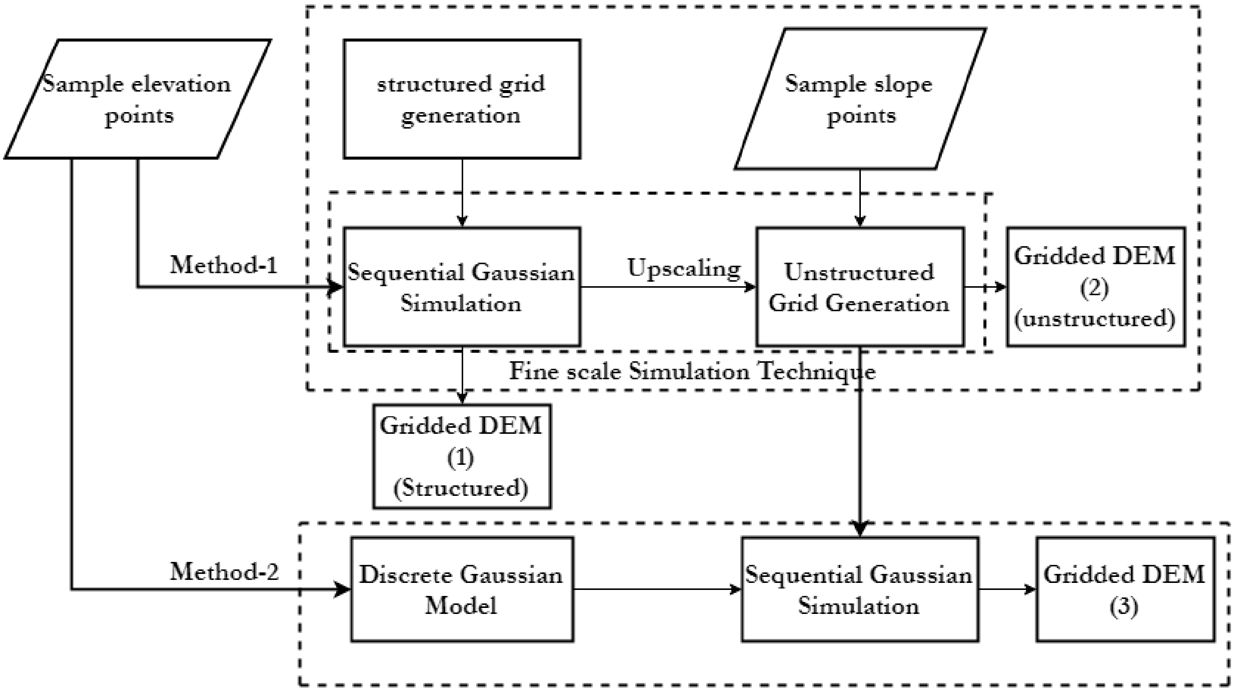

Figure 5-1 Flow diagram for geostatistical simulation

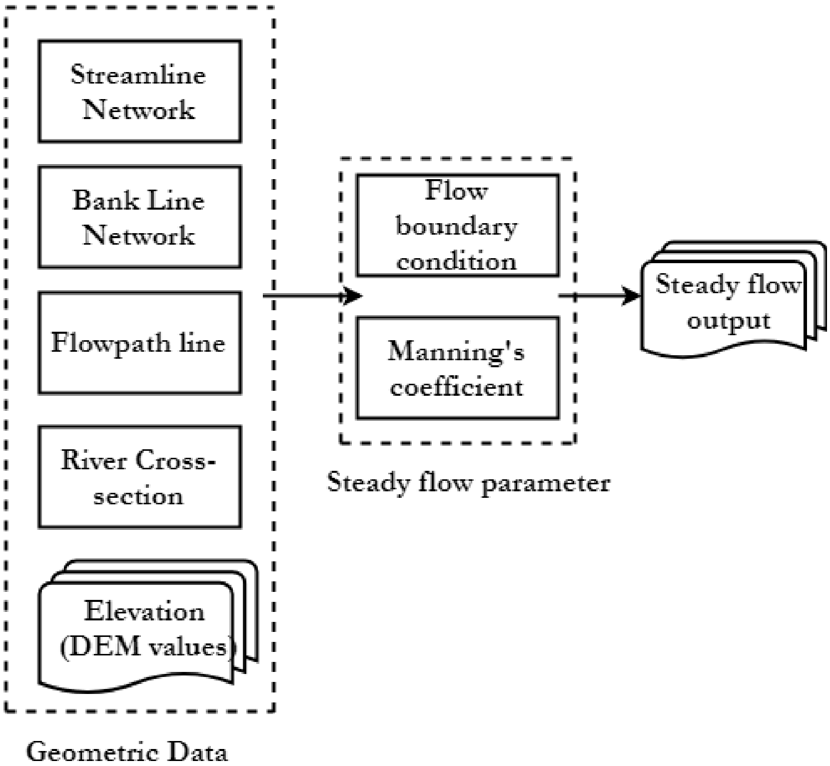

Figure 5-2 Flow Diagram for flow simulation

5.2. Description of flow diagram geostatistical simulation

5.2.1. Data used

Digital Elevation Model (DEM) was used for the study and was obtained from Cartosat-2 satellite. The spatial resolution of the same is 30m and for validation of the flow model CartoDEM of 10m resolution is used. From 30m DEM, 100 randomly sampled locations were chose as ground truth points.

5.2.2. Generation of unstructured grid

As mentioned in section 2.5, generation of grid follows certain steps:

1. Boundary Definition
2. Grid discretization
3. Mesh Generation

5.2.2.1. Boundary Definition

There are different shapes of unstructured grids like triangular, hexagon, Thiesson polygon etc. and different methods like triangulation, tessellation are there to generate the unstructured grid with different shape. But to generate the grids using any of this method, the need to define a boundary and set of distributed points over the polygon are required. Boundary of the grid was taken from the test area, whose bounding box coordinates has values of longitude from 77.66 to 77.72 decimal degrees and latitude from 30.42 to 30.45 decimal degrees.

5.2.2.2. Generation of sample points for grid generation

In order to generate these polygons, we need a set of sample points. The point data can be any parameter as it depends on the application of the grid. The slope map was generated from 30m DEM (input data). The map is converted to vector form, where the points are generated at the centroid of the each square block. Using these converted points, sample points area defined.

The main focus of unstructured grid generation is to show the structural features of surface using grid. The application is on hydrology, so the surface should be featured in such a way that river area should be more highlighted than other land use land cover features. The sample points are generated using the slope data. Since slope is generated from the DEM, the elevation values in the DEM shows the surface elevation above sea level. Thus the region of river will give height of same values. Which means it will give characteristics of a flat region and if we take a slope for that region it will be less than 10 degrees. The sample points are taken in such a way that the slope of these points are less than or equal to 5degrees.

5.2.2.3. Voronoi polygon generation

To generate an unstructured grid, Voronoi polygon method is used. Using the sample slope points, the grid is generated in R software using Dirichlet function. The generated polygon is of class Tess. Three kinds of grids are generated here, one using slope points 0-1 degrees (figure 5.3), one using slope points generated between 0-3 degrees (figure 5.4), and third one using the slope points greater than 3 i.e. slope degrees between 3-17 degrees (figure 5.5).

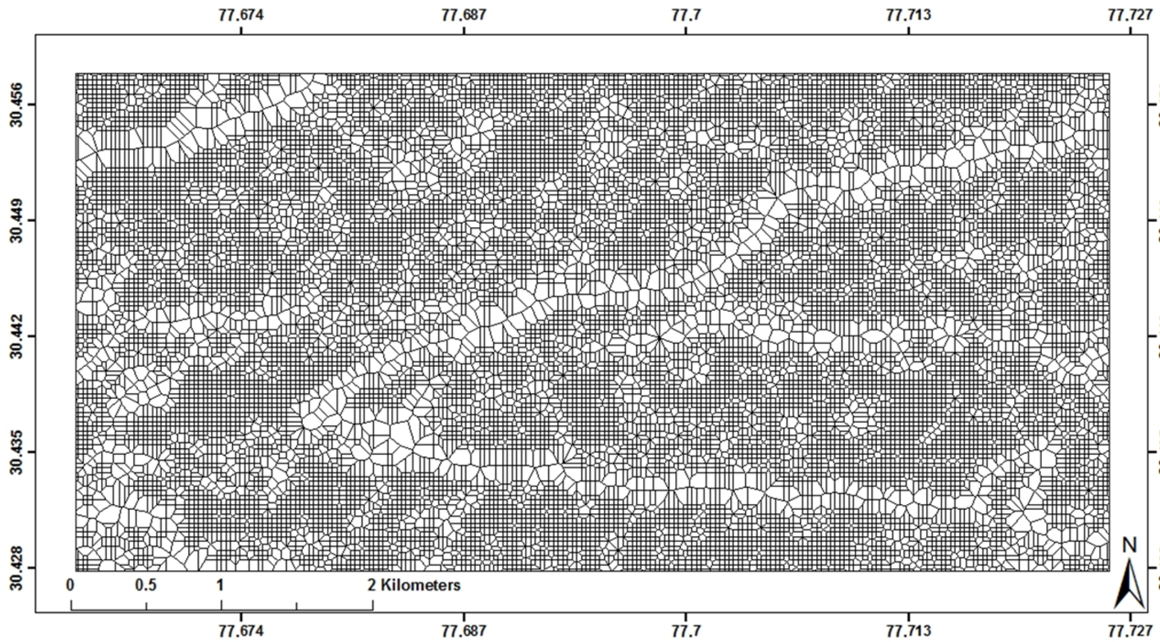

Figure 5-3 Grid generated using the slope points between 0-1 degrees

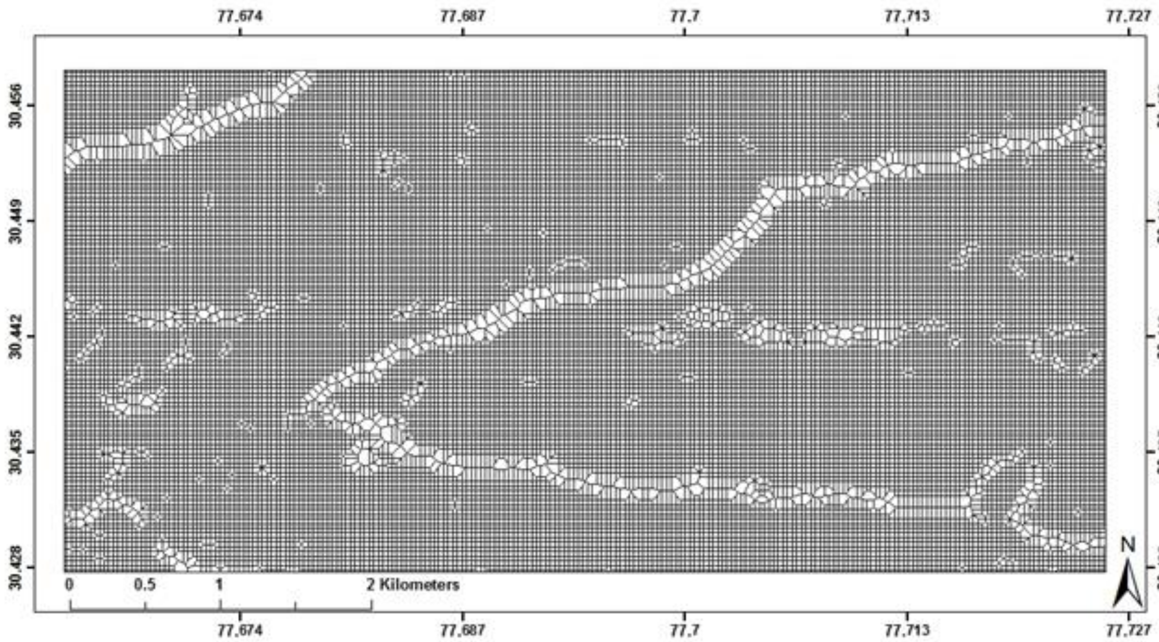

Figure 5-4 Grid generated using the slope points between 0-3 degrees

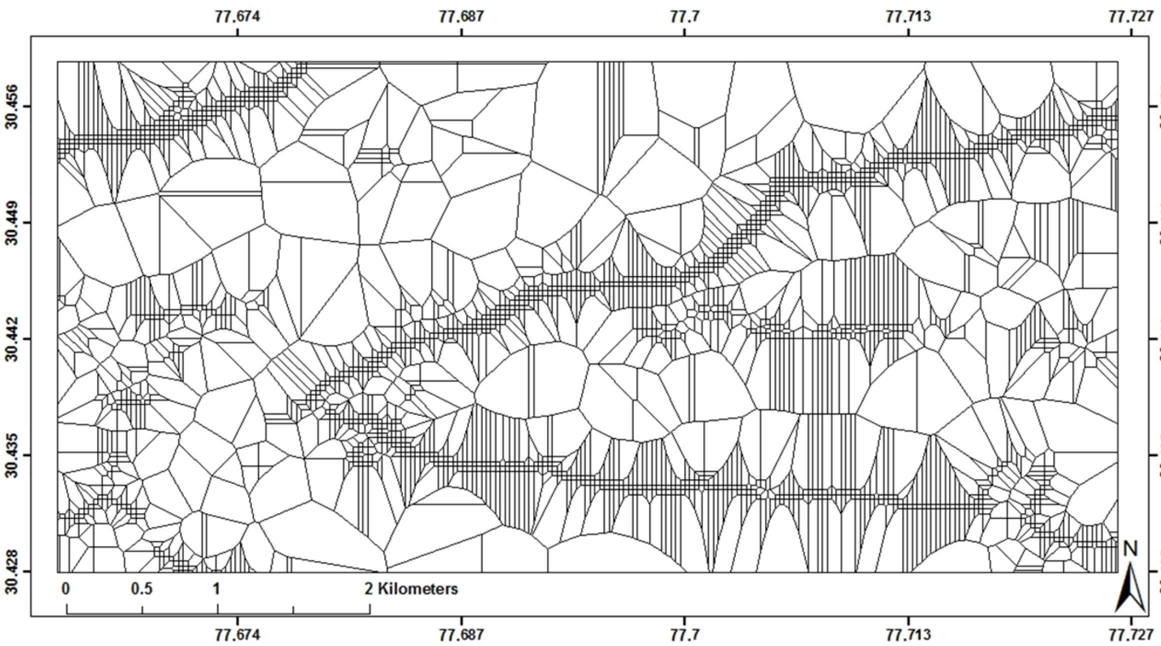

Figure 5-5 Grid generated using the slope points between 3-17 degrees

The grid generated has finer blocks due to high density slope point in that region and coarser blocks due to low density of slope points in that region. Further details is explained in section 6.1 of chapter 6.

5.2.3. Sample point generation

From the Cartosat 30m DEM, 100 sample points were generated from random location using ArcGIS software. The extent given for generation of random points is same as the extent of the grids generated.

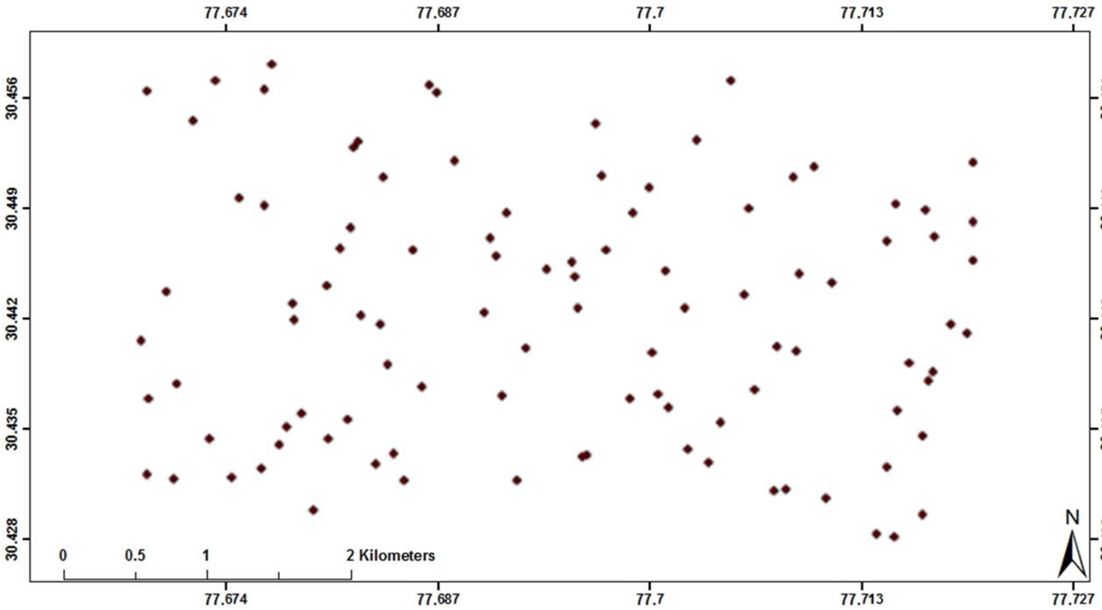

Figure 5-6 Generated sample ground points

5.3. Method-I Fine-scale simulaton technique

Algorithm for implementing fine-scale simulation

1. Generating structured grid
2. Variogram parameter estimation using the sample points
3. Fitting suitable variogram model
4. Applying Sequential Gaussian technique to the fitted variogram model
5. Upscaling the resultant output values to the generated unstructured grid.

5.3.1. Structured grid generation

From the generated unstructured grids using different slope points, grid generated with slope points of degree between 3-17 is taken for simulation because compared to other generated grids this grid is coarser so for further computation using this grid will be less time consuming and faster than the other finer grids. Now for fine scale simulation structured fine scale grid has to be generated whose grid cell size should be equal to the minimum area of the unstructured grid generated i.e. 821 m^2.

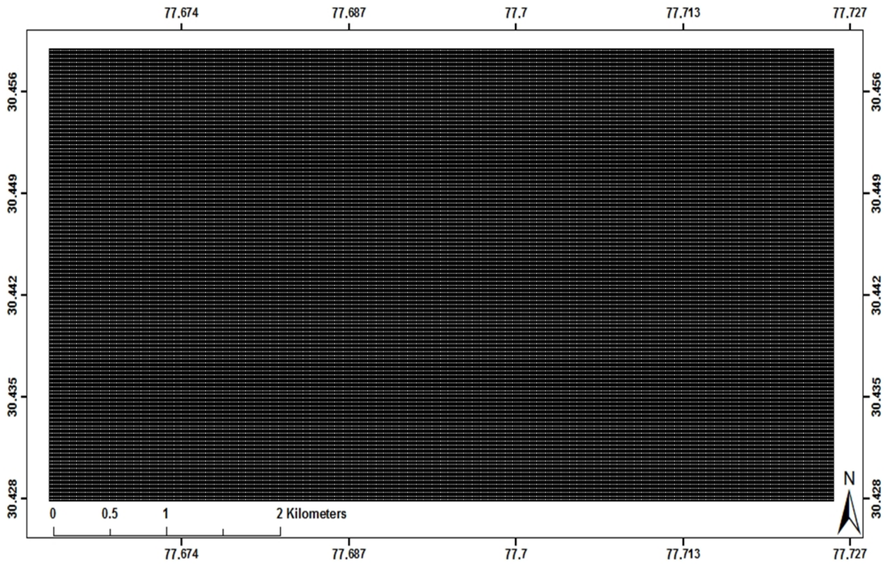

Figure 5-7 Generated structured grid using fine block size

5.3.2. Variogram selection

Table 2 Semi variogram for different fitted model

MODEL	PSILL	RANGE (m)	SSERR(m)
SPHERICAL	196.54	2734.66	0.56
EXPONENTIAL	382.83	3215.39	0.53

It can be observed from the Table 2 that the Standard error for exponential variogram is less compared to spherical variogram. Thus, exponential model is fitted to the variogram (Figure 5-8).

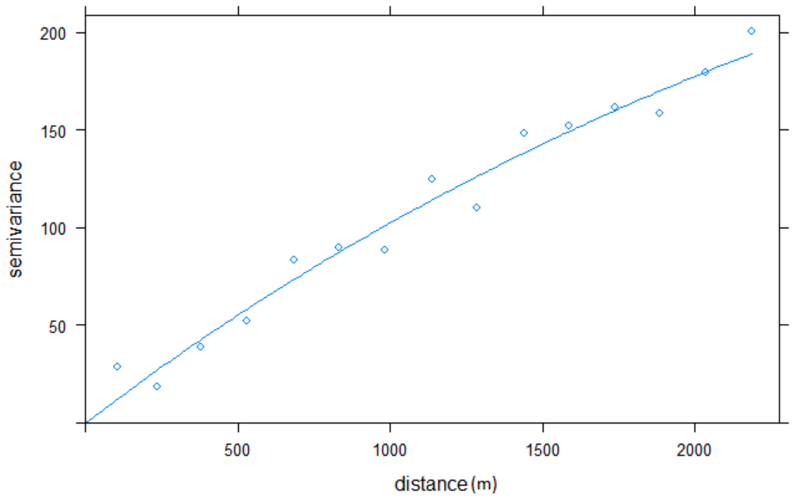

Figure 5-8 Semi-variogram with fitted exponential model

5.3.3. Sequential Gaussian Simulation (SGS)

'Krige' function from 'geostats' package of R language was used to perform Sequential Gaussian Simulation. In that Krige function sample points is given as the data, the estimated variogram is given as the model, the generated fine scale structured grid is given as the new data. The function is run for 100 times (nsim=100) to get a constant result in the end.

5.3.4. Upscaling

The result of this Sequential Gaussian simulation is the gridded DEM. The blocks of the grid which fall completely inside the polygon/block of the unstructured grid is averaged and that block is given the average value. In order to know the blocks which falls inside the block of unstructured grid, the resultant gridded DEM is converted into vector form. The vector point feature is generated in the centroid of each cell. This generated vector is overlaid with the unstructured grid and the points that are falling inside each block is averaged and the block is given that value.

5.4. Method-2 Discrete Gaussian Model (DGM)

5.4.1. DGM

Algorithm for implementing DGM is as follows

1. Given input data x, transform the data into Gaussian Transformation $\phi Y(x)$
2. Now, using point support covariance $C(x, x'),$ support co-efficient r is derived (equation 3.19).
3. Using equation 3.20, covariance between each pair of block $Cov\left(Y_{v_p} Y_{v_q}\right)$ is derived.

The model approach is given as flow diagram in figure 5-7.

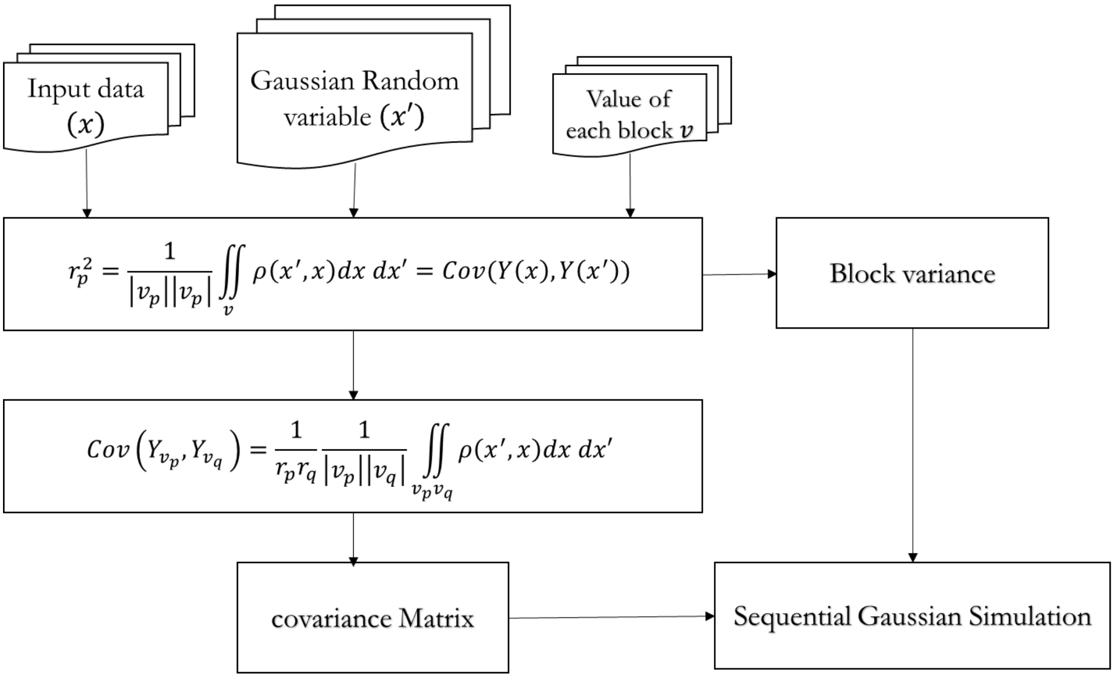

Figure 5-9 Discrete Gaussian Model approach (adapted from (Delfiner, 1999))

Basically the model helps to convert point support to block support before doing further geostatistical simulation. The model is implemented as per the algorithm given above in RStudio software. Input point support contains 100 values. Those points which are completely contained by the block are taken as block support samples. The value of the block represents the area of each block. The support size coefficient is determined by first, generating set of Gaussian random points having zero mean and standard deviation 1 in each block. Then, finding the covariance between the random points, which is assumed to be a bivariate Gaussian distribution function. Then for each block, the covariance is divided by its respective block area. Here, in case of structured grid the area is same for all the blocks so the support co-efficient generated will be a single value. But in case of unstructured grid, each block size in the grid varies, so is the area. Hence area/block value is divided with the covariance value and we get support size co-efficient for each block. Thus 100 variables are generated. The support size coefficient is also known as the block variance

In order to generate covariance matrix, first covariance between the random point in one block and random point in another block is calculated and the result is divided by the block value and support co-efficient value of their respective block (mathematical formula is illustrated in figure 5-7). A 100 x 100 matrix is generated whose diagonals represents the variance of the blocks and upper and lower triangle represents the covariance between two blocks. It is noted that once this change of support co-efficient and covariance between each pair of random variables in each block is known the later part of predicting random variables is done by any classical method such as SGS (Biver et al., 2017).

Now, In order to do simulation and predict the block values of unknown blocks we need to generate block sample values. The output of the DGM gives the variance of the block and point to block covariance matrix. Normally in kriging, the variance is calculated with the weight and covariance values which are calculated from the variogram. In this case we have the covariance matrix and variance value, the weight is calculated by the inverse of covariance matrix multiplied by the variance matrix. Later in loop, the weight is multiplied with the point support data, to generate the sample set of block support data.

The kriging weight factors of n valid input points $(i = 1, \dots n)$ are found by solving equation 5.1 (ILWIS, 2015)

$$\underbrace{\begin{pmatrix} 0 & \gamma(h_{12}) & \gamma(h_{13}) & \cdots & \gamma(h_{1n}) & 1 \\ \gamma(h_{21}) & 0 & \gamma(h_{23}) & \cdots & \gamma(h_{2n}) & 1 \\ \gamma(h_{31}) & \gamma(h_{32}) & 0 & \cdots & \gamma(h_{3n}) & 1 \\ \vdots & \cdots & \cdots & \ddots & \cdots & \vdots \\ \gamma(h_{n1}) & \gamma(h_{n2}) & \gamma(h_{n3}) & \cdots & 0 & 1 \\ 1 & 1 & 1 & 1 & 1 & 0 \end{pmatrix}}_{C} . \underbrace{\begin{pmatrix} w_1 \\ w_2 \\ w_3 \\ \vdots \\ w_n \\ \lambda \end{pmatrix}}_{W} = \underbrace{\begin{pmatrix} \gamma(h_{p1}) \\ \gamma(h_{p2}) \\ \gamma(h_{p3}) \\ \vdots \\ \gamma(h_{pn}) \\ 1 \end{pmatrix}}_{D} \quad (5.1)$$

$$C^{-1}.D = W \quad (5.2)$$

And kriging estimator is defined as $\widehat{Y_0} = w'Y$, where w is the weight matrix and Y is the point support data.

5.4.2. Variogram Selection

The using resultant block support data is used for variogram model. The model is then fitted using spherical variogram.

5.4.3. Sequential Gaussian simulation

The simulation is performed using krige function in R. Usually in krige function, in formula the attribute to be simulated is given (here elevation is given as attribute), spatial data frame which contains the simulation attribute is given as data parameter and in the slot for new data generally structured grid is given, which the function takes as a spatial points. In this case the generated unstructured in the form of spatial points are given as new data parameter and the krige function is performed.

5.5. Description of flow diagram for flow simulation

In this research, to find the surface properties of each DEM, 2 kinds of flow analysis were done. One is flow accumulation using ArcGIS and other steady flow analysis using HEC-RAS software.

5.5.1. Flow Accumulation

Flow Accumulation is performed in ArcGIS. First, flow direction is derived from each DEM. Each output flow direction is given as an input raster to the flow accumulation operation. The function creates a raster of accumulated flow to each cell. The flow accumulation is based on number of cells flowing into each cell in the output raster (Environmental Systems Research Institute, 2016).

5.5.2. Steady Flow Analysis

5.5.2.1. Geometric data preparation

Steady flow analysis is divided into 2 main sections (Figure 5-2), first section, pre-processing where geometric data is digitized. In this 4 features are digitized. One, the river centre stream line, which shows the river flow centre. The second one is the banks of the river, the third one is the flow path channel. Flow path is defined for flood simulation analysis, to show the maximum area the water can flow. In the direction towards downstream the river is digitized. The final parameter is the cross-section which is created from right bank to left bank, given here with width of 400 meters and spacing between each cross-section is kept as 300 meters. The length of the river network generated is 3641.761 meters. After generation of the data, elevation values are added to each attribute table. Here, each time, using different DEM, the geometric data's elevation was updated. Each file is exported into 'GIS2RAS' HEC-RAS format.

5.5.2.2. HEC-RAS Geometric data

1. In HEC-RAS new project has to be created.
2. In Geometric data editor, the exported file from ArcGIS has to be imported in HEC-RAS
3. After importing, the cross-section data has to be edited and Manning's coefficient value has to be added.
4. The next step is to enter the steady flow data. In order to run the steady flow analysis some boundary conditions are to be added.
    a. Number of profile has to be added. Number of profile refers to number of calculation which has to be performed. Since the steady flow analysis is done on each file having different DEM, the number of profile and the value must be kept same so as to compare the output relatively.
    b. Reach boundary conditions where normal upstream and downstream depth is defined. The normal depth is calculated by general profile plot of the 3D river line from ArcGIS. Mathematically it is, difference in the maximum and minimum elevation divided by the total length of the river. And the maximum steady profile rate which was used for steady flow analysis prediction was 200m^3/s, thus making this value as the maximum threshold for flow discharge. The steady flow analysis is predicted as per this given threshold value.

5.5.2.3. Steady flow analysis

After feeding the geometric data, the next step was to simulate the steady for analysis. Output of the simulated flow contains surface plot, a table (Table 3) representing the steady flow values. The manning's equation for velocity is given in Equation 5.3

$$\bar{u} = \frac{1}{n} R^{\frac{2}{3}} \sqrt{S} \tag{5.3}$$

And uniform flow rate is derived from the Equation 5.4

$$Q=\bar{u}A=\frac{1}{n}AR^{\frac{2}{3}}\sqrt{S} \tag{5.4}$$

Table 3 Steady flow output description

PARAMETER	**DESCRIPTION**
Q-TOTAL	Profile Discharge (m^3/s)
MIN CH EL:	Minimum Channel elevation [m]
W.S.EL:	Water Surface Elevation
CRIT W.S:	Critical Water Surface in the profile
E.G ELEV:	Energy Grade line Elevation
E.G SLOPE	Slope of Energy Grade line
VEL CHNL	Velocity in the channel
FLOW AREA	Cross-sectional Area of flow
TOP WIDTH	Width of the area of flow
FROUDE #CHL:	Froude number for each cross-section

6. RESULTS AND ANALYSIS

This chapter presents the results and analysis done on the study area as per the workflow mentioned in Chapter 5. The section is divided into 4 sections. Section 6.1, describes briefly about the resultant output of grid generation, while the geostatistically simulated output is given in Section 6.2 and the final flow simulation output and their analysis is discussed in Section 6.3. The resultant outputs of flow simulation are compared and validated in the Section 6.4.

6.1. Grid generation

In Geostatistical simulation, under Section 5.2.2.3, it can be observed that the unstructured grid is generated by Voronoi polygon method using R software. In this study three types of unstructured grids were generated as shown in Figure 5-3, Figure 5-4, Figure 5-5. As mentioned in previous chapter that the grids were generated using slope as the point parameter and it can be seen from those figures that Figure 5-3 generated with slope having 0-1 degrees and Figure 5-4 generated with slope point having value 0-3 degrees is giving very finer grid size than Figure 5-5, where grid is generated with slope point having range between 3 to 17 degrees. As the generated grid will be used for further computational analysis for the study, using the finer grid cell will make the computation more complex. Because finer grid has more number of grid cells than the coarser one and will require more storage space to store the value of each grid and computationally it will take time. Furthermore, due to high slope between the river bed and the land/urban areas there is finer and coarser grid variation separating the urban/non-river area and river bed region. As an objective for generating grid for hydrological model, the grid shown in Figure 5-5 is taken for further simulation analysis. Here Figure 6-1 shows the unstructured grid with 2400 blocks and each block whose area ranges from 0.4 x10^{-3} km^2 to 6 x10^{-3} km^2.

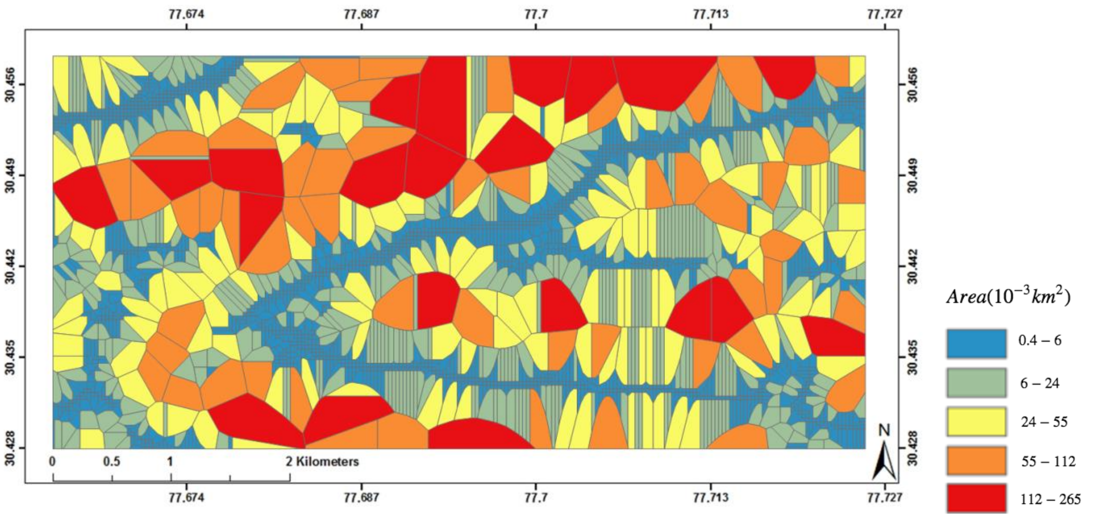

Figure 6-1 Unstructured Grid representing the variation in block area

When the generated unstructured grid is overlaid with a topographic base layer as shown in Figure 6-3, it can be seen that the finer blocks are generated in such a pattern that it distinguishes the urban land and the river bed. This separation is caused because those finer blocks were the regions having higher density of points whose slope ranges from 3 degrees to 17 degrees. From Figure 6-2, it can be noted that if rise is smaller than run, then the slope lesser than 30 degrees. In this case, region covering the river regions and the region covering the urban land were giving similar behaviour elevation value but the elevation values that are from river bank to urban land, there is this slight decrease in rise compared to other regions, which resulted in slope ranging from 3 to 17 degrees. Due to this denser points are generated in that region, making a separation between river bank and urban land.

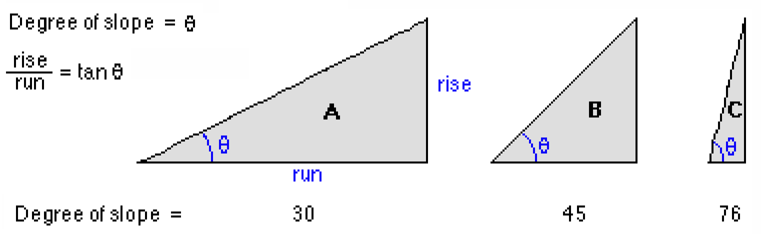

Figure 6-2 Comparing the values of Slope in degrees (adapted from (Environmental Systems Research Institute, 2010)

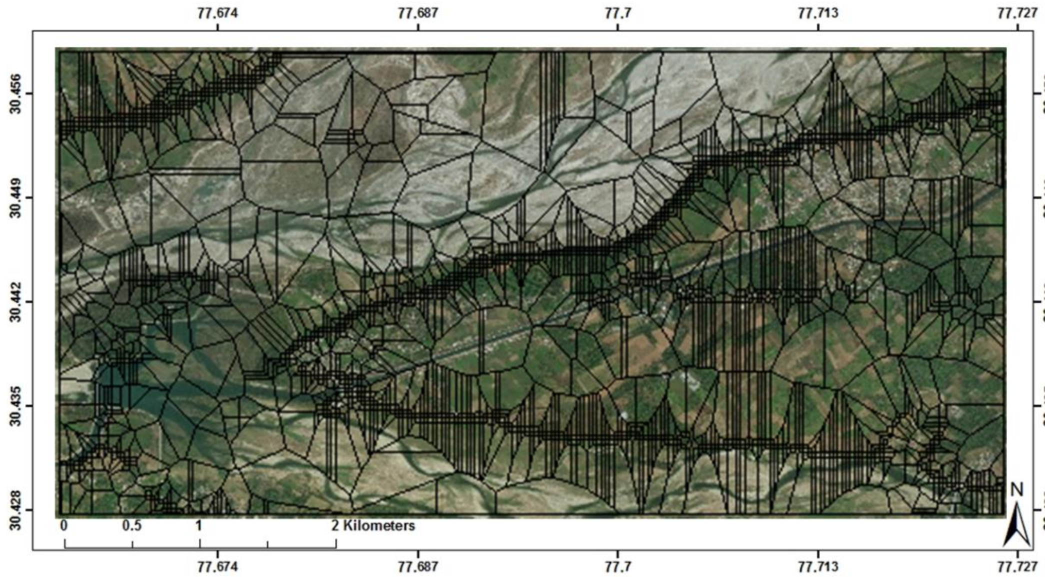

Figure 6-3 Unstructured Grid overlaid with a topographic base layer

6.2. Geostatistical simulation

Two approaches were taken in order to do geostatistical simulation by addressing the issue of support size effect. The first method is to do fine scale simulation, where the support size effect is addressed after applying sequential Gaussian simulation, while the second method is the discrete Gaussian method. In this method the support size effect is addressed before performing geostatistical simulation. The resultant outputs of both the approaches are shown in further sections.

6.2.1. Using fine-scale simulation approach

In this approach as mentioned in the Section 5.3 of methodology chapter, the structured grid generation is generated with block having value that is equal to the smallest area of a block in unstructured grid. As we can see from Figure 6-1 the smallest area of a block in unstructured grid is $0.4x10^{-3}$ km^2 (i.e.$411m^2$). The structured grid is generated in such a way that each block in structured grid is $411m^2$ of area as shown in Figure 5-7.Using this generated structured grid, sequential Gaussian simulation was applied with variogram having exponential model whose range is 3215.39m and semi variance is 382.83. Figure 6-4 shows the output for SGS. The resultant value of the gridded elevation model varies from 0 to 457.79m.

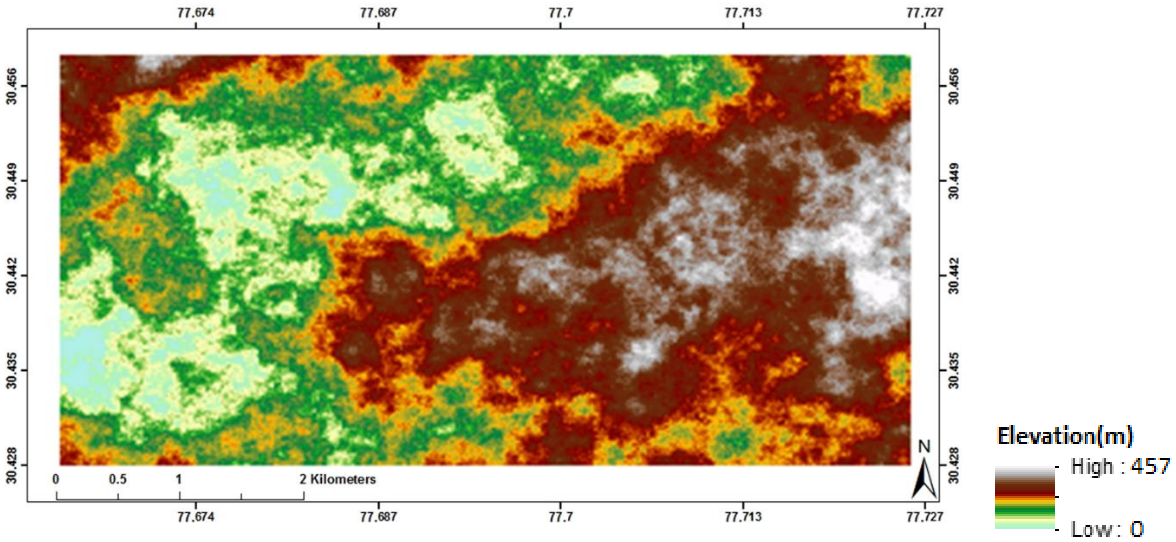

Figure 6-4 (Fine Scale Simulation Approach) Gridded DEM generated using SGS technique

From the above Figure 6-4 it can be observed that due to fine grid size, the gridded DEM that is generated gives a continuous and smoothened output surface. The mean value of the elevation, 419.64m is in the region where river is flowing and the elevation increases as we move away from the river. And the elevation value ranges from 0 to 457.79m.

In fine-scale simulation approach the support size effect is addressed by performing regularization to the point support data. Thus, regularisation is performed by up-scaling the structured simulated output to the generated unstructured grid as shown in Figure 6-5. The resultant output of upscaling is the unstructured DEM and values of this DEM ranges from 392.50m to 451.76m. It can be seen from both the figures that low elevated region is region where river is flowing and slightly elevated areas are near the border regions which is separating the river and the non-river areas and high elevated values are in the urban land areas. In addition to that from Figure 6-5 it can also be noted that due to the structure of the grid and the upscaling procedure, the output produced shows a discrete variation in the values.

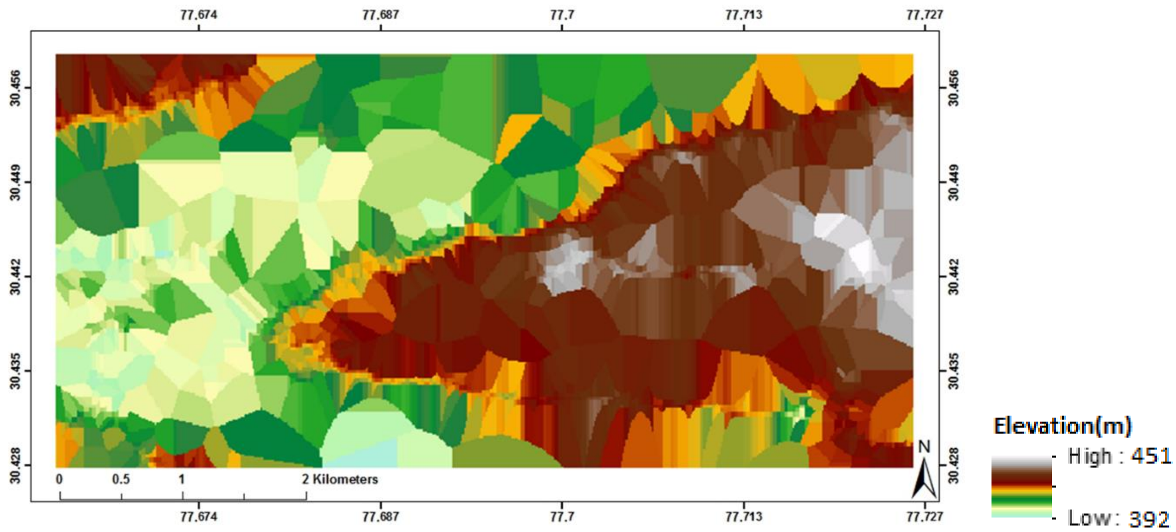

Figure 6-5 Unstructured DEM after upscaling

Table 4 Semi-variogram of fitted spherical model for up-scaled unstructured DEM

MODEL	PSILL	RANGE(m)	SSERR(m)
SPHERICAL	198.38	2952.44	98017

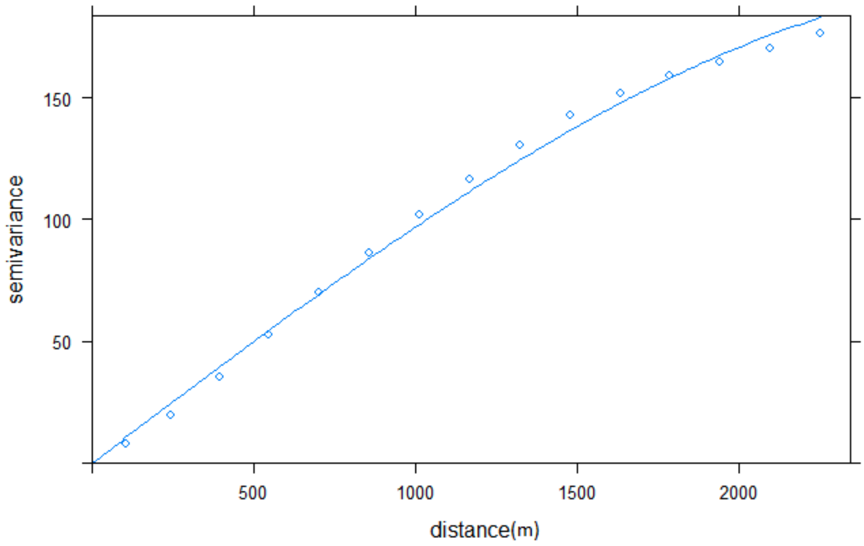

Figure 6-6 Semi-Variogram of up-scaled unstructured Grid

6.2.1.1. Change of support analysis - I

Figure 6-7 shows the variogram of the generated fine-scale structured DEM values and the up-scaled unstructured DEM values. As mentioned in Section 2.4 about the relation between the support size and variogram, we can see similar relation in Figure 6-7 given below. Basically the structured variogram is the point support variogram and the unstructured variogram is the block support variogram. It can be reframed that the semi-variogram plotted in Figure 6-7 is showing the relationship between the point support and block support.

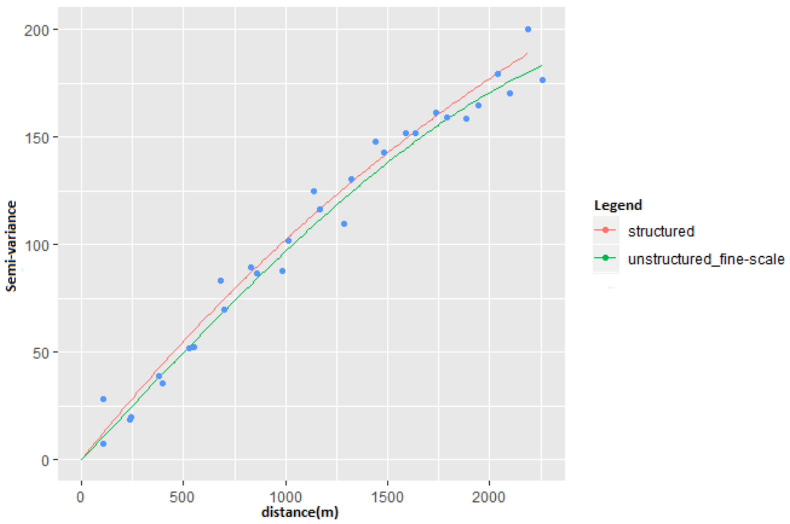

Figure 6-7 Variogram comparison between structured and unstructured grid.

From Figure 6-7 it can be observed that, the variance of unstructured grid when compared to the structured grid has decreased while the range of the same has increased which means that the spatial variability of unstructured grid has decreased when compared to the structured point support grid. By graphically comparing the Figure 6-7 and Figure 2-3, the semi-variance is $C(0) = 382.83$ and $C_v(0) =$

198.38 and range is $\gamma(h) = 3215.39m$ and $\gamma_v(h) = 2952.44m$ then $\bar{\gamma}(v, v)$ is $C(0) - C_v(0)$, i.e. $382.83 - 198.38 = 184.44$

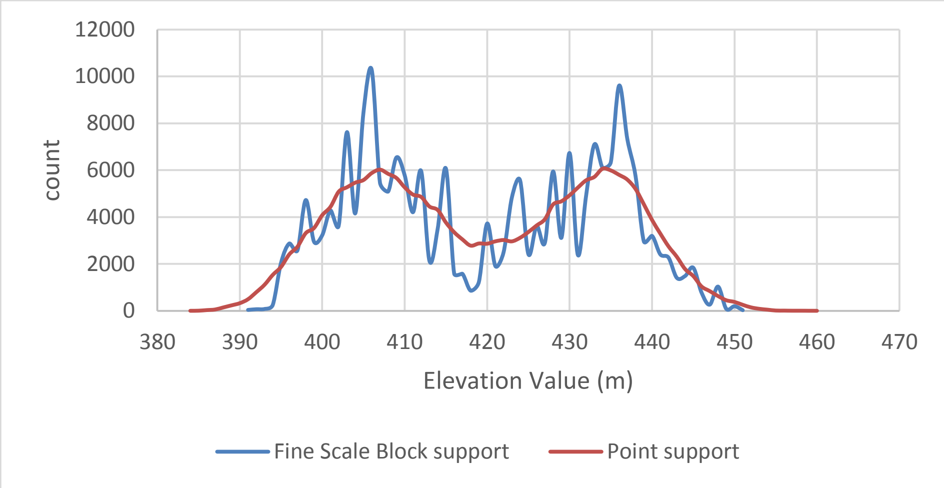

Figure 6-8 Histogram comparison between block support and point support

Figure 6-8 shows the frequency distribution of values between point support and block support. Difference in the variability of the elevation value can be seen from the distribution plot, as it shows the support effect due to different support sizes.

6.2.2. Discrete Gaussian Model Approach

The second method to address the issue of support size effect is using DGM. As mentioned earlier the generated grid consists of 2400 Voronoi polygon cells and Discrete Gaussian model is applied to it as mentioned in the methodology. The support size co-efficient is calculated as given in the Equation 3.19. From Figure 6-9 it can be observed that the support size co-efficient range from 0 to 3.50e-04. Normally as mentioned in literature, the value of support co-efficient should range between 0 to 1, where 0 represents support with large area and 1 represents point support. As our generated grid are coarser in size, the co-efficient of the support or the correlation-coefficient is in the above mentioned range is more tending towards zero.

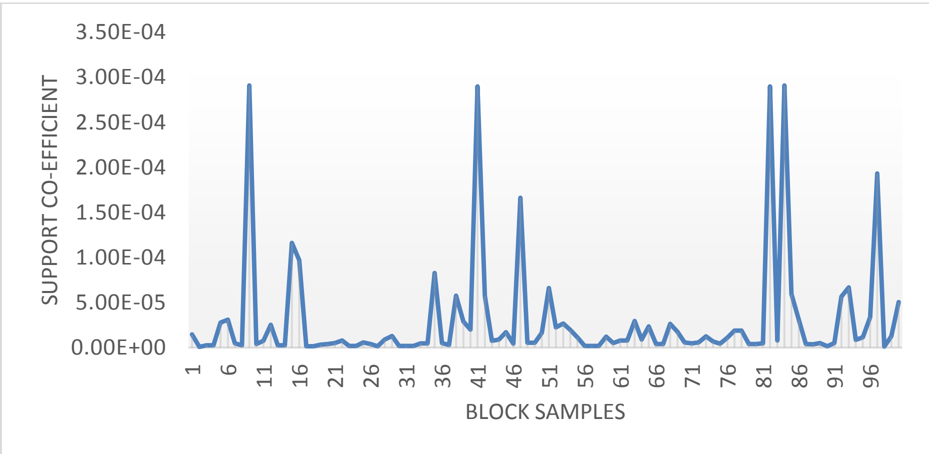

Figure 6-9 Plot showing the range of support size co-efficient

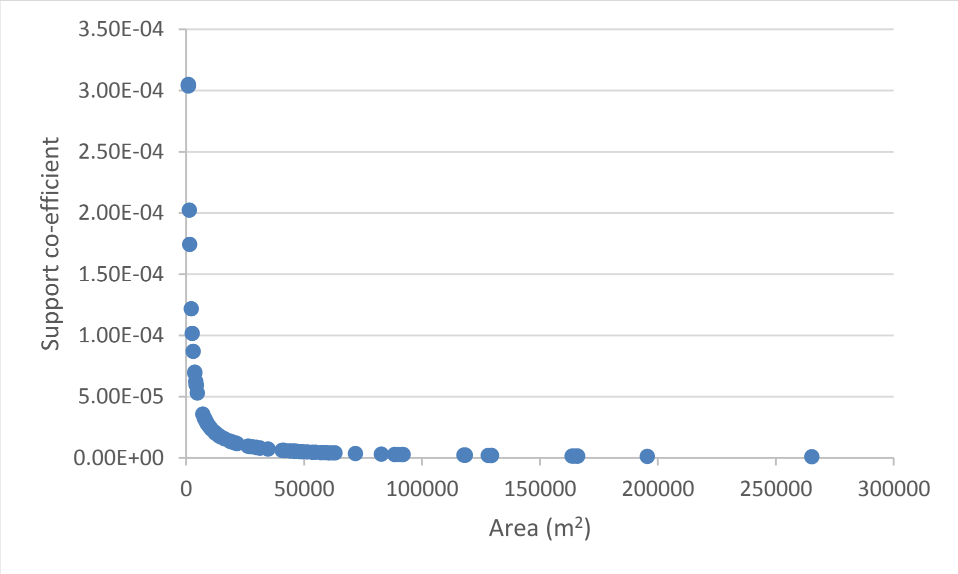

Figure 6-10 Variation of support co-efficient with respect to area

As stated in the previous section, ideally the support coefficient range should be between 0 to 1 denoting that if the value is 1 it is said to be point support and if it is 0 it is said to be block support. And it is also observed from Figure 6-9 that the range of the co-efficient is between 0 and 0.00035. From Figure 6-10 it can be further noted that as the area of the block in unstructured grid increases, the support co efficient tends towards zero. That is, it can also be stated that, larger the area, lesser will be the support co-efficient. Using Equation 3.20, the above correlation coefficient is used to find the block to block covariance. The resultant covariance is a covariance matrix of 100 rows and 100 columns. Now with block variance and block to block covariance, sequential Gaussian simulation is done on the unstructured grid, the variogram generated is shown in Figure 6-12 and the Semi-variance is given in Table 4 below

Table 5 Semi variogram for the generated DGM variogram with fitted spherical model

MODEL	PSILL	RANGE (m)	SSERR (m)
SPHERICAL	361.98	429.89	12.70

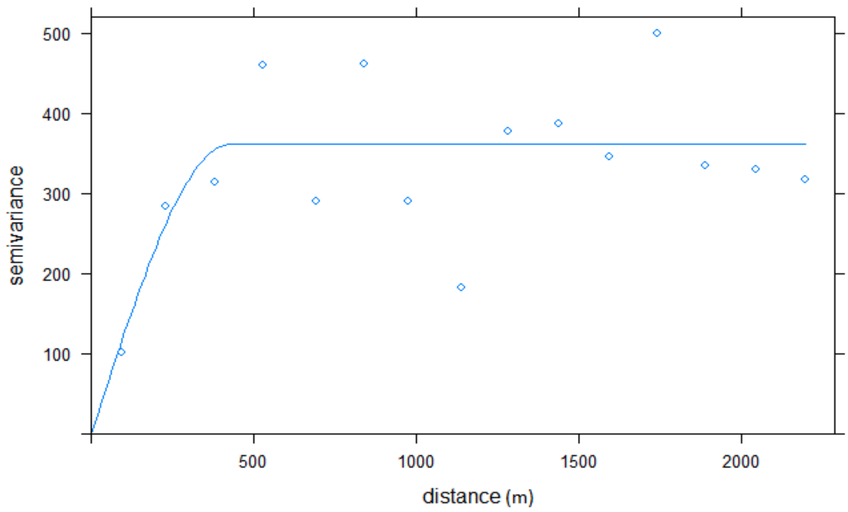

Figure 6-11 Variogram for DGM approach simulation with fitted spherical model

The output of Sequential Gaussian simulation with the above mentioned variogram is given in Figure 6-12. The Elevation values here ranges from 0 to 433 m.

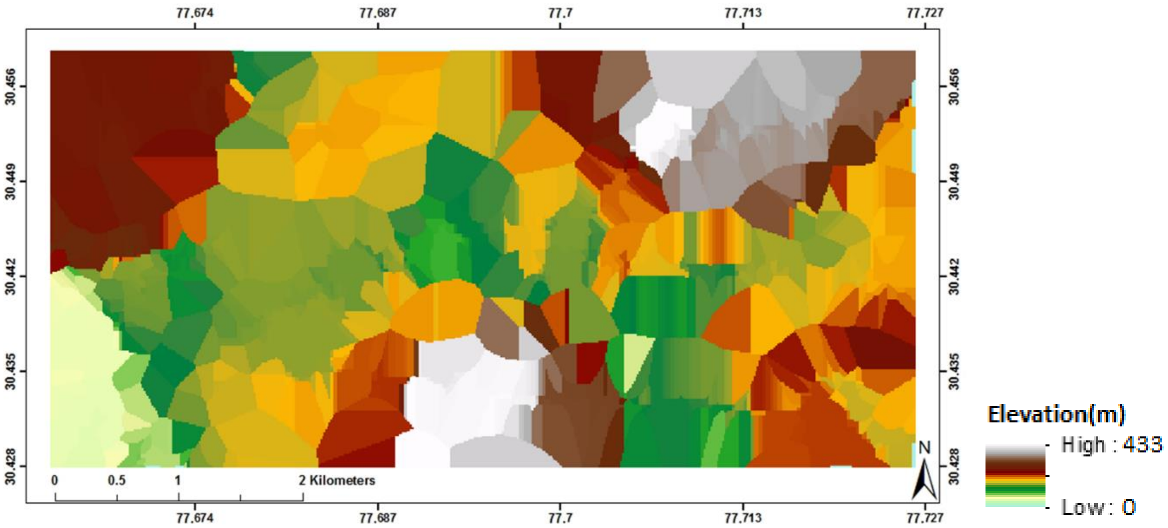

Figure 6-12 DEM generated using DGM model

6.2.2.1. Change of support Analysis – II

Similar to change of support analysis –I, Figure 6-13 shows the graphical comparison of point support and block support (generated using DGM). It is already mentioned in Section 6.2.1.1 and Figure 6-7 about the comparison between the point support and block support using fine-scale simulation approach.

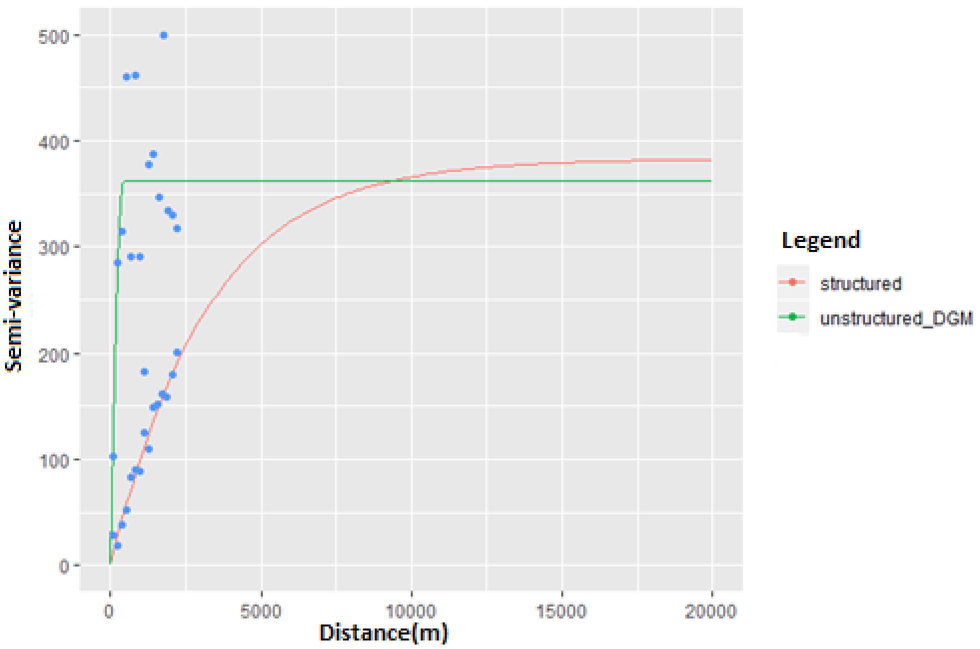

Figure 6-13 Semi variogram comparison between point support and block support generated using DGM

Just like fine-scale approach, gamma, the range of the variogram also decreases as support increases. Variogram being inversely proportional to correlogram, the correlation increases as the size of the support increases. Figure 6-15 shows the value distribution based on the point support and block support generated using different approaches. Similar to Figure 6-8, in this Figure also it can be observed that the average mean value of the distribution is same while the variability among the values for different support varies. Figure 6-14 shows the plot between the block support generated using Fine scale simulation approach and the block support generated using the DGM approach. It can be observed that the variance difference between the two block support variogram is $361.98 - 198.38 = 163.60$ and the range difference is $2952.44 - 429.89 = 2522.54\ m$. The difference in measured value to the inferred value of semi-variance denoted by $\bar{\gamma}(v, v)$, for fine-scale approach is 184.44 and DGM approach 20.84.

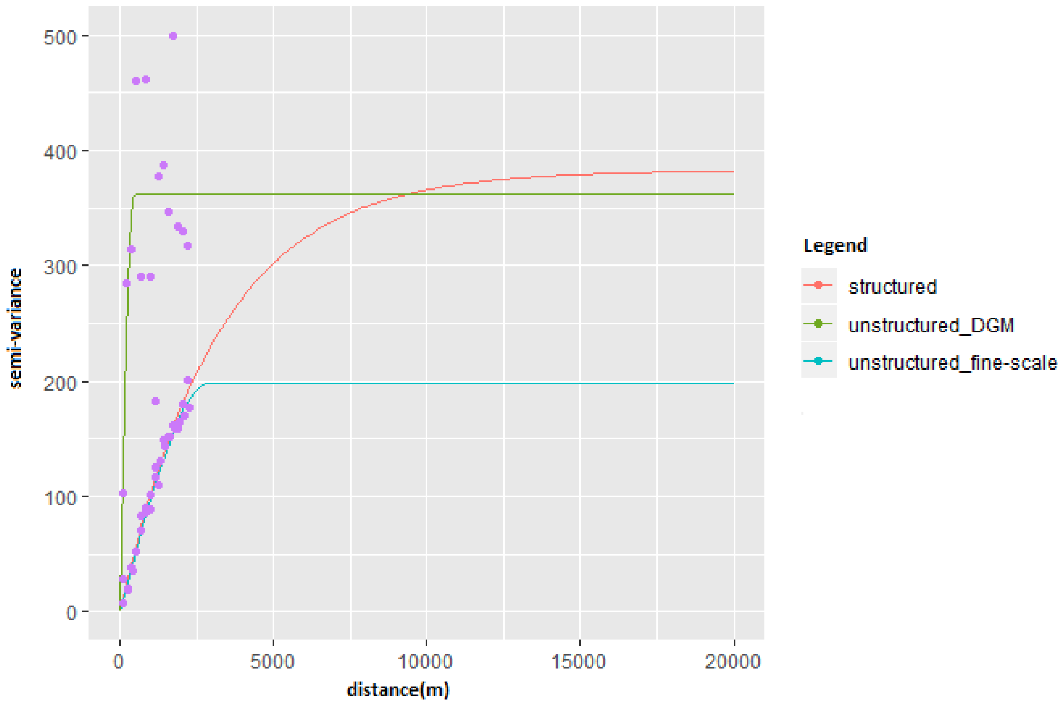

Figure 6-14 Semi-Variogram comparison between fine-scale approach and DGM approach

Figure 6-14 shows the comparative plot of 2 different variograms, point support, unstructured grid using fine-scale simulation approach and unstructured grid using DGM approach.

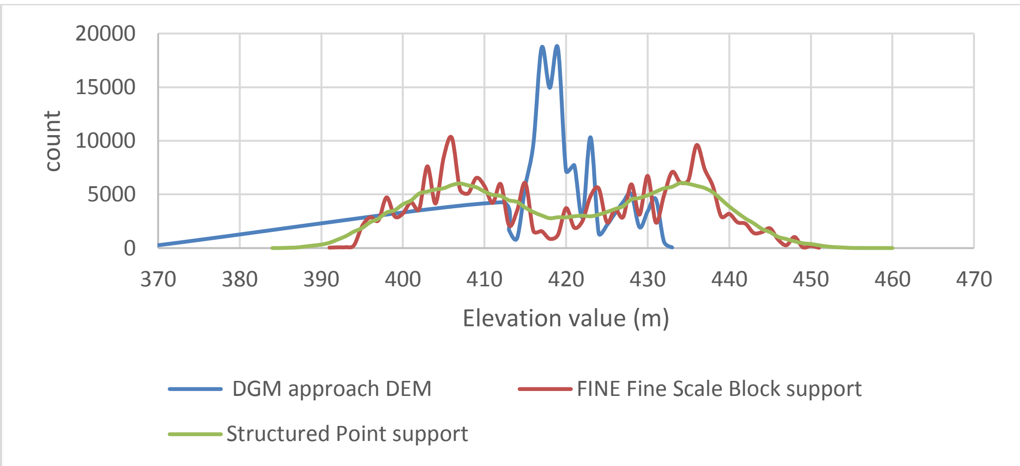

Figure 6-15 Frequency distribution (histogram) for different support sizes

6.3. Flow simulation

6.3.1. Flow Accumulation

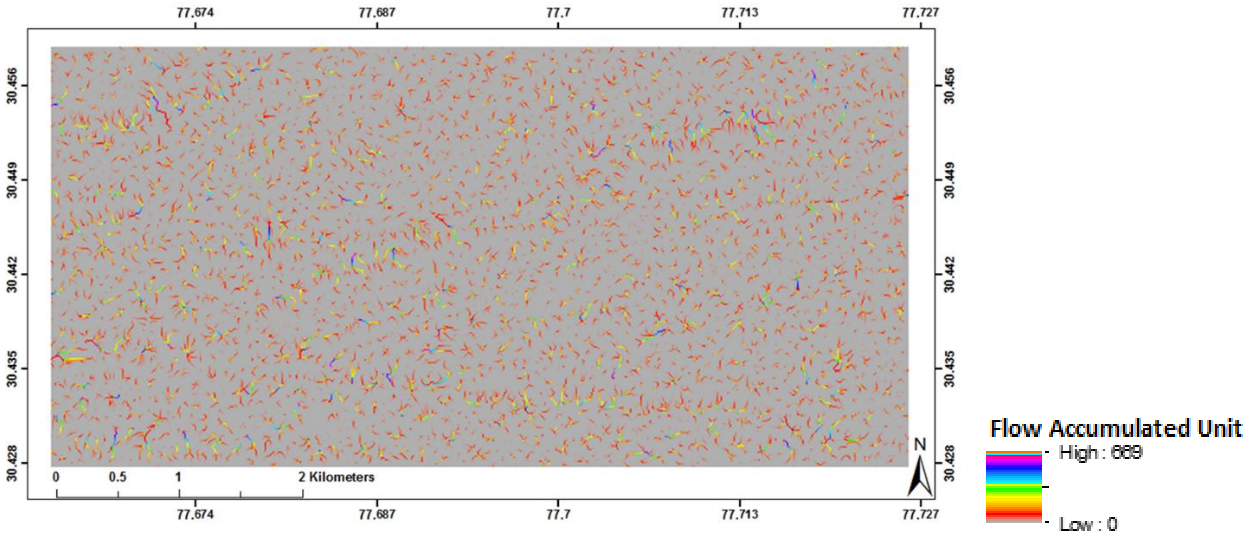

Figure 6-16 Flow accumulation map of 10m Reference DEM

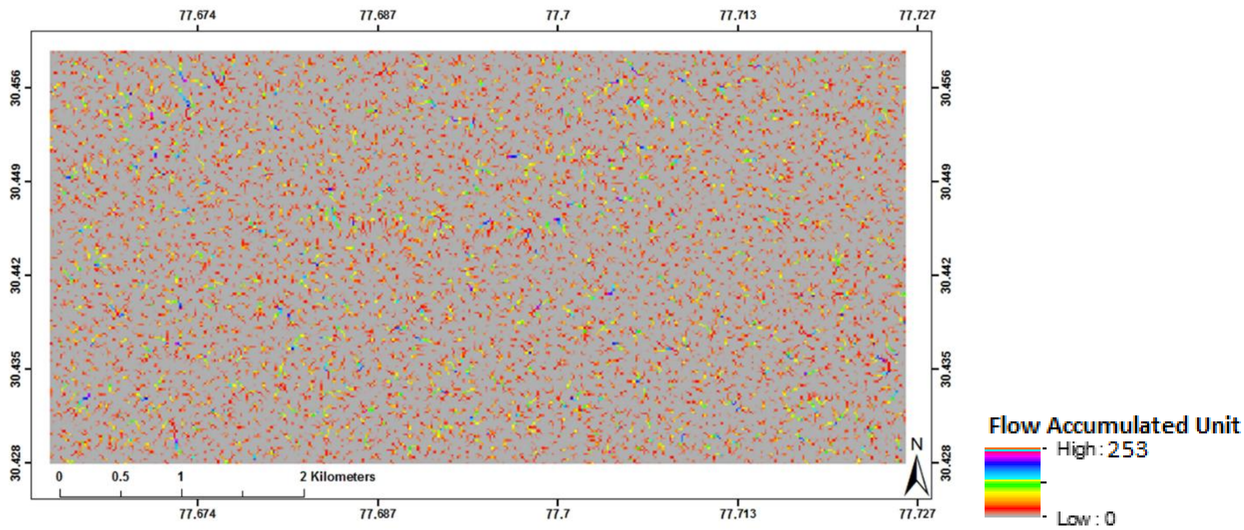

Figure 6-17 Flow Accumulation Map of structured DEM

It can be seen in the table that Figure 6-16 shows the accumulation output for Reference DEM. Figure 6-17 shows the output of the accumulation generated for the fine-scale simulation structured DEM. Figure 6-18 is the accumulation output for the up-scaled unstructured DEM and Figure 6-19 is the output for unstructured DEM generated using DGM approach. It can be visually observed that simulated structured grid in Figure 6-17 gives visually similar to the accumulated flow of Figure 6-16 due to its gridded structure. The unstructured grid, due to its regularisation in the value, tends to give a larger accumulated flow. But it is to be noted that all the accumulation is in the regions similar to that of Figure 6-16.Basically this accumulation map shows the drainage path based on the flow direction map which is generated from each DEM.

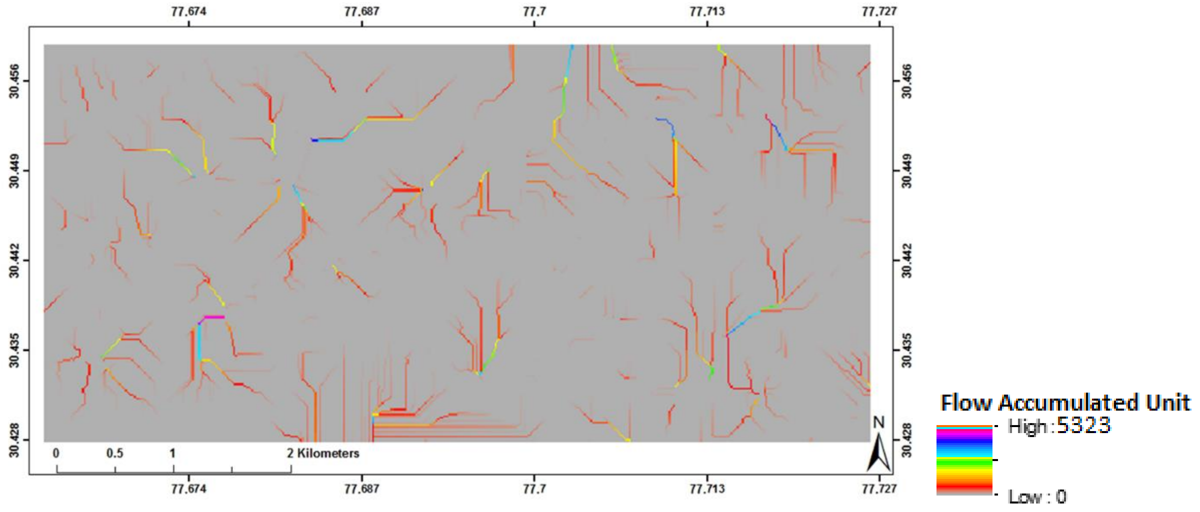

Figure 6-18 Flow Accumulation of Unstructured DEM generated using Fine scale simulation

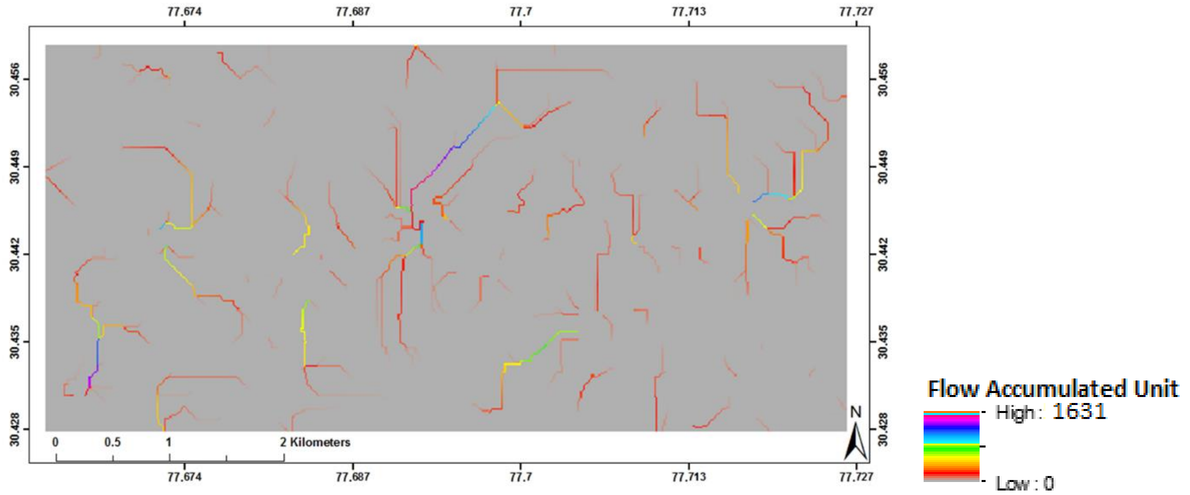

Figure 6-19 Flow Accumulation Map generated for unstructured grid generated using DGM

6.3.2. Steady Flow Analysis

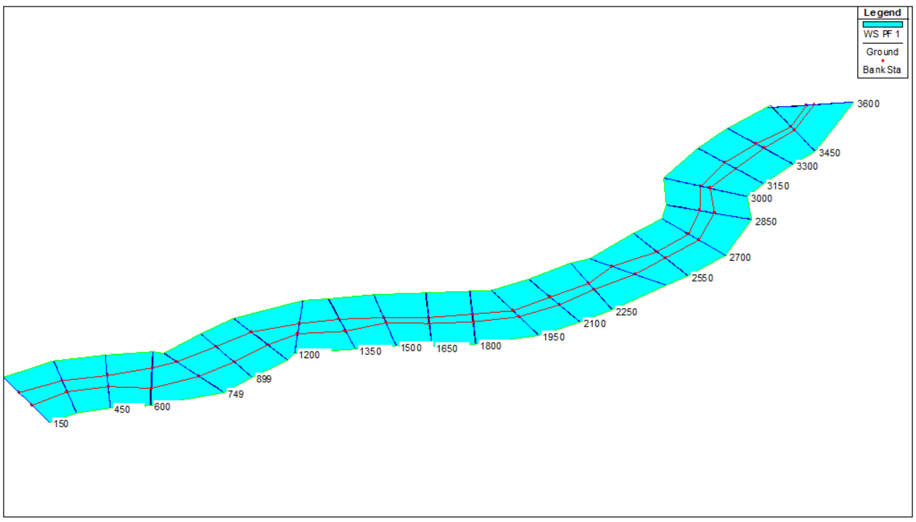

Figure 6-20 3-D Multiple cross-section plot

Figure 6-20 shows the 3-D multiple cross-section outputs showing from upstream to downstream, which is generated during the digitization of geometric data using ArcGIS. These cross-section models are one of the key parameter HEC-RAS. The cross-section model shows the stream centreline, right and left bank, and the cross-section generated for width 400m and interval 300m. The cross-section model is kept the same as they are used to extract elevation data from the DEM to create a ground profile across the channel. Thus each time when different DEM is given and the elevation value is updated to get different general elevation profile plot. The steady flow analysis for Asan river area in the study was performed using HEC-RAS. The energy equation and Manning's equation helped in solving the steady flow. The detailed summary table of the output is given in Appendix-A.

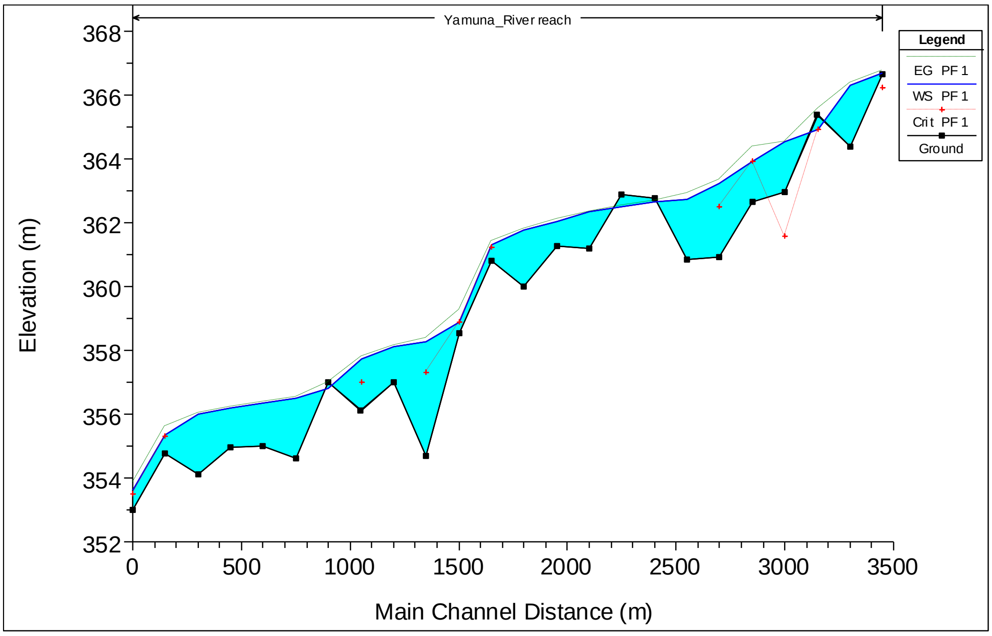

Figure 6-21Water surface profile for reference DEM

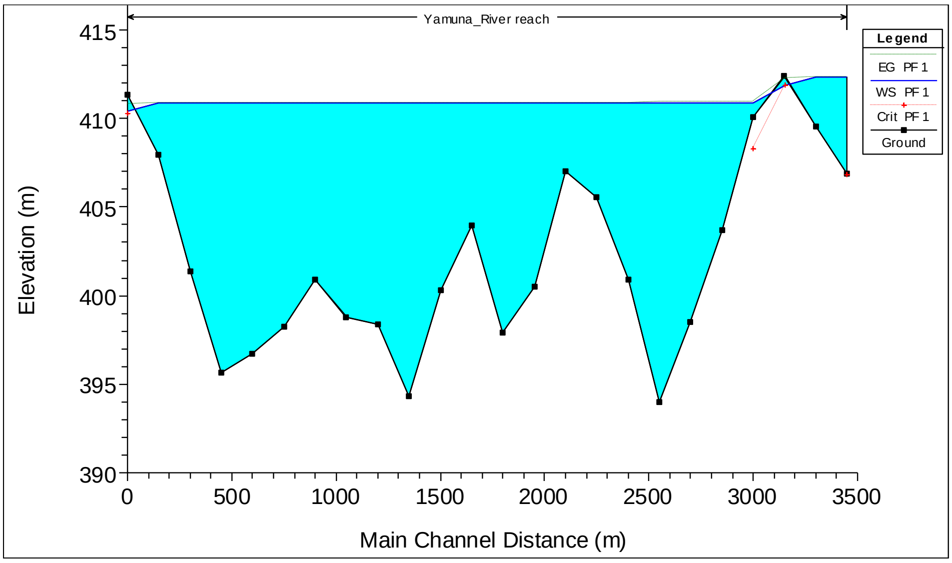

Figure 6-22 Water surface profile for structured DEM

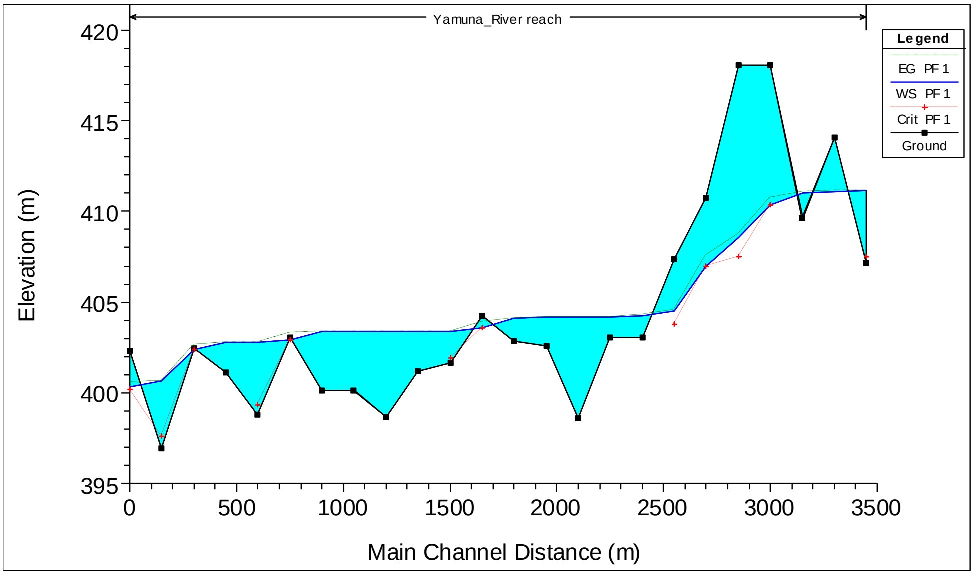

Figure 6-23 Water surface profile for Unstructured DEM generated using fine-scale simulation

Figure 6-21 shows the water surface profile for the Reference DEM, which was taken for validating the other outputs. Figure 6-22 is the surface plot for structured gridded DEM. Figure 6-23 shows the Elevation vs Channel Distance plot for unstructured Grid generated using fine-scale simulation, and Figure 6-24 is the surface plot for the Unstructured grid generated using DGM approach. It can be observed that Figure 6-23 gives a similar result, having high elevation in upstream and low elevation in downstream, to that of reference DEM surface profile. It can also be observed that in these in reference DEM, the surface elevation is a gradually decreasing while in unstructured DEM of fine-scale simulation, the water surface elevation at from upstream till a distance of 3000m there is a steep decrease and then the water surface decreases gradually. But in case of structured DEM, the water surface elevation almost looks flat and it can also be observed that the figure shows the depth to be deeper in the structured DEM. In the case of unstructured DEM of DGM, the difference between the water surface profile and the ground is too large and stating that the river is too deeper.

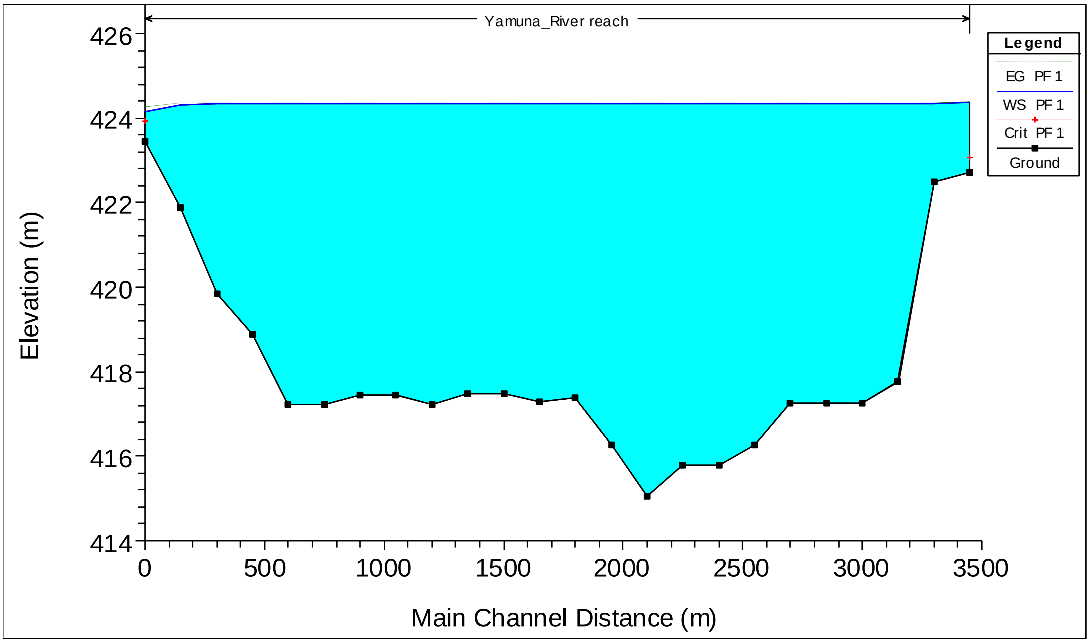

Figure 6-24 Water surface profile for Unstructured DEM generated using DGM

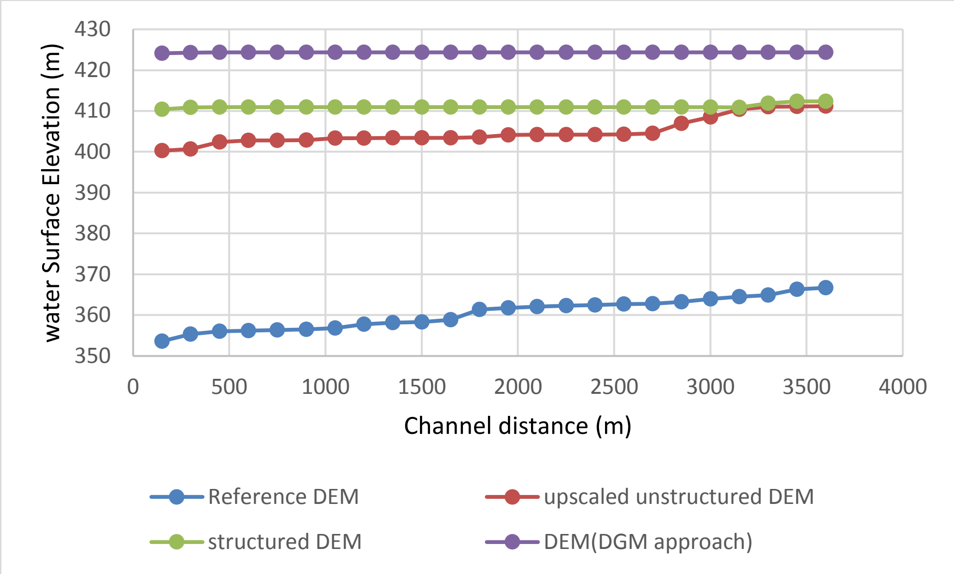

Figure 6-25 Water Surface elevation plot

The water surface profile is plotted between the elevation and the main channel distance. The profiles are generated at each cross-section by creating an energy grade line, a water surface profile, and a critical profile line. Figure 6-25, and Table 6, the water surface elevation difference can be observed. It is noted that the elevation difference for the unstructured grid (fine-scale simulation approach) has almost near to same value to that of the reference DEM. This can be added to the behaviour of the water surface profile from Figure 6-21 and Figure 6-23 that the Fine-scale Unstructured DEM gives similar water surface elevation to that of reference DEM. And similarly the difference in elevation for the structured grid and the unstructured DGM is very less, stating that the water level is flat without much roughness in the flow.

Table 6 Elevation difference from upstream to downstream

DEM	Water surface Elevation Difference (m)
Reference DEM	13.07
Structured Grid	1.92
Unstructured grid(fine – scale simulation)	10.87
Unstructured Grid(DGM approach)	0.21

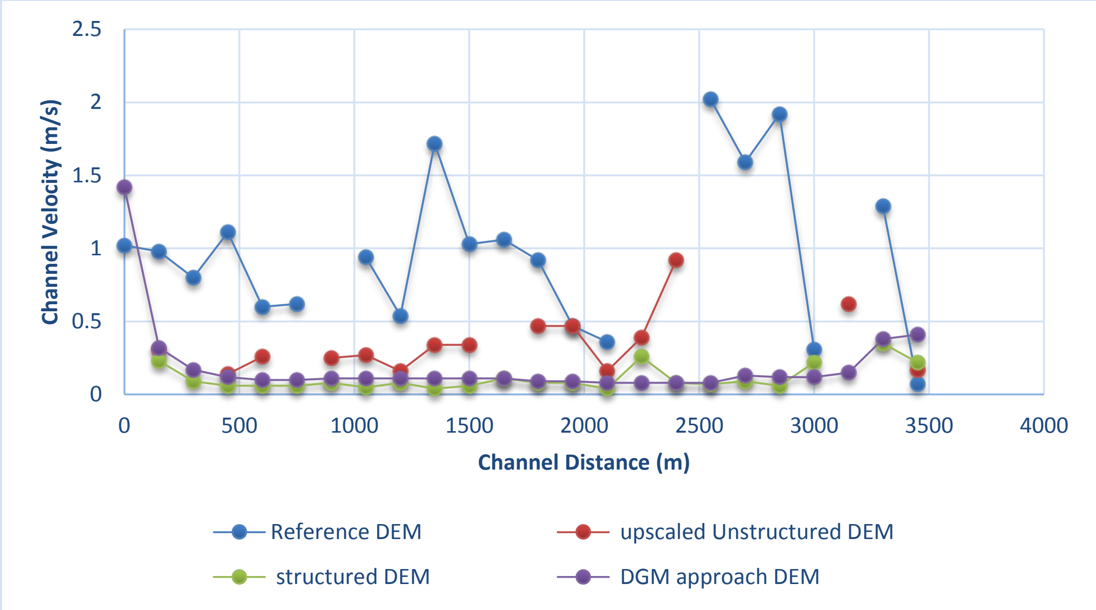

Figure 6-26 General Profile Velocity Plot

Figure 6-26 shows the general profile velocity plot, which is plotted between Channel velocity (m/s) and the channel distance. It is to be noted that the velocity profile not only shows the magnitude of velocity but also shows the characteristics of flow direction, change in shape of the domain, etc. In the plot distance 0 refers to downstream and distance 4000m represents upstream. In this case Figure 6-26 shows the increase/decrease in the velocity magnitude with respect to the geometry. The relative accurate DEM that is the Reference DEM shows an increase in velocity as we move from upstream to downstream. The velocity increases from 0.7m/s to 1m/s, with high velocity of 2.02m/s at a distance of 2500m. In structured DEM due to less variation in the surface elevation, velocity of the flow is also in a steady state. While in Unstructured DGM Approach, there is maintained velocity similar to structured grid due to the

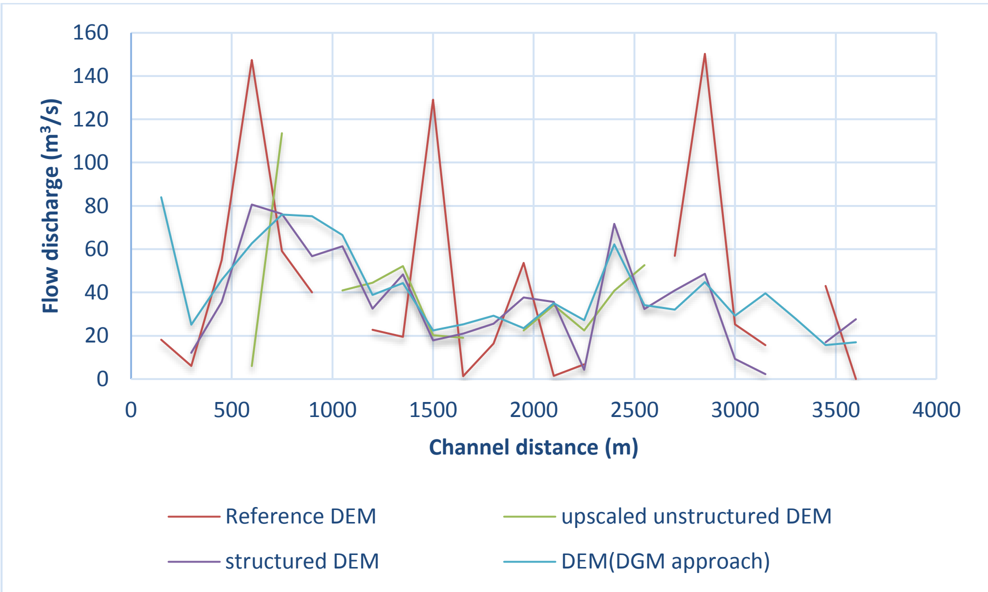

Figure 6-27 Channel profile discharge (m^3/s)

The flow discharge characteristics of the river are shown in Figure 6-27. The X-axis, channel distance, represents downstream to upstream flow and their corresponding discharge in terms of (m^3/s) in Y-axis. The Reference DEM shows that the flow discharges in high velocity at the upstream with discharge of

150m³/s at distance of 2700m as the highest. The other 3 DEM shows similar behaviour where the discharge is increasing as the station moves from upstream to downstream

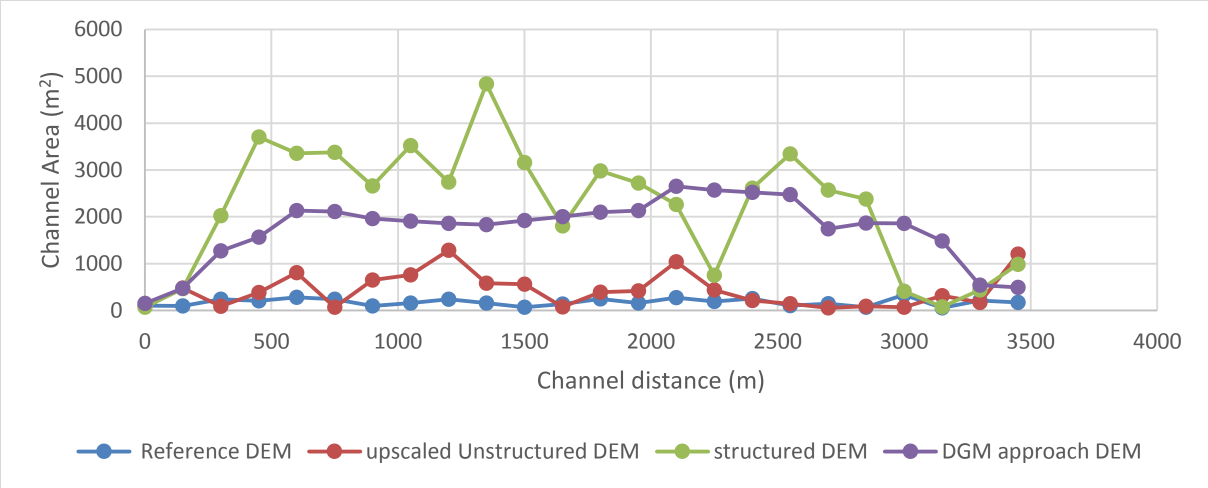

Figure 6-28 Plot representing the flow area for each cross-section

Figure 6-28 shows the plot representing the flow area for each cross-section. It can be observed from the above plot that, the flow area for the upmost stream and the flow area for downstream is the same for all the DEMs. It is also observed that the flow area pattern for the unstructured grid generated using DGM and Fine-scale approach is similar to the reference DEM while for structured DEM, there is too much variation in comparison to the structured DEM.

6.4. Validation

In order to compare the performance of the flow in each simulated DEM, Validation is needed to check which DEM behaves similarly to that of Reference DEM. Here the 3 simulated DEM is taken as the predicted value, and the RMSE is found with the original Reference DEM with respect to the steady flow properties. Table 7 shows the comparison of DEM values with mean elevation, flow discharge and mean velocity. The statistical comparison for the same is plotted in Bar graph as shown in **Error! Reference ource not found.** and **Error! Reference source not found.**.

Table 7 Mean values for all the parameters

DEM	**Mean Elevation (m)**	**Mean flow Discharge (m^3/s)**	**Mean Velocity (m/s)**
Reference DEM	360.36	43.38	0.96
Structured	411.04	36.13	3.73
Unstructured DEM –Fine scale Approach	404.86	34.32	5.09
Unstructured- DGM Approach	424.32	40.98	4.13

Table 8 statistical comparison of data for surface water elevation (m)

DEM	Mean (m)	RMSE (m)	Standard Deviation (m)	Correlation coefficient	R^2
Structured	424.47	0.87	1.20	0.84	0.72
Unstructured DEM (Fine scale Approach)	417.42	0.89	4.47	0.90	0.82
Unstructured- DGM Approach	436.57	0.83	1.13	0.93	0.86

Table 8 shows the statistical comparison of water surface elevation for different elevation profile. Comparing the RMSE value, it can be noted that the unstructured DEM generated using DGM has the lowest RMSE while the second lowest is the structured DEM. Similarly, the standard deviation of the unstructured DEM generated using DGM gives the lower value and also in addition to that, it has a high correlation to the reference DEM.

Table 10 shows the statistical analysis of channel velocity for different DEMs. The RMSE is calculated keeping the reference DEM values as the actual values. Comparing the values to the reference DEM it can be noted that the RMSE value is less with 0.38m^3/s for unstructured grid generated with fine-scale simulation and the second lowest is for the unstructured grid generated using DGM. It is the same case for the standard deviation values that is, lowest is for unstructured grids having 0.58m/s and the highest is for the structured grid. While comparing correlation, unstructured grid generated using DGM gives more correlation to the reference DEM.

Table 9 statistical comparison of data for flow discharge (m^3/s)

DEM	RMSE (m^3/s)	Standard Deviation (m^3/s)	Correlation coefficient
Structured	1.22	2020.37	-0.39
Unstructured DEM –Fine scale Approach	1.33	2263.25	-0.26
Unstructured- DGM Approach	1.18	1939.13	-0.40

Table 10 statistical comparison of data for channel velocity (m/s)

DEM	RMSE (m/s)	Standard Deviation (m/s)	Correlation coefficient	R^2
Structured	0.65	1.25	0.64	0.42
Unstructured DEM (Fine scale Approach)	0.38	0.95	0.46	0.21
Unstructured- DGM Approach	0.58	0.95	0.84	0.70

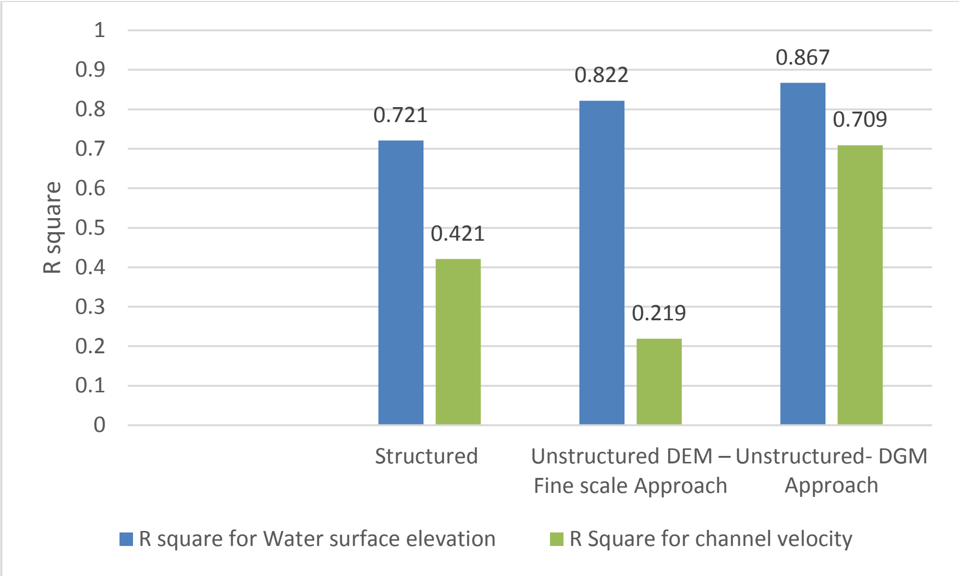

Figure 6-29 Plot showing the R^2 value for water surface elevation and channel velocity between different DEM values

Figure 6-29 shows the R^2 value which is plotted between reference DEM and the simulated DEM. It can be observed that the R^2 value is high in DGM generated DEM for both water surface elevation and channel velocity. Which means that the extent of DGM generated DEM is a highly reliable model and can be used to predict the flow analysis compared to other DEM as it shows a high correlation to the reference DEM.

7. DISCUSSION

The main objective of this research is to do a geostatistical simulation on the unstructured grid by addressing the support size effect and implementing the resultant output of the simulation to the surface flow simulation. This chapter discusses the results and its analysis obtained by understanding the effect of support size effect in the application of hydrology.

7.1. Support size effect

The support size effect is usually addressed in the area of mining and petroleum sectors, where point and block support can make a major impact in variable estimation as stated in chapter 2. However, in this study support size effect has been performed to analyse the effect on hydrology. As mentioned in one of the chapters, Digital Elevation model is used as a key parameter for this analysis due to its crucial role in hydrological parameter estimations. As per the methodological workflow, in order to address this support size effect, two approaches have been followed. One is the classical approach, that is, the fine-scale simulation approach and the other one is the Discrete Gaussian model. From both these approaches it can be observed that, due to the difference in the size of the support, variability in the data increases leading to support effect. As observed in Figure 6-8 and Figure 6-15, the value distribution of point support and the block support has the same average value but the variability of the values differ. It can be noted that the variability of block support is smaller than the variability of the point support. In addition to this, the decrease in variability can also be seen in Figure 6-14 where the semi-variance (sill) is decreased in block support as compared to point support. The reason is stated in Section 2.4.2, as the variability decrease the sill value also decreases. Comparing the classical model, fine-scale simulation and the discrete Gaussian model in response to support size effect it can be noted that, even though the support size is addressed in fine-scale simulation but as per the literature and the practical analysis DGM gives a better result.

7.2. Geostatistical simulation

As discussed in the previous section about support size effect, the geostatistical simulation is done on accounting this support size effect i.e. as per the support size effect approach this simulation is also done on two types of grids. In fine-scale simulation approach, the geostatistical simulation, Sequential Gaussian simulation, is done on the generated structured grid and then the values are up-scaled to the unstructured grid. This method means that the simulation does not directly involve with unstructured grid and the support size effect is addressed after the geostatistical simulation. While in Discrete Gaussian model approach, the simulation is done after addressing the support size effect using the model given. That is the point support data is converted to block support, block is the cells of the generated unstructured grid. The conversion includes finding the support size co-efficient, also known as correlation coefficient or block variance, which is calculated as given in Equation 3.19. Ideally, the value of coefficient should vary between 0 to 1, denoting that if the value is 0 means that the size of the support is too large (block) and if the value is 1 the size of the support is too small (point). In this study the support coefficient varies from 0 to 3.50e-04, denoting that the value which is near to 1 has finer block size and the values which are closer to 0 have very large block area. The resultant output of unstructured gridded DEM as shown in Figure 6-4 and Figure 6-5 shows variation in their output due to direct and indirect simulation approach. As in Fine-scale simulation approach, the value of the grid is obtained by up-scaling the variability between the point support and block support is less. While in the case of DGM approach, the simulation is done directly on the unstructured grid, the variation between the structured point support and unstructured block support is large, Figure 6-15.

7.3. Dynamic simulation

As per the objective, the dynamic simulation or the flow simulation is done to analyse the effect of support size in hydrology. As the hydrological input parameter, elevation values, the geostatistical simulation is done to generate different digital elevation models by addressing this support size effect. The resultant model shows different variability in the elevation values. In order to analyse the effect on hydrology, two hydrological simulations are done, one is the flow accumulation analysis and the other is the steady flow analyses.

In the flow simulation, as observed in Figure 6-16, Figure 6-17, Figure 6-18 and Figure 6-19, the flow accumulation varies for different DEMs. The variation is caused due to the variability in the values of the DEM. But overall if it is observed clearly, it can be noted that the flow accumulated in a large area in un-structured grids than compared to structured grids and at the same time, there flow accumulated regions are less in comparison to the structured grid. It can be said that the size of the block does affect the flow accumulation analysis due to the variation in vertical as well as the horizontal resolution of each DEM.

Steady flow analysis is done by updating the elevation values of different elevation models in the geometric data. As per the observation done it can be noted that due to the difference in the elevation values of each DEM, the velocity of the flow in the channel also varies. From this, it can be said that performing geostatistical simulation by addressing the support size effect gives a high impact on the flow simulation due to the variation in the values. Comparative analysis was performed to find which DEM gives an output similar to the high-resolution reference DEM. Furthermore, in order to validate the results of the flow simulations, the outputs are compared with the reference DEM. It can be noted the all the 3 generated DEM, gives the RMSE in a similar range with not much variation in the value. The coefficient of determination also gives similar results. But among the values obtained the DEM generated using DGM approach gives high correlation with the reference DEM, compared to the structured DEM. This can be observed from Table 8, Table 9 and Table 10 that the performance DGM generated DEM gives better results compared to other generated DEM. As Digital Elevation Model is a primary parameter in flow analysis, the variation of flow is reasonable due to the variability in the value of each DEM. It is also to be noted that this flow variation is also affected if the support change effect occurs. Sahid, Nurrohman, & Hadi, (2018) has also mentioned in their research about the DEM structure influence on flood modelling, where they had concluded that the vertical as well as the horizontal accuracy of the DEM influence the flood modelling.

8. CONCLUSION AND RECOMMENDATIONS

This chapter is about the overall research conclusion, which is given by answering the research questions given in Chapter 1 and along with that recommendations are given for future scope.

8.1. Conclusion

The overall research objective of this study was divided into 2 parts. One was to generate an adaptive unstructured grid for the hydrological model and to address the support size effect issue and the other one is to do surface flow simulation on the generated unstructured grid and compare it with the structured grid. The research is being done in order to attain the objective goals as per the workflow mentioned in chapter 5. The unstructured grid is generated in such a way that it represents the boundary of the river and the urban land in finer grid blocks and the other areas in coarser grid blocks, thus making a clear distinguishing structure between river and land. The support size effect is addressed using two different approaches and as per the ideal statement; the variability of the block support is decreased compared to the point support. The output of the geostatistical simulation, after addressing the support size effect is used as the elevation input for the flow simulation. It can be observed that in surface flow simulation, the variation in support shows the impact on the velocity of flow in the channel as there is the difference in flow velocity through the channel when the DEM is structured and unstructured. Since in the flow simulation in comparison with the DEM, along with the vertical comparison (in the elevation values), in horizontal comparison (area) the values gave abrupt change in the flow of the water across the channel. The resultant output of the flow simulation when validated with the reference DEM shows that the DEM generated using DGM model gives more accurate results as it has the minimum RMSE value and maximum coefficient of determination when compared to other DEMs.

As mentioned in chapter 1 this study answers the following questions

1. What are the different types of unstructured grids available in the previous study and which can be used for hydrological modelling?
   As per the literature, there are many different types of unstructured grids like triangular, hexagon, octahedral, Voronoi polygons. In this study as well as basically in hydrological modelling so far, Voronoi polygons are used due to their adaptive nature and easy to construct capability.

2. How the issue of support size effect is relevant in relation to unstructured grids and hydrological modelling?
   As mentioned in an earlier chapter the issue of support size effect can be easily addressed using unstructured grids due to their geometrical behaviour. Basically, this support size effect was effectively addressed in the domain of petroleum and mining areas and in hydrology it is addressed to estimate sub-surface flow. In this research, the support size effect is studied for hydrological modelling for surface flow estimation. It is observed that the size of the support in our case elevation value varies abruptly. Due to regionalisation of the data, the variability changes with distance this leads to change of support value leading to variation in the flow.

3. How does the structure of grid vary over a typical terrain?

   The main key in grid generation is the point parameter which is here is taken as the slope points. So depending on the slope points, these Voronoi polygons are generated. Denser the points the finer the grid blocks are generated. In this study, there were many attempts made using different slope angle to generate different kinds of an unstructured grid. The final chosen structure varies in such a way that it distinguisher the river area and the urban land area by finer blocks in between and coarser blocks on the other sides.

4. How to address this support size effect?

   In this research the support size effect is addressed in two approaches, one is the classical approach that is the fine-scale simulation approach, where the geostatistical simulation is done on the structured grid and then the values are upscaled to the unstructured grid. The second approach is that using DGM model, where the simulation is done directly on the unstructured grid, by considered each block to block and point to block variance and area while doing the structural analysis.

5. How to validate the results?
   The results are validated by comparing the output DEM with high-resolution DEM taken as reference and using RMSE (Root Mean Square Error), mean and standard deviation and along with this, the output from the flow simulation of each DEM is also compared to know the performance of each DEM in reference to the high-resolution DEM.

8.2. Recommendation

This research is done by addressing the support size effect with minimum parameter (DEM). As unstructured grids are famous for its complexity. Using different parameters, the change of support can be explored. Also, in this study unstructured grid is generated based on the slope points as the point data, due to this, the finer and the coarser blocks of the grid are generated depending on the density of the points. As a future scope, the grid can be generated in such a way that the blocks have user constrained volume and the finer and coarseness of the block can be controlled. In this research, the change of support is studied on the structural aspect. A detailed exploration of the change of support models can be done to address the support size effect and its behaviour in different parameters. Furthermore, in the application with hydrology, the unsteady surface flow simulation and in sub-surface flow, the effect of support effect analysis can be done.

LIST OF REFERENCES

Ahmad, H. F., Bhat, M. S., & Ahmad, S. (2016). One Dimensional Steady Flow Analysis Using HEC- RAS – A case of River Jhelum , Jammu and Kashmir, *12*(32), 340–350. https://doi.org/10.19044/esj.2016.v12n32p340

Baddeley, A., Turner, R., & Rubak, E. (2019). spatstat: Spatial Point Pattern Analysis, Model-Fitting, Simulation, Tests.

Balan, B., & Schlumberger, G. (1997). Structured versus Unstructured (PEBI) Grids in Reservoir Modeling and Simulation. *Soagi.Ru*, (June), 37998–37998. Retrieved from http://soagi.ru/Free_article/Structured versus Unstructured.pdf

Bergamaschi, L. (2005). Geostatistics in Hydrology: Kriging Interpolation. *Course Materials*. Retrieved from http://scholar.google.com/scholar?hl=en&btnG=Search&q=intitle:Geostatistics+in+Hydrology+:+Kriging+interpolation#6

Bertoncello, A., Caers, J., Biver, P., Caumon, G., & France, N. (2009). Geostatistics on Stratigraphic Grid Gridding and Reservoir Geometry Representation 1-Definition of the Grids, 1–16.

Biver, P., Zaytsev, V., Allard, D., & Wackernagel, H. (2017). Geostatistics on unstructured grids , theoretical background and applications . *Geostatistics Valencia 2016*, 449–458.

Bowyer, A. (1981). Computing Dirichlet tessallation. *Computer Journal*, *24*(2), 162–166.

Braun, P., Molnar, T., & Kleeberg, H. B. (1997). The problem of scaling in grid-related hydrological process modelling. *Hydrological Processes*, *11*(9), 1219–1230. https://doi.org/10.1002/(SICI)1099-1085(199707)11:9<1219::AID-HYP553>3.3.CO;2-J

Chawner, J. (2013). Quality and Control – Two Reasons Why Structured Grids Aren't Going Away. Retrieved July 4, 2018, from http://www.pointwise.com/theconnector/2013-March/Quality-Control-Two-Reasons-Structured-Grids-Arent-Going-Away.html

Chilès, J. ., & Delfiner, P. . (2014). Geostatistics : Modeling Spatial Uncertainty Geostatistics : Modeling Spatial Uncertainty, (November). https://doi.org/10.1007/s11004-012-9429-y

Chiles, J. P. (2014). Validity range of the discrete Gaussian change-of-support model and its variant. *Journal of the Southern African Institute of Mining and Metallurgy*, *114*(3), 231–235.

Clark, I., & Harper, W. V. (2000). *Practical Geostatistics*. Columbus, Ohio : Ecosse North America, c2008.

Conroy, C. J., Kubatko, E. J., & West, D. W. (2012). ADMESH : An advanced , automatic unstructured mesh generator for shallow water models, 1503–1517. https://doi.org/10.1007/s10236-012-0574-0

Dehotin, J., & Braud, I. (2008). Which spatial discretization for distributed hydrological models? Proposition of a methodology and illustration for medium to large-scale catchments. *Hydrology and Earth System Sciences*, *12*(3), 769–796. https://doi.org/10.5194/hess-12-769-2008

Delfiner, P. (1999). *Geostatistics:modeling spatial uncertainity* (1st ed.). New York:John Wiley & Sons.

Delfiner, P. (2012). *Geostatistics : modeling spatial uncertainty* (2nd ed.). Wiley. Retrieved from https://ebookcentral.proquest.com

Desbarats, A. J. (1996). Modeling spatial variability using geostatistical simulation, *1283*, 32–48.

Durlofsky, L. J. (2005). Upscaling and Gridding of Fine Scale Geological Models for Flow Simulation. *E 8th International Forum on Reservoir Simulation*, 1–59. https://doi.org/10.1002/er.3246

Dusserre, M. G., Garbolino, M. E., Jaber, M. A., Guarnieri, M. F., & Karim, M. H. (2016a). de l ' Université de recherche Paris Sciences et Lettres.

Dusserre, M. G., Garbolino, M. E., Jaber, M. A., Guarnieri, M. F., & Karim, M. H. (2016b). *Stochastic methods for modeling uncertainties on unstructured meshes*. PSL Research University.

Emery, X. (2007). Change of Support for Estimating Local Block Grade.

Emery, X., & Ortiz, J. M. (2011). Two approaches to direct block-support conditional co-simulation. *Computers and Geosciences*, *37*(8), 1015–1025. https://doi.org/10.1016/j.cageo.2010.07.012

Environmental Systems Research Institute, I. (2010). How Slope works. Retrieved from http://desktop.arcgis.com/en/arcmap/10.3/tools/spatial-analyst-toolbox/how-slope-works.htm

Environmental Systems Research Institute, I. (2016). Flow Accumulation. Retrieved February 13, 2019, from http://desktop.arcgis.com/en/arcmap/10.3/tools/spatial-analyst-toolbox/flow-accumulation.htm

Environmental Systems Research Institute, I. (2018). ArcMap. Retrieved February 13, 2019, from http://desktop.arcgis.com/en/arcmap/

Fields, R., Soni, B. K., Thompson, J. F., Hausser, H., Gable, C. W., Trease, H. E., & Cherry, T. a. (1996).

Geological Applications of Automatic Grid Generation Tools for Finite Elements Applied to Porous Flow Modeling From : Numerical Grid Generation in Computational Fluid Dynamics and From : Numerical Grid Generation in Computational Fluid Dynamics and From : *Methods*, (June), 1–9.

Franz, D. D. (2015). Full Equations (FEQ) Model for the Solution of the Full, Dynamic Equations of Motion for One-Dimensional Unsteady Flow in Open Channels and Through Control Structures. Retrieved February 15, 2019, from https://il.water.usgs.gov/proj/feq/feqdoc/contents_1.html

Gold, B. (2012). Surface Water Hydrology Predictive Study. In *APPLICATION FOR AN ENVIRONMENTAL ASSESSMENT CERTIFICATE / ENVIRONMENTAL IMPACT STATEMENT*.

Gómez, H., Rodrigo, I., Rodrigo, C., & Vargas, G. (2017). *Geostatistics Valencia 2016*. Springer International Publishing. Retrieved from https://books.google.nl/books?id=My1IDgAAQBAJ

Grid Systems. (2015). Retrieved July 5, 2018, from https://www.flow3d.com/resources/cfd-101/general-cfd/grid-systems/

Hagen, E. D. M., Huthoff, F., & Warmink, J. J. (2014). Hydrodynamic modelling with unstructured grid using D-Flow-FM : case study Afferden-Deest, 39–40.

Hengl, T. (2006). Finding the right pixel size. *Computers and Geosciences*, *32*(9), 1283–1298. https://doi.org/10.1016/j.cageo.2005.11.008

Hengl, T. (2009). *Geostatistical Mapping*. https://doi.org/10.1016/0277-9390(86)90082-8

Hodges, B. R. (2014). *Hydrodynamical Modeling. Reference Module in Earth Systems and Environmental Sciences*. Elsevier Inc. https://doi.org/10.1016/B978-0-12-409548-9.09123-5

Hurtado, F. S. V. (2004). The element-based finite volume method applied to petroleum reservoir simulation. In *Rio Oil & Gas Expo and Conference 2004* (Vol. M).

ILWIS. (2015). Kriging-Algorithm. Retrieved February 13, 2019, from http://spatial-analyst.net/ILWIS/htm/ilwisapp/kriging_algorithm.htm

Jamal, H. (2018). Applications of Hydrology in Civil Engineering Subscribe to our Newsletter.

Journel, A. ., & Huijbregts, C. J. (1978). *Mining geostatistics*. academic press london.

Loseille, A. (2017). Unstructured Mesh Generation and Adaptation. In *Handbook of Numerical Methods for Hyperbolic Problems - Applied and Modern Issues*. Elsevier Inc.

Manchuk, J. (2010). *Geostatistical Modeling of Unstructured Grids for Flow Simulation*. University of Alberta.

Manchuk, J. G., & Deutsch, C. V. (2009). Algorithms for Unstructured Grids, *2009*, 1–8. Retrieved from http://www.ccgalberta.com

Manchuk, J., Leuangthong, O., & Deutsch, C. V. (2005). Direct Geostatistical Simulation on Unstructured Grids. In O. Leuangthong & C. V Deutsch (Eds.), *Geostatistics Banff 2004* (pp. 85–94). Dordrecht: Springer Netherlands. https://doi.org/10.1007/978-1-4020-3610-1_9

Marsh, C. B., Spiteri, R. J., Pomeroy, J. W., & Wheater, H. S. (2018). Multi-objective unstructured triangular mesh generation for use in hydrological and land surface models. *Computers and Geosciences*, *119*(September 2017), 49–67. https://doi.org/10.1016/j.cageo.2018.06.009

Matheron, G. (1985). Change of support for diffusion-type random functions. *Journal of the International Association for Mathematical Geology*, *17*(2), 137–165. https://doi.org/10.1007/BF01033151

Mavriplis, D. J. (1997). Unstructured Grid Techniques. *Annual Review of Fluid Mechanics*, *29*(1), 473–514. https://doi.org/10.1146/annurev.fluid.29.1.473

Moog, G. J. E. A. (2013). Advanced Discretization Methods for Flow Simulation Using Unstructured Grids, (June), 161. Retrieved from https://pangea.stanford.edu/ERE/pdf/pereports/PhD/Moog2013.pdf

Morgan, C. J. (2005). *Analysing spatial data via geostatistical methods*. Retrieved from http://hdl.handle.net/10539/1768

Morgan, C. J. (2012). The influence of support size on semi- variogram parameters, 50–59.

Morgan, C. J. (2012). *Theoretical and practical aspects of variography: in particular, estimation and modelling of semi-variograms over areas of limited and clustered or widely spaced data in a two-dimensional South African gold mining context*. Retrieved from http://hdl.handle.net/10539/11193

Pebesma, E., & Graeler, B. (2018). gstat: Spatial and Spatio-Temporal Geostatistical Modelling, Prediction and Simulation.

Rendu. (1981). *An Introduction to Geostatistical Methods of Mineral Evaluation* (2nd ed.). Johannesburg: South African Institute of Mining and Metallurgy.

Sahid, Nurrohman, A. W., & Hadi, M. P. (2018). An investigation of Digital Elevation Model (DEM) structure influence on flood modelling. *IOP Conference Series: Earth and Environmental Science*, *148*,

012001. https://doi.org/10.1088/1755-1315/148/1/012001
Tate, E. (1999). Introduction to HEC-RAS. Retrieved February 16, 2019, from http://www.ce.utexas.edu/prof/maidment/grad/tate/research/rasexercise/webfiles/hecras.html
Team, R. D. C. (2018). The R Project for Statistical Computing. Retrieved February 13, 2019, from https://www.r-project.org/
U.S. Army Corps of Engineers. (2019). Hydorlogical Engineering Center-River Analysis System. Retrieved February 13, 2019, from https://www.hec.usace.army.mil/software/hec-ras/
Usul, N., & Pasaogullari, O. (2004). Effect of map scale and grid size for hydrological modelling. In F. Chen, YB and Takara, K and Cluckie, ID and DeSmedt (Ed.), *GIS and Remote Sensing in Hydrology, Water Resources and Environment* (Vol. 289, pp. 91–100). INST OF HYDROLOGY, WALLINGFORD OX10 8BB, ENGLAND: INT ASSOC HYDROLOGICAL SCIENCES.
Vieux, B. E. (2016). *Distributed hydrologic modeling using gis* (3rd ed.). Springer.
Watson, D. (1981). Computing the ndimensional Delaunay tessalation with application to Voronoi polytopes. *Computer Journal*, *24*(2), 167–171.
Webster, R., & Oliver, M. A. (2002). *Geostatistics for Environmental Scientists*. *Vadose Zone Journal* (Vol. 1). https://doi.org/10.2136/vzj2002.0321
Wikipedia contributors. (2018). Surface-water hydrology.
Willse, J. T. (2018). CTT: Classical Test Theory Functions. Retrieved February 13, 2019, from https://cran.r-project.org/web/packages/CTT/index.html
Yakar, M., Yilmaz, H. M., & Yurt, K. (2010). The effect of grid resolution in defining terrain surface. *Experimental Techniques*, *34*(6), 23–29. https://doi.org/10.1111/j.1747-1567.2009.00553.x
Yang, J., Townsend, R. D., & Daneshfar, B. (2006). Applying the HEC-RAS model and GIS techniques in river network floodplain delineation. *Canadian Journal of Civil Engineering*, *33*(1), 19–28. https://doi.org/10.1139/l05-102
Zainalfikry, M. K., & Ghani, A. A. (2018). HEC-RAS One-Dimensional Hydrodynamic Modelling for Recent Major Flood Events in Pahang River Corporation Engineers Hydraulic Engineering Centre to, 1–10.
Zaytsev, V., Biver, P., Wackernagel, H., & Allard, D. (2016a). Change-of-Support Models on Irregular Grids for Geostatistical Simulation. *Mathematical Geosciences*, *48*(4), 353–369. https://doi.org/10.1007/s11004-015-9614-x
Zaytsev, V., Biver, P., Wackernagel, H., & Allard, D. (2016b). Geostatistical Simulations on Irregular Reservoir Models Using Methods of Nonlinear Geostatistics.
Zhou, Q., Pilesjö, P., & Chen, Y. (2011). Estimating surface flow paths on a digital elevation model using a triangular facet network. *Water Resources Research*, *47*(7), 1–12. https://doi.org/10.1029/2010WR009961

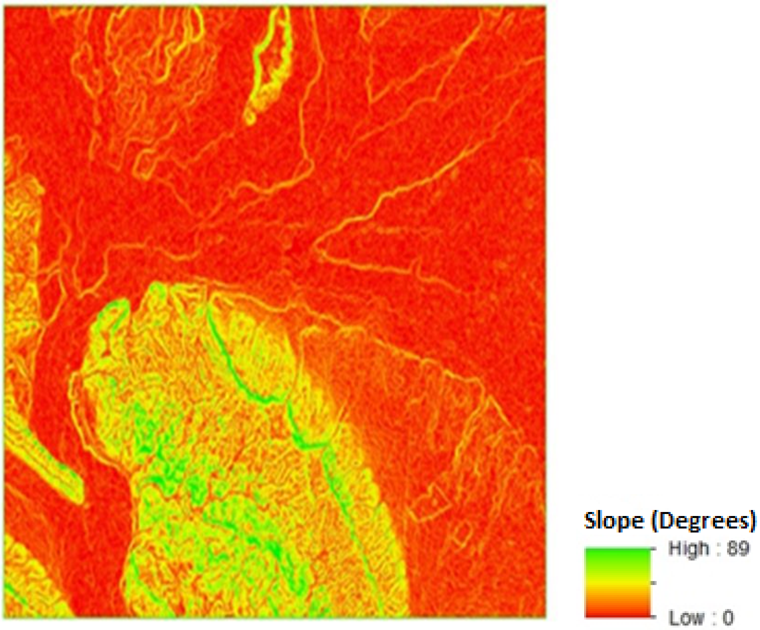

Slope generated from CartoDEM 30m

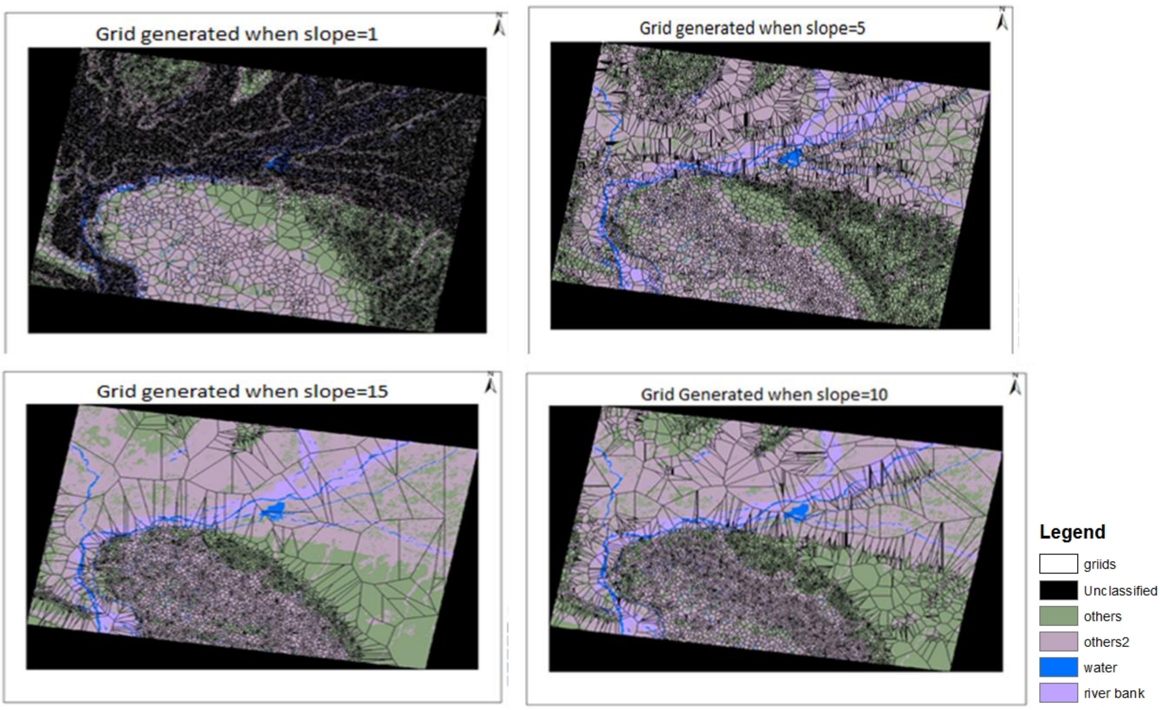

Grid generated for different slope points for the full study area without taking subset.

APPENDIX-B

The output of the steady flow analysis for different DEM inputs are given below

Reach	River Sta	Profile	Q Total	Min Ch El	W.S. Elev	Crit W.S.	E.G. Elev	E.G. Slope	Vel Chnl	Flow Area	Top Width	Froude # Chl
			(m3/s)	(m)	(m)	(m)	(m)	(m/m)	(m/s)	(m2)	(m)	
reach	3600	PF 1	200.00	366.66	366.69	366.25	366.77	0.001194	0.07	171.08	193.68	0.18
reach	3450	PF 1	200.00	364.39	366.32		366.38	0.000900	1.29	217.95	288.30	0.34
reach	3300	PF 1	200.00	365.39	364.92	364.92	365.56	0.008220		56.36	44.01	0.00
reach	3150	PF 1	200.00	362.96	364.52	361.57	364.54	0.000081	0.31	340.51	156.36	0.10
reach	3000	PF 1	200.00	362.66	363.92	363.92	364.40	0.006688	1.92	69.47	76.58	0.80
reach	2850	PF 1	200.00	360.94	363.23	362.49	363.34	0.001050	1.59	149.60	135.32	0.38
reach	2700	PF 1	200.00	360.86	362.74		362.92	0.002387	2.02	108.93	106.28	0.55
reach	2550	PF 1	200.00	362.78	362.66		362.69	0.000214		253.82	142.00	0.00
reach	2400	PF 1	200.00	362.88	362.49		362.55	0.000680		191.04	154.01	0.00
reach	2250	PF 1	200.00	361.21	362.33		362.36	0.000316	0.36	278.52	243.87	0.17
reach	2100	PF 1	200.00	361.27	362.03		362.12	0.001599	0.47	159.89	234.38	0.33
reach	1950	PF 1	200.00	360.00	361.78		361.81	0.000472	0.92	250.22	240.38	0.25
reach	1800	PF 1	200.00	360.82	361.32	361.21	361.44	0.003645	1.06	137.30	251.42	0.55
reach	1650	PF 1	200.00	358.52	358.88	358.88	359.27	0.009281	1.03	73.07	98.17	0.77
reach	1500	PF 1	200.00	354.68	358.28	357.29	358.39	0.000847	1.72	157.56	176.42	0.36
reach	1350	PF 1	200.00	357.00	358.10		358.14	0.000632	0.54	241.11	271.19	0.24
reach	1200	PF 1	200.00	356.11	357.74	357.02	357.82	0.001193	0.94	162.75	164.32	0.35
reach	1050	PF 1	200.00	357.00	356.80		357.00	0.004668		101.93	130.67	0.00
reach	899.9999	PF 1	200.00	354.63	356.50		356.54	0.000480	0.62	245.49	242.62	0.22
reach	749.9999	PF 1	200.00	355.00	356.36		356.39	0.000385	0.60	282.02	260.69	0.20
reach	600.0001	PF 1	200.00	354.96	356.18		356.23	0.000920	1.11	205.74	244.23	0.33
reach	450	PF 1	200.00	354.13	356.01		356.05	0.000505	0.80	243.51	216.88	0.24
reach	299.9999	PF 1	200.00	354.77	355.35	355.29	355.60	0.004940	0.98	97.95	151.14	0.60
reach	150	PF 1	200.00	353.00	353.62	353.51	353.84	0.004205	1.02	105.80	157.38	0.57

Summary table for Reference DEM Steady Flow report

Reach	River Sta	Profile	Q Total	Min Ch El	W.S. Elev	Crit W.S.	E.G. Elev	E.G. Slope	Vel Chnl	Flow Area	Top Width	Froude # Chl
			(m3/s)	(m)	(m)	(m)	(m)	(m/m)	(m/s)	(m2)	(m)	
reach	3600	PF 1	200.00	407.16	411.18	407.52	411.18	0.000004	0.17	1204.56	300.00	0.03
reach	3450	PF 1	200.00	414.11	411.10		411.17	0.000261		172.69	50.13	0.00
reach	3300	PF 1	200.00	409.63	411.04		411.06	0.000249	0.62	314.94	234.91	0.17
reach	3150	PF 1	200.00	418.05	410.37	410.37	410.73	0.009951		74.80	103.38	0.00
reach	3000	PF 1	200.00	418.05	408.54	407.52	408.77	0.001487		93.11	40.05	0.00
reach	2850	PF 1	200.00	410.79	406.97	406.97	407.54	0.008866		59.92	53.29	0.00
reach	2700	PF 1	200.00	407.38	404.50	403.79	404.59	0.001082		146.16	103.21	0.00
reach	2550	PF 1	200.00	403.02	404.24		404.28	0.000612	0.92	215.23	180.48	0.27
reach	2400	PF 1	200.00	403.02	404.19		404.20	0.000108	0.39	438.00	300.00	0.11
reach	2250	PF 1	200.00	398.60	404.19		404.19	0.000005	0.16	1040.15	300.00	0.03
reach	2100	PF 1	200.00	402.58	404.18		404.19	0.000131	0.47	419.18	300.00	0.13
reach	1950	PF 1	200.00	402.82	404.12		404.14	0.000158	0.47	395.47	300.00	0.14
reach	1800	PF 1	200.00	404.25	403.59	403.59	403.91	0.010499		80.16	127.67	0.00
reach	1650	PF 1	200.00	401.68	403.40	401.91	403.40	0.000050	0.34	562.13	300.00	0.08
reach	1500	PF 1	200.00	401.16	403.38		403.38	0.000043	0.34	585.77	300.00	0.08
reach	1350	PF 1	200.00	398.67	403.38		403.38	0.000003	0.16	1285.73	300.00	0.02
reach	1200	PF 1	200.00	400.11	403.37		403.38	0.000016	0.27	764.34	300.00	0.05
reach	1050	PF 1	200.00	400.11	403.37		403.37	0.000027	0.25	649.85	300.00	0.06
reach	899.9999	PF 1	200.00	403.05	402.89	402.89	403.29	0.009878		71.13	87.19	0.00
reach	749.9999	PF 1	200.00	398.82	402.78	399.30	402.78	0.000010	0.26	806.52	218.15	0.04
reach	600.0001	PF 1	200.00	401.13	402.75		402.77	0.000064	0.14	385.58	300.00	0.07
reach	450	PF 1	200.00	402.47	402.37	402.37	402.66	0.005859		94.64	154.40	0.00
reach	299.9999	PF 1	200.00	396.94	400.63	397.58	400.63	0.000030	0.31	481.77	136.46	0.06
reach	150	PF 1	200.00	402.29	400.31	400.16	400.57	0.005705		88.10	100.69	0.00

Summary table for up-scaled Unstructured DEM Steady Flow report

Reach	River Sta	Profile	Q Total	Min Ch El	W.S. Elev	Crit W.S.	E.G. Elev	E.G. Slope	Vel Chnl	Flow Area	Top Width	Froude # Chl
			(m3/s)	(m)	(m)	(m)	(m)	(m/m)	(m/s)	(m2)	(m)	
reach	3600	PF 1	200.00	406.86	412.34	406.81	412.34	0.000005	0.22	986.24	246.71	0.03
reach	3450	PF 1	200.00	409.55	412.33		412.34	0.000040	0.35	436.94	152.78	0.08
reach	3300	PF 1	200.00	412.39	411.87	411.87	412.25	0.008120		75.78	103.39	0.00
reach	3150	PF 1	200.00	410.09	410.90	408.31	410.92	0.000076	0.22	410.31	195.08	0.09
reach	3000	PF 1	200.00	403.72	410.91		410.91	0.000000	0.06	2377.12	300.00	0.01
reach	2850	PF 1	200.00	398.51	410.91		410.91	0.000000	0.09	2567.59	300.00	0.01
reach	2700	PF 1	200.00	394.00	410.91		410.91	0.000000	0.07	3341.98	300.00	0.01
reach	2550	PF 1	200.00	400.90	410.91		410.91	0.000000	0.08	2613.77	300.00	0.01
reach	2400	PF 1	200.00	405.54	410.91		410.91	0.000012	0.26	755.84	255.33	0.04
reach	2250	PF 1	200.00	407.04	410.91		410.91	0.000000	0.04	2264.31	300.00	0.01
reach	2100	PF 1	200.00	400.53	410.91		410.91	0.000000	0.08	2720.92	300.00	0.01
reach	1950	PF 1	200.00	397.88	410.91		410.91	0.000000	0.08	2981.44	300.00	0.01
reach	1800	PF 1	200.00	403.94	410.91		410.91	0.000001	0.11	1805.89	300.00	0.01
reach	1650	PF 1	200.00	400.33	410.91		410.91	0.000000	0.06	3155.09	300.00	0.01
reach	1500	PF 1	200.00	394.34	410.91		410.91	0.000000	0.04	4833.37	300.00	0.00
reach	1350	PF 1	200.00	398.40	410.91		410.91	0.000000	0.08	2738.10	300.00	0.01
reach	1200	PF 1	200.00	398.77	410.91		410.91	0.000000	0.05	3517.31	300.00	0.01
reach	1050	PF 1	200.00	400.93	410.91		410.91	0.000000	0.08	2657.45	300.00	0.01
reach	899.9999	PF 1	200.00	398.22	410.91		410.91	0.000000	0.06	3375.46	300.00	0.01
reach	749.9999	PF 1	200.00	396.69	410.91		410.91	0.000000	0.06	3358.04	300.00	0.01
reach	600.0001	PF 1	200.00	395.63	410.91		410.91	0.000000	0.06	3700.14	300.00	0.01
reach	450	PF 1	200.00	401.38	410.91		410.91	0.000001	0.09	2024.26	300.00	0.01
reach	299.9999	PF 1	200.00	407.93	410.89		410.91	0.000043	0.23	470.71	220.32	0.07
reach	150	PF 1	200.00	411.32	410.42	410.27	410.81	0.005713		72.77	64.68	0.00

Summary table for up-scaled structured DEM Steady Flow report.

Reach	River Sta	Profile	Q Total	Min Ch El	W.S. Elev	Crit W.S.	E.G. Elev	E.G. Slope	Vel Chnl	Flow Area	Top Width	Froude # Chl
			(m3/s)	(m)	(m)	(m)	(m)	(m/m)	(m/s)	(m2)	(m)	
reach	3600	PF 1	200.00	422.72	424.36	423.07	424.37	0.000078	0.41	491.48	300.00	0.10
reach	3450	PF 1	200.00	422.50	424.33		424.34	0.000058	0.38	539.19	300.00	0.09
reach	3300	PF 1	200.00	417.78	424.34		424.34	0.000002	0.15	1486.20	300.00	0.02
reach	3150	PF 1	200.00	417.27	424.34		424.34	0.000001	0.12	1860.96	300.00	0.01
reach	3000	PF 1	200.00	417.27	424.34		424.34	0.000001	0.12	1864.99	300.00	0.01
reach	2850	PF 1	200.00	417.27	424.33		424.34	0.000001	0.13	1744.73	300.00	0.02
reach	2700	PF 1	200.00	416.26	424.33		424.34	0.000000	0.08	2471.86	300.00	0.01
reach	2550	PF 1	200.00	415.79	424.33		424.33	0.000000	0.08	2519.29	300.00	0.01
reach	2400	PF 1	200.00	415.79	424.33		424.33	0.000000	0.08	2572.49	300.00	0.01
reach	2250	PF 1	200.00	415.05	424.33		424.33	0.000000	0.08	2654.67	300.00	0.01
reach	2100	PF 1	200.00	416.26	424.33		424.33	0.000001	0.09	2134.70	300.00	0.01
reach	1950	PF 1	200.00	417.38	424.33		424.33	0.000001	0.09	2098.51	300.00	0.01
reach	1800	PF 1	200.00	417.30	424.33		424.33	0.000001	0.11	2003.91	300.00	0.01
reach	1650	PF 1	200.00	417.47	424.33		424.33	0.000001	0.11	1919.54	300.00	0.01
reach	1500	PF 1	200.00	417.47	424.33		424.33	0.000001	0.11	1835.04	300.00	0.01
reach	1350	PF 1	200.00	417.22	424.33		424.33	0.000001	0.11	1858.25	300.00	0.01
reach	1200	PF 1	200.00	417.44	424.33		424.33	0.000001	0.11	1905.28	300.00	0.01
reach	1050	PF 1	200.00	417.44	424.33		424.33	0.000001	0.11	1964.32	300.00	0.01
reach	899.9999	PF 1	200.00	417.23	424.33		424.33	0.000001	0.10	2110.26	300.00	0.01
reach	749.9999	PF 1	200.00	417.22	424.33		424.33	0.000001	0.10	2131.77	300.00	0.01
reach	600.0001	PF 1	200.00	418.87	424.33		424.33	0.000002	0.12	1565.97	300.00	0.02
reach	450	PF 1	200.00	419.84	424.33		424.33	0.000003	0.17	1270.17	300.00	0.03
reach	299.9999	PF 1	200.00	421.89	424.32		424.33	0.000073	0.32	470.88	300.00	0.09
reach	150	PF 1	200.00	423.44	424.15	423.92	424.25	0.002863	1.42	152.36	300.00	0.54

Summary table for DGM approach DEM Steady Flow report

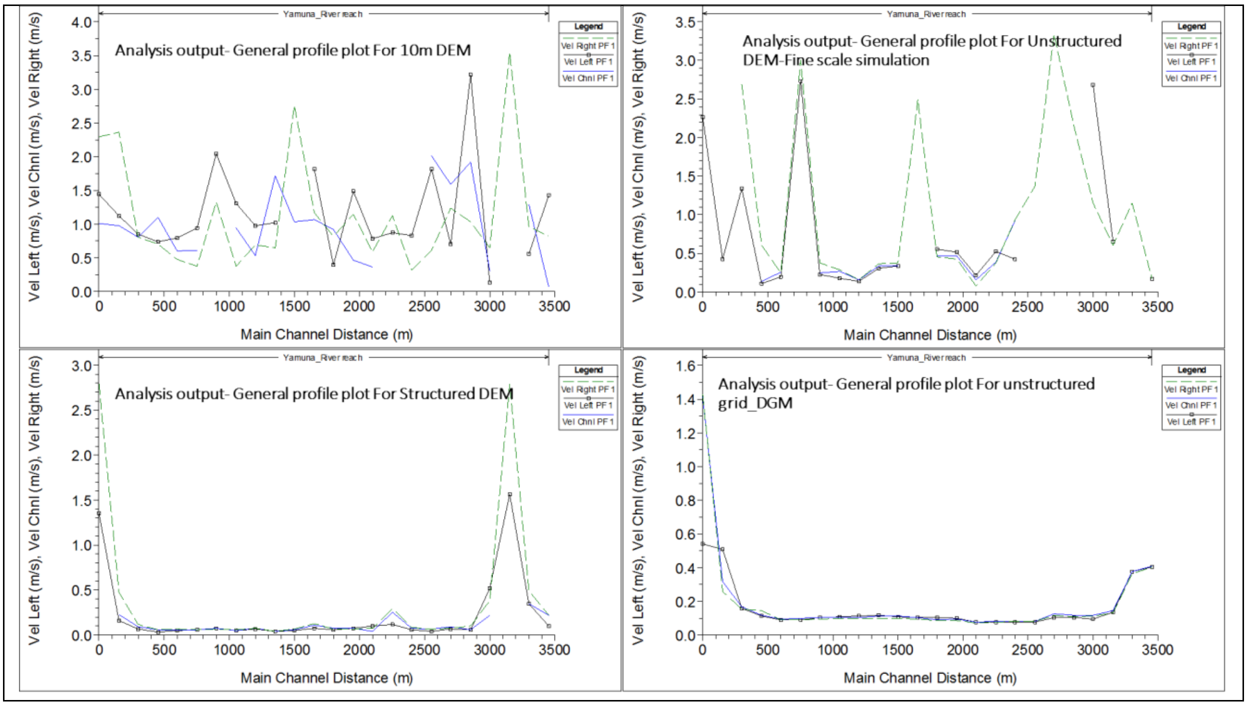

The above Figure shows the general surface plot generated from HEC-RAS

APPENDIX-C

R-Codes

1. **Fine scaled structured grid generation**

```
xy <- expand.grid(x=seq(77.66292, 77.72597 ,length=450), y=seq( 30.42708,
30.45792,length=450))
xys <- SpatialPoints(xy)
gridded (xys) <- TRUE
```

2. **Generation of unstructured Grid (Voronoi polygon)**

```
Library (spatstat)
Diri<- Dirichlet (sample points)
```

3. **Sequential Gaussian Simulation**

```
Library (gstat)
lzn.condsim = krige (elevation_value~1, elevation_data, xys, model = fit.variog,nmax = 30,
nsim = 100)
spplot (lzn.condsim,main='conditional simulation')
```

4. **Discrete Gaussian Model**

   i. Support Co-efficient calculation

```
x1 = rnorm(n=100, mean=0, sd=1)
x2 = rnorm(n=100, mean=0, sd=1)
cova1 <- cov(x1, x2) #0.057105
correlation_coeff<- cova1/ (polygon_area^2) # r square= block variance of y(v)
r<-sqrt(correlation_coeff)
```

   ii. Covariance Matrix

```
area<-as.matrix(poly_area)
area2<-as.matrix(t(area))
support_coeff<-as.matrix(r)
support_coeff2<-as.matrix(t(support_coeff))
Y_v<-as.numeric(transformed$new.scores*r)
###using the formulae of DGM2 cov(Vp,Vq)
bloc<- matrix(ncol = 100, nrow = 100)
bloc_val<-area %*% area2
block_value<-1/bloc_val
rp<-matrix(ncol = 100, nrow = 100)
rp<-support_coeff%*%support_coeff2
rp_coeff<-1/rp
cova1
cova_matrix<-matrix(ncol = 100, nrow = 100)
cova_mat<-block_value%*%rp_coeff
cova_matrix<-cova_mat*cova1
for (i in seq(1:100))
{
 U[i]=sum(weigh[i]%*%((Y_v[i])))
}
```